DIRECTED EVOLUTION OF CYANIDE DEGRADING ENZYMES

A Dissertation

by

MARY ABOU NADER

Submitted to the Office of Graduate Studies of
Texas A&M University
in partial fulfillment of the requirements for the degree of

DOCTOR OF PHILOSOPHY

Approved by:

Chair of Committee,	Michael Benedik
Committee Members,	Carlos Gonzalez
	Matthew Sachs
	Wayne Versaw
Head of Department,	U. J. McMahan

December 2012

Major Subject: Microbiology

ABSTRACT

Cyanide is acutely toxic to the environment. However, this simple nitrile is used in several industrial applications especially the mining industry. Due to its high affinity to metals, cyanide has been used for years to extract gold and other precious metals from the ore. Cyanide nitrilases are considered for the detoxification of the industrial wastewaters contaminated with cyanide. Their application in cyanide remediation promises cheaper and safer processes compared to chemical detoxification. However, application of these enzymes in industry requires improving their characteristics.

The goal of this dissertation is to better understand cyanide nitrilases, in particular the cyanide dihydratase from of *Bacillus pumilus* and *Pseudomonas stutzeri* and to improve their activity and stability. The lack of any high resolution structure of these enzymes calls for isolating or screening for mutants showing enhancement in enzyme properties.

Described first is a simple and efficient method utilizing *in vivo* recombination to create recombinant libraries incorporating the products of PCR amplification. This method is useful for generating large pools of randomly mutagenized clones after error-prone PCR mutagenesis. Several parameters were investigated to optimize this technique; length of homology region, vector treatment, induction time and ratio of fragment to vector.

Using error-prone PCR for random mutagenesis, several $CynD_{pum}$ mutants were isolated for higher catalysis at pH 7.7. Three point mutations, K93R, D172N and E327K

increased the enzyme's thermostability. The D172N mutation also increased the affinity of the enzyme for its substrate at pH 7.7 suggesting an effect on the active site. However, the A202T mutation located in the dimerization or the A surface rendered the enzyme inactive by destabilizing it. No significant effect on activity at alkaline pH was observed for any of the purified mutants.

Lastly, an important region for $CynD_{stut}$ activity was identified in the C-terminus. This same region increased the stability of $CynD_{pum}$ compared to the wild-type enzyme. Also, $CynD_{pum\text{-}stut}$ hybrid was found to be highly more stable than $CynD_{pum}$. This same hybrid exhibited 100% activity at pH9, a pH where the parent enzyme is inactive, and retained 40% of its activity at pH 9.5 making it a true pH tolerant mutant.

DEDICATION

To my parents, my sisters, my husband and my precious Blueberry for their endless love, support and encouragement.

"*Scientific research constitutes for you, as it does for many, the way for the personal encounter with truth, and perhaps the privileged place for the encounter itself with God, the Creator of heaven and earth.*" Pope John Paul II

ACKNOWLEDGEMENTS

I would like to express my gratitude for my graduate advisor, Dr. Michael Benedik, for providing me with invaluable support, guidance and assistance throughout my graduate studies. It has been a blessing and honor to be part of his lab.

I also would like to thank my committee members, Dr. Carlos Gonzalez, Dr. Matthew Sachs and Dr. Wayne Versaw, for their constant guidance and evaluation during these years.

A special thanks to Dr. Trevor Sewell for his advice and collaboration on the cyanide project and Dr. Bruce Riley for allowing me to rotate in his laboratory during my first semester at Texas A&M University.

For their invaluable help, I would like to thank all the undergraduates that I had the opportunity to work with especially Kate Brels, Ilka Maza and Henry Lessen.

I would like to thank my labmates and friends, Lacy Basile, Tysheena Charles, Lan Wang, Allyson Martinez, Alvaro Rodriguez and Jason Park.

I would like to express my love and gratitude for my family and friends in Lebanon, Australia and USA. Thank you for supporting and encouraging me all these years.

NOMENCLATURE

HCN	Hydrogen cyanide
CN^-	Cyanide ion
NaCN	Sodium cyanide
KCN	Potassium cyanide
CynD	Cyanide dihydratase
CHT	Cyanide hydratase
$CynD_{pum}$	Cyanide dihydratase from *Bacillus pumilus*
$CynD_{stut}$	Cyanide dihydratase from *Pseudomonas stutzeri* AK61
CHT_{crassa}	Cyanide hydratase from *Neurospora crassa*
EP-PCR	Error-prone PCR

TABLE OF CONTENTS

LIST OF FIGURES

Page

LIST OF TABLES

Page

CHAPTER I

INTRODUCTION AND LITERATURE REVIEW

OVERVIEW

Cyanide is a powerful poison that nevertheless has great applications in several industries such as mining and electroplating. Since large volumes of cyanide-contaminated effluents are generated from these industries, cyanide wastewater has to be detoxified before being discharged in the environment. Unfortunately, chemical methods that are currently used are expensive and generate toxic products. This makes the bioremediation of cyanide a potential and practical alternative solution.

Several animals, plants and microorganisms express enzymes able to degrade cyanide. In particular the nitrilases, cyanide dihydratase and cyanide hydratase, hold great promise in bioremediation of cyanide waste. Cyanide dihydratases of bacterial origin convert cyanide into ammonia and formate. These rare enzymes are found in the very disparate strains of *Bacillus pumilus* (87), *Pseudomonas stutzeri AK61* (146) and *Alcaligenes xylosoxidans subsp. denitrificans* (60) . On the other hand, cyanide hydratases of fungal origin hydrolyse cyanide into formamide. They are found in a wide spectrum of fungi and best characterized in *Neurospora crassa*, *Gloeocercospora sorghi* and *Fusarium lateritium* (9). Neither enzyme requires any cofactors or secondary substrate to catalyze the reaction, making them ideal for industrial processes. Uses of the native cyanide dihydratase from *Alcaligenes xylosoxidans subsp. denitrificans* and cyanide hydratase from *Fusarium lateritium* have been patented for industrial cyanide

detoxification. My research work has been focused on optimizing the cyanide dihydratases from *Bacillus pumilus* and *Pseudomonas stutzeri* to improve their stability and increase their degrading activity, thereby yielding a promising and practical enzyme.

CYANIDE CHEMICAL PROPERTIES

Also known as prussic acid, hydrogen cyanide (HCN) forms a colorless gas with a bitter almond odor. It is the simplest of the nitriles (R–CN). Cyanide is a very weak acid, with a pK_a value of 9.22 and soluble in water at 25°C; it evaporates above room temperature. This nitrile is less dense than air and therefore, it disperses rapidly (26). In the environment cyanide can be present in different forms; other than gas and liquid, it can be found as a solid in the form of simple salt crystals like sodium cyanide (NaCN) and potassium cyanide (KCN). In alkaline solutions (pH>9), approximately 60% of cyanide remains in solution as CN^- but at physiological pH 7.4, 99% of cyanide exists as the volatile hydrogen cyanide (HCN) (20).

Despite its toxicity and due to its ability to form complexes with numerous metals thereby making them soluble, cyanide is used in many industrial processes such as gold and silver mining and electroplating (29). It is also widely used in the synthesis of organic and inorganic chemicals such as nitriles, carboxylic acids, amides, and esters (99).

CYANIDE TOXICITY

Hydrogen cyanide (HCN) is extremely hazardous. By binding more strongly than oxygen to the cytochrome c oxidase, it inhibits cellular respiration causing death in seconds (148). Also, cyanide binds and inhibits several metalloenzymes due to its high affinity for metals. Thus, it affects the function and activity of different body organs such as the kidneys, liver and central nervous system (148). The average lethal dose of ingested cyanide is 1.52 mg/kg body weight (151).

Although cyanide acts rapidly, cyanide antidote treatments are available. Hydroxocobalamin, a precursor of vitamin B12, binds the cyanide ion to form cyanocobalamin (vitamin B-12) which is excreted in the urine (17). The kit is FDA approved and is sold under the brand name Cyanokit. Another antidote kit consists of amyl nitrite, sodium nitrite and sodium thiosulfate. Nitrite (NO_2^-) reacts with hemoglobin to form methemoglobin, which draws cyanide out of cytochrome system to form cyanomethemoglobin. The mitochondrial enzyme rhodanese combines thiosulfate ($S_2O_3^{2-}$) with cyanomethemoglobin to form the less toxic thiocyanate (CNS^-), which is excreted by the kidneys. Finally, methemoglobin is converted back to hemoglobin by the enzyme methemoglobin reductase (47).

CYANIDE IN NATURE

Cyanide is commonly found in nature. It is produced by some bacteria, fungi, algae and plants (71). Cyanogenic fungi (that produce cyanide) such as *Marasmius oreades* are often plant pathogens (15). In bacteria, certain Pseudomonads (44, 120) and

Chromobacterium violaceum (88) produce cyanide as a secondary metabolite. In plants, cyanide is stored in the vacuoles as cyanogenic glycosides such as amygdalin and other natural compounds. Several food plants contain varying amounts of cyanide compounds and cause death if ingested in large quantities. Some of these foods include almonds, cassava roots, millet sprouts, lima beans, bamboo shoots, apple seeds and apricot seeds.

Almond trees, one of the earliest domesticated trees, are native to the southwestern Asia. However, the seeds are of two kinds, sweet and bitter. Only sweet almonds are edible and bitter almonds are toxic. Domestication of almonds was made possible due to a mutation inhibiting the production of amygdalin, a cyanogenic glycoside. One bitter almond contains around 6 mg of cyanide (127). The seeds contain an enzyme called emulsin. Emulsin degrades amygdalin into benzaldehyde, cyanide and 2 molecules of glucose. In the early 1950s, amygdalin was promoted as a cancer cure and was marketed under the name laetrile. It was thought that cyanide might act as an active anticancer compound (92). When the pills are ingested and amygdalin is released, several glycosidase enzymes act on the amygdalin and release cyanide. Numerous cyanide poisoning cases were recorded in patients who took laetrile as cancer treatment (12).

In the tropics, cassava is the third most important food source after rice and maize according to the Food and Agriculture Organization of the United Nations. Cassava tolerates drought, grows on poor soil and the roots are an important carbohydrate source. Tapioca is the powdered form of cassava. The roots and leafs contain valine- and isoleucine-derived cyanogenic glycosides, linamarin and lotaustralin.

When chewed, the enzyme linamarase found in cell wall comes in contact with the cyanogenic glycosides and degrades them to release glucose and a precursor of cyanide, acetone cyanohydrin (91). This latter product is degraded into acetone and cyanide either spontaneously or through the action of α-hydroxynitrile lyase (57). The leaves and the skin layer of the roots of this plant have high amounts of cyanide. Sweet cassavas have less cyanogen compared to the bitter cassavas. The bitter taste is largely due to the linamarin. In order to be safely consumed, cassava roots have to be properly cooked and processed; sun drying, heap fermentation, boiling. In Africa, during famine periods, shortcuts in processing techniques are sometimes used but they fail to lower the linamarin content to safe consumption levels. Some cyanide-related health disorders such as Konzo, an irreversible paraparesis and Tropical Ataxic Neuropathy (TAN) are linked to chronic low-level cyanide consumption especially in malnourished individual

CYANIDE IN INDUSTRY

Hydrogen cyanide is an important chemical in industrial applications. Cyanide has a high affinity to metals; it binds them and dissolving them in solution. Thus, for decades cyanide has been used as lixiviant in metal mining for extraction of precious metals from the ore. Other industries also use cyanide such as electroplating, nylon and plastic manufacturing, photography, pesticide and insecticide production.

Gold cyanidation is a technique for extracting gold from ore using cyanide solution (77). It is also known as MacArthur-Forrest process developed in 1887. To extract the gold, the ore is ground and water is added. This slurry is then mixed with a

sodium cyanide or calcium cyanide solution. The use of cyanide in gold mining has greatly increased gold production because of the high recovery rate (84). Gold dust particles and fine grain gold are not wasted and low-grade ores are now possible to mine. Lime or soda is also present in the mixture to maintain an alkaline medium (pH10-11) and prevent to creation of poisonous hydrogen cyanide. To recover the gold from solution, several techniques can be used such as carbon-in-pulp (112). In the carbon-in-pulp technique, activated carbon is mixed with ore and cyanide solution and gold-cyanide complex is adsorbed. The carbon particles are then separated from the ore using caustic solution under high temperate and pressure. Finally gold is recovered by electrolysis or by zinc precipitation (89).

The large quantities of cyanide pollutants created by these industries have to be properly disposed of. Several cyanide spills have occurred in different parts of the world such in Europe, Africa and America, the majority of them have occurred in mining facilities (115). In 2006 a leak in Ghana from a gold mining company polluted the Ajoo stream killing fish, crabs and lobsters. People who drank water from the stream showed symptoms of cyanide poisoning. Another spill from a chemical company occurred in Czech Republic in 2006. Cyanide was released in the Elbe River, one of the major rivers in central Europe. Other cyanide spills have taken place in Romania, Australia, China, Philippines and elsewhere (72). These spills had disastrous effect on the environment and human life.

A different kind of industry, the marine ornamental industry, also uses cyanide. Cyanide fishing is the practice of collecting aquarium ornamental fish using cyanide. It

is mainly practiced in Southeast Asia (8). The fish habitat is sprayed with a solution of sodium cyanide to stun and capture the fish. Using a net to collect fish is less productive and more time consuming so using cyanide increases the collection and brings more money. This technique is harmful to marine ecosystems and is illegal however the majority of the collection is done this way (64).

CYANIDE DETOXIFICATION

Cyanide effluents from various industries differ in their cyanide concentration, chemical contaminants and cyanide-metal complexes. Thus, several decontamination methods are commonly employed. In effluents, cyanide compounds are classified in three categories. Depending on the category, different adequate processes and treatment strategies are then applied. The first is the free cyanide category, which includes cyanide ion (CN^-) and hydrogen cyanide (HCN). Compounds in this category are considered extremely toxic. The second category includes the WAD (Weak Acid Dissociable) cyanide, which are weak and moderately stable metal-cyanide complexes, such as those of sodium, cadmium, copper, nickel and zinc. The last category consists of strong metal-cyanide complexes such as those of gold, silver and iron. This category is considered the least toxic. This classification of cyanide discharge is important to consider when choosing a detoxification technique.

Natural degradation or attenuation of cyanide relies on holding the wastewaters for a long period in ponds (116). The outcome of this technique depends strongly on the cyanide species in the solution, their concentration and the storage conditions such as

temperature, aeration, depth and area of the ponds. In this technique, free cyanide (HCN, CN^-) is subjected to volatilization and when free cyanide reacts with air, oxidation would take place to produce ammonia and bicarbonate. Depending on the pH, WAD cyanide species can also dissociated. This occurs at a pH 4.5 and hence hydrogen cyanide can then evaporate. Iron-cyanide complexes can also be dissociated through the action of UV radiation (sunlight). This process is defined as photodecomposition. Natural degradation is a lengthy process and only 60% of the cyanide is removed in a period of 9 months (18).

Another method marketed by Cyanide Destruct Systems, Inc (Canada) uses the thermal hydrolysis of cyanide solutions. This naturally occurring reaction has a slow rate and cyanide is converted into ammonia and formic acid (132) (Eq 1.1). In order to speed up the reaction, temperatures of 400 - 450^oF is required and high pressure of 300 to 500 psi is employed to keep the liquid phase during the reaction. This method does not require any chemicals and is able to destroy all cyanide complexes including iron-cyanide (117).

$$HCN + 2H_2O \rightarrow NH_3 + HCOOH \qquad \text{Eq 1.1}$$

In addition to these non-chemical cyanide remediation ways, there are a variety of chemical methods, each having its advantages and disadvantages. However, they all rely on the destruction of cyanide through oxidation.

Alkaline chlorination is the traditional decontamination technique. This technique is well established and requires the use of hypochlorite ion which can originate from chlorine or sodium hypochlorite (bleach) (Eq 1.2). The advantage of this technique is that it is successful in breaking cyanide into a less toxic product cyanate. It is suitable for destroying free and WAD cyanide. Gold, silver, copper and nickel cyanide complexes can also be destroyed but the reaction requires longer time. Some of the disadvantages of this technique is that it is not suitable of ferrocyanide [$Fe(CN)_6^{-4}$] destruction and that chlorine is toxic and can generate toxic intermediates.

$$CN^- + OCl^- \rightarrow CNO^- + Cl^- \qquad \text{Eq 1.2}$$

Due to the disadvantages of the alkaline chlorination method, hydrogen peroxide has become a preferable reagent for cyanide oxidation (70). This reaction, in alkaline medium with a catalyst such copper, produces cyanate, which is less toxic then cyanide (Eq 1.3-a). Cyanate is then hydrolyzed to give carbon dioxide and ammonia (Eq 1.3-b). The reaction is simple to operate and it is environmentally favorable since excess hydrogen peroxide decomposes to water and oxygen. Free cyanide as well as WAD cyanide can easily be destroyed with this method but other cyanide complexes with nickel, silver and iron require additional steps. Ferrocyanide [$Fe(CN)_6^{-4}$] is not oxidized because of the high stability of the complex in the dark. However, it can undergo precipitation using heavy metals such as copper or photolytic degradation using UV

irradiation (73). The major drawbacks of this technique are the relatively high reagent cost and the continuous and accurate measurements of the reagent dose to be used (93).

$$CN^- + H_2O_2 \rightarrow OCN^- + H_2O \qquad \text{Eq 1.3-a}$$

$$CNO^- + 2H_2O \rightarrow NH_3 + CO_2 + OH^- \qquad \text{Eq 1.3-b}$$

Also, cyanide and thiocyanate anions can be oxidized using sulfur dioxide (SO_2) and air in the presence of a soluble metal catalyst such as copper (Cu) (33) (Eq1.4-a). This sulfur dioxide mediated destruction technique is known as INCO and marketed by INCO Ltd. The process oxidizes free and WAD cyanide and thiocyanate (Eq 1.4-b) but ferrocyanides [$Fe(CN)_6^{-4}$] have to be precipitated using heavy metals such as copper. This technique is useful in cyanide detoxification of slurry. The reagents are inexpensive however the capital cost is high due to the complex chemical handling systems used and the licensing fees to INCO (93).

$$CN^- + SO_2 + H_2O + O_2 \rightarrow OCN^- + H_2SO_4 \qquad \text{Eq 1.4-a}$$

$$SCN^- + 4SO_2 + 5H_2O + 4O_2 \rightarrow OCN^- + 5H_2SO_4 \qquad \text{Eq 1.4-b}$$

These processes are successful in yielding low non-toxic cyanide concentrated effluents. However, these current practices have limitations because (1) they can be expensive, (2) cyanide is not recovered and (3) additional treatment of the products is necessary before the effluent can be released into the environment.

For these reasons, the bioremediation of cyanide waste is presently being considered as an alternative safe, inexpensive and environmentally-friendly method compared to the chemical processes.

CYANIDE DEGRADING ENZYMES

Since cyanide is commonly found in nature, several organisms produce enzymes capable of degrading cyanide for detoxification or for assimilation as a nitrogen source. The enzymes differ remarkably in their reaction conditions, co-factor requirements or additional substrates.

Three pathways, reduction, oxidation and hydrolysis are degradative pathways: they degrade cyanide into simpler and less toxic molecules. The fourth pathway, substitution/transfer, is used for the assimilation of cyanide into the organism's primary metabolism as a source of nitrogen.

Reduction pathway

Some microorganisms such as cyanobacteria use nitrogenase to fix atmospheric nitrogen gas. This reaction requires anaerobic conditions since the enzyme mediating the pathway, nitrogenase, is inhibited by oxygen. Also the enzyme requires low potential reductants such as sodium dithionite ($Na_2S_2O_4$), ATP and protons. Nitrogenase is formed of two protein complexes, an iron containing homodimer (Fe protein) and an iron-molybdenum heterotetramer (MoFe protein). Fe protein forms a complex with MoFe protein while binding 2 molecules of ATP. In this complex one electron is transferred

from Fe protein to MoFe and accompanied by hydrolysis of ATP into ADP. The complex is then dissociated and the 2 molecules of ADP are replaced by ATP (34). Other than N_2, nitrogenase catalyzes the reduction of several substrates such as azide, nitrous oxide, cyclopropene and acetylene. In 1967, Hardy and Knight showed that HCN was reduced to methane and ammonia through the action of nitrogenase (Eq 1.5) (45, 52).

However CN^-, which concentration depends on the pH of the medium, stops electron flow through the enzymes and thus acts as an inhibitor (79). Cyanide solutions are kept at alkaline pH to inhibit the production of hydrogen cyanide. At pH 7, HCN constitutes 99% of total cyanide ($HCN+CN^-$) present in the aqueous solution. However, at pH 9.5, 80% of total cyanide is present as CN^- (20). This percentage increases with an increase of the solution's pH value. Nitrogenase cannot be used in these alkaline solutions because its catalysis reaction is inhibited by the substrate CN^-. Several bacteria were shown to mediate cyanide degradation through the action of their nitrogenase such as *Rhodopseudomonas gelatinosa* (85) and *Klebsiella oxytoca* (65). Nitrogenase of cyanide-degrading *Klebsiella oxytoca* strain is induced by the presence of potassium cyanide in the medium as a sole nitrogen source.

$$HCN + 6e^- + 6H^+ \rightarrow CH_4 + NH_3 \qquad \text{Eq 1.5}$$

Oxidation pathway

Pseudomonas fluorescens NCIMB 11764 was isolated for its ability to utilize cyanide as a sole source of nitrogen in the presence of a carbon source such as glucose (54). Using fed-batch cultures, the cells, pulsed with vapor cyanide in aerobic conditions, degraded cyanide and produced stoichiometric amounts of ammonia while stimulating oxygen uptake (54). However in *Pseudomonas fluorescens* NCIMB 11764 cell-free extract, cyanide degradation required the presence of NADH (53). Two pathways were proposed. The first pathway involves a cyanide monoxygenase that converts cyanide to cyanate (Eq 1.6-a). The latter product would be converted to ammonia and carbon dioxide through the action of the cyanase, an enzyme found in bacteria and plants such as *Escherichia coli* (5) and *Arabidopsis thaliana* (113) which catalyzes the reaction of cyanate with bicarbonate to produce ammonia and carbon dioxide .This first pathway was supported by the presence of cyanate degrading activity in extract of this bacterium (53, 76). In the second pathway, a NADH-requiring cyanide dioxygenase (also known as oxygenase CNO) catalyzes the conversion of cyanide into ammonia and carbon dioxide (53) (Eq 1.6-b). Further research demonstrated that there is no co-induction between cyanide oxygenase and cyanase activities, excluding the coupled pathway of a cyanide oxygenase with cyanase (35).

Cyanide monoxygenase:

$$HCN + O_2 + H^+ + NADH \rightarrow HOCN + NAD^+ + H_2O \quad \text{Eq 1.6-a}$$

Cyanide dioxygenase:

$$HCN + O_2 + H^+ + NADH \rightarrow CO_2 + NH_3 + NAD^+ \quad \text{Eq 1.6-b}$$

To understand the reaction mechanism of CNO and determine if the enzyme is a monoxygenase or a dioxygenase, isotopic labeling of oxygen 18 was conducted. It was shown that during cyanide conversion, a single atom of molecular oxygen was incorporated during the reaction and an intermediate X-OH is formed (Eq 1.7-a). This first step indicated that the enzyme is indeed a monoxygenase (143). A second atom of oxygen from water is then incorporated and the hydrolysis of the substrate into ammonia and carbon dioxide is completed (Eq 1.7-b).

$$HCN + O_2 + 2NADH + 2H^+ \rightarrow [X\text{-}OH] + H_2O + NAD^+ \quad \text{Eq 1.7-a}$$

$$[X\text{-}OH] + H_2O \rightarrow NH_3 + CO_2 \quad \text{Eq 1.7-b}$$

Studies on purified CNO showed that the enzyme is pterin-dependent (75), requires NADH and converts cyanide into formate and ammonia when the cyanide concentration in the medium was 10 to 50 μM (Eq 1.8-a) (41). Formate is further oxidized by formate dehydrogenase (FDH) into carbon dioxide (Eq 1.8-b).

$$HCN + O_2 + NADH + H^+ \rightarrow HNCO + H_2O + NAD^+$$

$$HNCO + NADH + H^+ \rightarrow HCONH_2 + NAD^+$$

$$HCONH_2 + H_2O \rightarrow HCO_2H + NH_3 \qquad \text{Eq 1.8-a}$$

$$HCO_2H + NAD^+ \rightarrow CO_2 + NADH + H^+ \qquad \text{Eq 1.8-b}$$

At higher cyanide concentration (1 mM), the major end product of the reaction is formamide (formamide/formate ratio, 0.6:0.3) which accumulates in the medium and it is not further degraded (41). As for the structure, CNO is proposed to consist of 4 different components; NADH oxidase, NADH peroxidase, cyanide dihydratase and carbonic anhydrase (42). CNO activity is detected only when all four components are combined and NADH and reduced pterin are added to the reaction mixture, the products formed are formate and ammonia. When FDH is present, formate is oxidized into CO_2 (42).

Hydrolysis pathway

Cyanide degradation through a hydrolytic pathway is catalyzed by two major enzymes types: cyanide hydratase and cyanide dihydratase. Cyanide hydratase (CHT) converts cyanide into formamide (Eq 1.9-a). It is found in fungi such as *Neurospora crassa, Gloeocercospora sorghi* and *Fusarium lateritium*. Cyanide dihydratase (CynD) also referred to as cyanidase, converts cyanide into ammonia and formate (Eq 1.9-b). It is found in some bacteria such as *Bacillus pumilus*, *Pseudomonas stutzeri* and *Alcaligenes xylosoxidans* subsp*. denitrificans*. The primary substrate for cyanide

hydratase and cyanide dihydratase is cyanide and the hydrolysis reaction does not require secondary substrates or cofactors making these two enzymes the best candidates for industrial remediation processes. Also, biosensors are being developed using these enzymes as analytical devices for rapid and accurate detection of cyanide (67). When cyanide is present it is degraded by cyanide dihydratase and the produced ammonia is then detected by an ammonia electrode.

These enzymes will be further discussed in the sections to follow.

$$HCN + H_2O \rightarrow CH_3NO \qquad \text{Eq 1.9-a}$$

$$HCN + 2H_2O \rightarrow NH_3 + HCOOH \qquad \text{Eq 1.9-b}$$

Substitution/transfer pathway

Two types of cyanide assimilation reactions exist in this pathway; substitution reactions and amino acid synthesis reactions. As mentioned earlier, in this pathway cyanide is not degraded but is assimilated into primary metabolism and used as a source for nitrogen and carbon for growth. Focused studies of cyanide assimilation have been done on *Chromobacterium violaceum* (which is also a cyanogenic bacterium), *Bacillus megaterium* and *Citrobacter freundii* (88, 110, 118). In fungi, only few species such as *Rhizopus oryzae* (106) and *Rhizoctonia solani* (94) demonstrated the ability for cyanide assimilation. On the other hand, all plants perform cyanide assimilation and do not appear to have degradation pathways. Enzymes involved in the assimilation of cyanide are present in cyanogenic organisms in order to prevent cyanide self poisoning (82, 118).

For example, in plants this pathway is a protective behavior from cyanide poisoning since cyanide is a co-product of the oxidation of 1-aminocyclopropane-1-carboxylic acid (ACC) in ethylene biosynthesis (154) and is released when cyanogenic glycosides and cyanolipids are catabolized (107, 111).

Amino acid synthesis reactions

These reactions are performed by the following enzymes: β-cyanoalanine synthase and γ-cyano-α-aminobutyric acid synthase.

β-cyanoalanine synthase (CAS) is a mitochondrial enzyme widely distributed in higher plants (56), insects (101) and some bacteria (37, 82)(21, 37). Even in non-cyanogenic plants, β-cyanoalanine synthase was detected but had lower activity than that found in cyanogenic species (90). This enzyme catalyzed the conversion of cyanide and cysteine to β-cyanoalanine and sulfide (Eq 1.10).

$$HCN + HSCH_2CHNH_2CO_2H \rightarrow NCCH_2CHNH_2CO_2H + H_2S \qquad \text{Eq 1.10}$$

Even though L-cysteine is the primary substrate, CAS also recognizes, less effectively, L-serine and L-cystine as substrates too (4, 82). β-cyanoalanine is then hydrolyzed into aspartic acid or asparagine through the action of β-cyanoalanine hydrolase (16, 21, 24) or asparaginase (78).

Ethylene biosynthesis induced by drought stress leads to an increase in cyanogenesis as cyanide is a co-product of this pathway (81). After 2 days of drought

stress, CAS activity in tobacco sharply increased in response to high levels of endogenous cyanide indicating a role of CAS in cyanide detoxification in plants under drought stress (81). Being predominately localized in the mitochondria, the role of CAS is likely to protect the cytochrome-c oxidase from cyanide. Activation of CAS renders some grass weeds and plants resistant to auxin herbicides such as quinclorac (1). This herbicide promotes grass weed death by activating the ACC synthase and inducing ACC production (49). ACC (1-aminocyclopropane-1-carboxylic acid) is converted to ethylene and cyanide by ACC oxidase. The excess of accumulated cyanide generated from this reaction is believed to cause the phytotoxic effects leading to cell death. Quinclorac-resistant grass weeds showed a 4 fold increase in CAS activity compared to sensitive grass weeds.

When cyanide was added to a *Chromobacterium violaceum* culture, γ-cyano-α-aminobutyric acid was formed in addition to β-cyanoalanine (22). The enzyme catalyzing the synthesis of this product was characterized as γ-cyano-α-aminobutyric acid synthase (114). This enzyme requires a co-factor, pyridoxal phosphate and converts cyanide and homocystine into thiocyanate, homocysteine and γ-cyano-α-aminobutyric acid (114) (Eq1.11-c). This reaction occurs in two steps. In the first nonenzymatic step, homocystine and cyanide react to form homocysteine and γ- thiocyano-α-aminobutyric acid (Eq 1.11-a). The second step is catalyzed by γ-cyano-α-aminobutyric acid synthase where γ- thiocyano-α-aminobutyric acid and cyanide are converted to thiocyanate and γ-cyano-α-aminobutyric acid (Eq 1.11-b).

$COOH(NH_2)CH(CH_2)_2.S\text{-}S\text{-}(CH_2)_2CH(NH_2)COOH + HCN \rightarrow$

$COOH(NH_2)CH(CH_2)_2SH + CNS\text{-}(CH_2)_2CH(NH_2)COOH$ Eq 1.11-a

$CNS\text{-}(CH_2)_2CH(NH_2)COOH + HCN \rightarrow CNSH + CNS\text{-}(CH_2)_2CH(NH_2)COOH$ Eq 1.11-b

$COOH(NH_2)CH(CH_2)_2.S\text{-}S\text{-}(CH_2)_2CH(NH_2)COOH + 2HCN \rightarrow CNSH +$

$COOH(NH_2)CH(CH_2)_2SH + CN\text{-}(CH_2)_2CH(NH_2)COOH$ Eq 1.11-c

Substitution reactions

Another enzyme involved in this pathway is a sulfur transferase. In 1933, K. Lang discovered rhodanese, which catalyzes the reaction between cyanide and thiosulfate to produce thiocyanate and sulfite (Eq 1.12).

$S_2O_3^{2-} + CN^- \rightarrow SO_3^{2-} + SCN^-$ Eq 1.12

Rhodanese, also known as thiosulfate:cyanide sulfurtransferase, is found in animals with high levels primarily in the mitochondrial fraction of the liver and kidneys. It also occurs in plants like the leaf of the cassava plant *Manihot utilissima* and microorganisms such as *Bacillus subtilis* and *Pseudomonas aeruginosa*. This mitochondrial enzyme is the key enzyme used by our bodies for detoxification of cyanide. It is suggested that a low-protein diet is responsible for the chronic disease linked to consumption of cyanogenic foods such as cassava. With a constant intake of non-lethal dose of cyanogens, the body increases the synthesis of rhodanese and the

demand for sulfur containing amino acids. Chronic consumption of cyanogenic food should be combined with a rich protein diet to avoid cyanide linked diseases such as konzo, a permanent paraparesis (Cassava is not a good source of protein). Rhodanese deficiency is also linked to the Leber's hereditary optic neuropathy, a rare mitochondrially inherited loss of vision (109).

3-mercaptopyruvate sulfurtransferase is also a member of the transferases family. The enzyme has two substrates, 3-mercaptopyruvate and cyanide and catalyses their conversion to pyruvate and thiocyanate (Eq 1.13).

$$COOHCOCH_2SH + CN^- \rightarrow CH_3COCOOH + SCN^- \qquad \text{Eq 1.13}$$

The crystal structure of 3-mercaptopyruvate sulfurtransferase from *Leishmania major* showed that the enzyme forms a persulfurated cysteine in its active site. The enzyme then interacts with cyanide to form thiocyanate. This enzyme is involved in cysteine metabolism via the mercaptopyruvate pathway. Cysteine is metabolized to form mercaptopyruvate by cysteine transaminase. 3-Mercaptopyruvate is then converted to pyruvate by 3-mercaptopyruvate sulfurtransferase. This enzyme is widely distributed in prokaryotes and eukaryotes and is evolutionary related to rhodanese. In mammalian cells, the enzyme is present in the mitochondria as well as in the cytoplasm.

In the past, efforts were employed in finding a cyanide-antidote administered to mass-exposed cyanide victims. Such an antidote is advantageous in the case of chemical disaster or terrorist attack. As mentioned earlier, current thiosulfate antidotes rely on

rhodanese which is concentrated in the mitochondria of the liver and kidneys but not in the other major organs such as the heart and the central nervous system. 3-mercaptopyruvate sulfurtransferase seems to be a better candidate for cyanide detoxification. Sulfanegen sodium, a novel prodrug of 3-mercaptopyruvate, alleviated cyanide toxicity when tested in animals (14, 19). 3-Mercaptopyruvate, the natural substrate of 3-mercaptopyruvate sulfurtransferase cannot be used as a drug due to its instability when administered intravenously (27).

NITRILASE SUPERFAMILY

In 2001, Brenner described the nitrilase enzyme superfamily (104). Nitrilases are found in both eukaryotes and prokaryotes. Enzymes in this superfamily catalyze the hydrolysis of nonpeptide carbon-nitrogen bonds. All the members of the superfamily share similar architecture with homodimeric αββα building blocks and a catalytic tetrad formed by four positionally conserved amino acids: cysteine, glutamate, glutamate and lysine. Seven branches of the superfamily include proteins in which the nitrilase-related domain is fused to some other conserved domain. Three of these branches have all their members fused to the additional conserved domain whereas only some members of the other four branches include such fusion. This domain fusion generally predicts specific biological functions or cellular localization for these enzymes (83). An example of Rosetta-stone protein is *C. elegans* protein VF11C1L.1 which harbors two domains found in two separate proteins in *Saccharomyces cerevisiae*. The first domain is from CCT3 protein and is involved in microtubule and actin assembly. The second domain is

from MSS4 protein which is involved in the organization of the actin cytoskeleton. The fusion of these two domains predicts that CCT3 and MSS4 cooperate in the cytoskeleton assembly and organization (40). Another example of domains predicted to interact are the *E. coli* gyrase A and gyrase B found fused in the yeast topoisomerase II and shown to interact from experiments (133).

The nitrilase superfamily is classified in 13 branches on the basis of sequence analysis. The first branch, nitrilase, consists of enzymes that hydrolyze nitriles whereas the other branches are amidases, carbamylases and N-acyl transferases. Branch 2 comprises the aliphatic amidases, which catalyze the hydrolysis of aliphatic amides such as the carboxamide side chain of glutamine and asparagine. An aliphatic amidase from *Pseudomonas aeruginosa* hydrolyzes acetamide (66). This bacterium is able to grow on acetamide as a sole carbon and nitrogen source. Branch 3 contains amino-terminal amidases. NTA1 amidase from *Saccharomyces cerevisiae* is a member of this branch (7). It regulates the degradation of proteins bearing N-terminal asparagine or glutamine by deaminating these residues. Biotinidase, which is in the fourth branch of the superfamily, is an amidases that catalyzes the hydrolysis of biotin from biocytin and biotinyl-peptides (59). Branches 5 and 6 consist of enzymes performing carbamoylase reaction such as β-ureidopropionases and carbamylases respectively. Branches 7 and 8 consist of prokaryotic and eukaryotic glutamine-dependent NAD synthetases respectively. NAD synthetases containing GAT (glutamine amidotransferase) domain use glutamine as an ammonia source, which is the case for all eukaryotic NAD synthetases but only few prokaryotic NAD synthetases (155). The N-acyltransferases in

branch 9 have a proposed function in post-translational modification. For example, *Escherichia coli* apolipoprotein N-acyltransferase (Lnt) transfers an acyl group to lipoproteins during lipoprotein synthesis (51). Branch 10 includes the Nit protein, which is fused to a tumor suppressor protein Fhit in invertebrates. Fhit and Nit proteins show coordinated levels of mRNA expression and tissue co-localization in mice (108). Based on these observations, Nit is assumed to have the same function of Fhit, a tumor suppressor, or be involved in the same pathway. Branch 11 is defined by an enzyme from *Pseudomonas aeruginosa PAO1*, AguB (97). This enzyme is a carbamylase involved in the metabolism of arginine into spermidine and succinate. Enzymes in branch 12 are thought to have a role in post-translational modifications since they are fused to N-terminal acetyltransferases. Lastly, enzymes in branch 13 are still not well defined.

Nitrilases

Nitrilases constitute the first branch in the nitrilase superfamily (104). They are found in both prokaryotes and eukaryotes. In 1964, Thimann and Mahadevan first described a nitrilase (134) that converts indole 3-acetonitrile to indole 3-acetic acid. Nitrilases convert their substrates (nitriles) to the corresponding carboxylic acids and ammonia, and occasionally to amides. Nitrile hydrolysis is considered as the best method for carboxylic acids production. However, the chemical hydrolysis of nitriles requires harsh reaction conditions such as high temperature, strong acids (example hydrochloric or phosphoric acid) or strong bases (example potassium or sodium

hydroxide). The neutralization of the medium at the end of the reaction generates large quantities of inorganic waste.

Nitriles are broadly used in chemical industries. For example adiponitrile is a precursor of nylon and acrylonitrile is a precursor of acrylic fibers and plastics. Several herbicides used in agriculture are nitriles, including the herbicides Casoron, Bentrol and Buctril. Hydrogen cyanide is the simplest nitrile and it is extensively used in industry. All of these nitriles are harmful to the environment if they are not disposed of properly. Nitrilases have gained great importance in industrial application as green catalysts for easily and efficiently generating several carboxylic acid derivatives and as important agents in bioremediation of nitrile contaminated wastewaters (129).

Enzymes in the nitrilase branch are classified into three major categories according to their substrate specificity: 1) aromatic nitrilases, which act on aromatic nitriles such as benzonitrile, 2) aliphatic nitrilases, which act on aliphatic nitriles such as acrylonitrile and 3) arylacetonitrilases, which act on arylacetonitriles such as phenylacetonitrile.

Cyanide hydratase and cyanide dihydratase are aliphatic members of the nitrilase branch. They both recognize cyanide as a substrate but the hydrolysis reaction end product differs. Cyanide dihydratase (CynD), also known as cyanidases, is of bacterial origin and degrades cyanide into ammonia and formate. On the other hand, cyanide hydratase (CHT) is of fungal origin and converts cyanide into formamide.

In 1988, a cyanide dihydratase from a *Pseudomonas sp* able to degrade cyanide to formate and ammonia was isolated from wastewaters of a coke plant (149). Other

organisms with cyanide degrading activity such as *Alcaligenes xylosoxidans* subsp. *denitrificans*, were also isolated by enrichment cultures from soil and water in medium containing cyanide (60). *Bacillus pumilus* C1, isolated from a cyanide wastewater dam, was found to express a cyanide dihydratase converting cyanide to formate and ammonia (86). *Pseudomonas stutzeri* strain AK61 was isolated from metal-plating plant wastewaters on the basis of its cyanide degrading activity (146).

Cyanide hydratases were isolated from both plant pathogenic and non-pathogenic fungi such as the phytopathogens *Gloeocercospora sorghi* (145) and *Fusarium solani* (36). These enzymes have been shown to degrade metal cyanide in addition to HCN or cyanide salts.

In fungi, the expression of cyanide hydratase is induced by the presence of cyanide in the growth media. This indicates a role of the enzyme in detoxification. In bacteria, the nitrilase is not known to have any biological role nor is it cyanide regulated. The expression of nitrilase gene in *Bacillus pumilus* C1 is not regulated by the presence of cyanide in the medium; instead it was found to be regulated by the SpoOA regulator of the sporulation pathway (87). Mutants of the transcription factor SpoOA do not express the enzyme. However the *cynD* can be induced by addition of Mn^{2+} (87). On the other hand, *Bacillus subtilis ZJB-063* constitutively expresses its nitrilase (156). Both nitrilases, cyanide dihydratase and cyanide hydratase, do not require any cofactors or secondary substrates for the hydrolysis of cyanide, making them ideal candidates for cyanide bioremediation.

Nitrilase structure

Cyanide nitrilases from *Bacillus pumilus* and *Pseudomonas stutzeri* are similar with 76% identity in their amino acid sequences. They share a similar monomer structure and have a αββα building block as seen with other nitrilases. For example, the monomer from N-carbamyl-d-amino acid amidohydrolase (Dcase), which catalyzes the hydrolysis of N-carbamyl-D-amino acids to the corresponding D-amino acids, has β sheets flanked by two α helices, α1 and α3 from one side and α5 and α6 from the other side (98). The size of the monomer varies between 35 and 42 KDa.

Also, oligomerization of the monomers is thought to be important for the activity of these enzymes, but the sizes of the oligomers vary between the members of the family. An example is the nitrilase from *Rhodococcus rhodochrous* J1, which converts acrylonitrile and 3-cyanopyridine to acrylic acid and nicotinic acid respectively. The enzyme is primarily found as inactive dimers but when it is incubated with benzonitrile, it forms an active decamer (96). This oligomerization requires the deletion of 39 amino acids by processing from the C-terminal of the protein (136). Other nitrilases do not require this processing.

The crystal structure of several members of the superfamily has been solved, such as *N*-carbamyl-d-amino acid amidohydrolase (Dcase)(98) from *Agrobacterium* sp. strain KNK712 (98) and the Nit domain of NitFhit fusion protein (105). Based on sequence homology with known nitrilase crystal structures and using negative stain electron microscopy, the structure of cyanide dihydratase from *Bacillus pumilus* ($CynD_{pum}$) and *Pseudomonas stutzeri* ($CynD_{stut}$) was modeled (62)(125). $CynD_{stut}$ is a 38

KDa monomer and forms a 14-subunit spiral with 2-fold symmetry while CynD$_{pum}$ is a 37 KDa subunit. At pH 8, its optimal pH, CynD$_{pum}$ forms an 18-subunit spiral with 2-fold symmetry. But at pH5.4, the enzyme's subunits associate to form extended rods.

Several surfaces were described in the structure of the enzymes (126). Surface A is defined as the dimer interface and involves 2 helices and residues in the C-terminus (case of CynD$_{stut}$ and CynD$_{pum}$) (FIG.1.1). Interactions at the C surface are essential for the formation of the spiral structure. In CynD$_{stut}$ and CynD$_{pum}$, it is thought that this spiral structure is made possible by two insertions of 12 and 14 amino acids and an extension of 35 amino acids at the C-terminus since the non-spiral nitrilases do not have these insertions. Mutations in the C surface abolish the activity of cyanide dihydratases. The interactions at this surface are mainly hydrophobic. The D surface is defined as the interactions across the groove when the spiral completes one turn (FIG.1.2). Mutations in this D surface did not alter the activity of CynD$_{pum}$ (126). Another interaction across the groove is responsible for terminating the spiral. This surface is called surface E (FIG.1.2).

The C-terminus of CynD$_{pum}$ and CynD$_{stut}$ is composed of a 28 and 33 amino acid extension respectively compared to the Nit sequence. Deletion of this region had different effects for each of the enzymes. CynD$_{pum}$ seems to tolerate deletion in its tail, losing activity only after removal of more than 28 residues. That is not the case of CynD$_{stut}$ where amino acid deletions in the protein's C-terminal render it inactive.

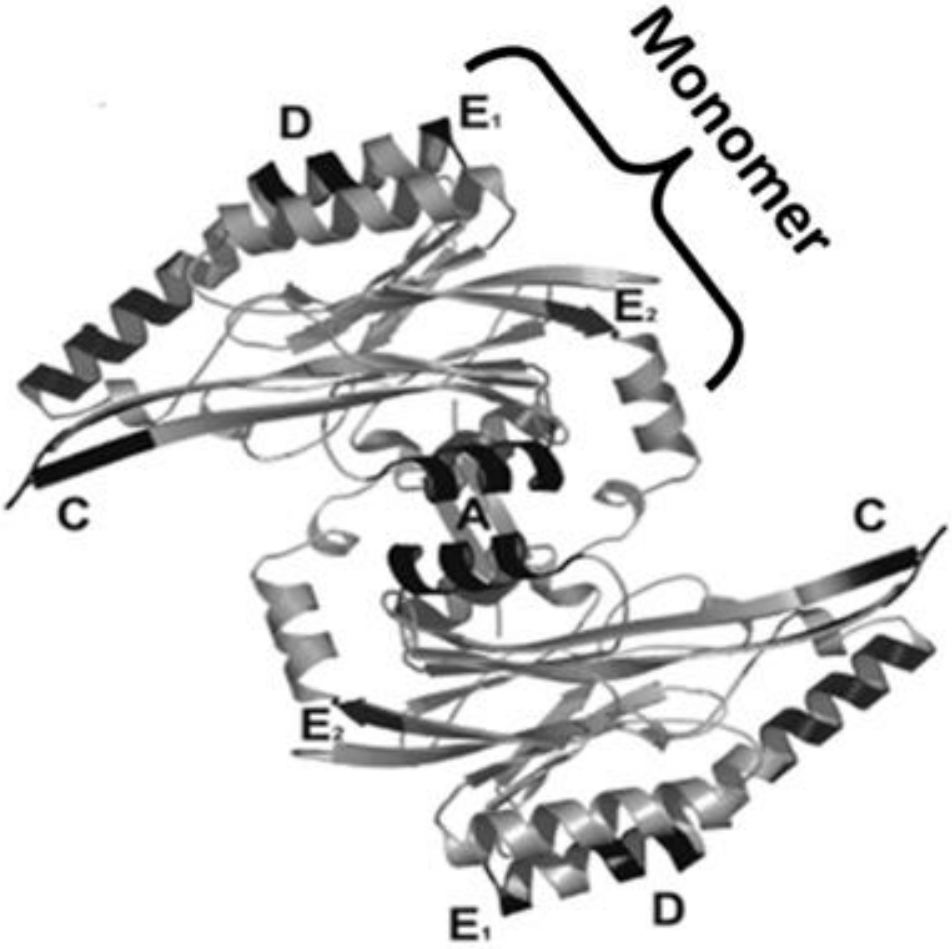

FIG.1.1. Dimer model of cyanide dihydratase from *Pseudomonas stutzeri* AK61. The structure of the monomer of $CynD_{stut}$ is also indicated. The ribbon diagram shows the predicted surfaces A, C, D and E highlighted in black. Surface B is formed by β-sheets situated between A and D surfaces and holds the active site (42).

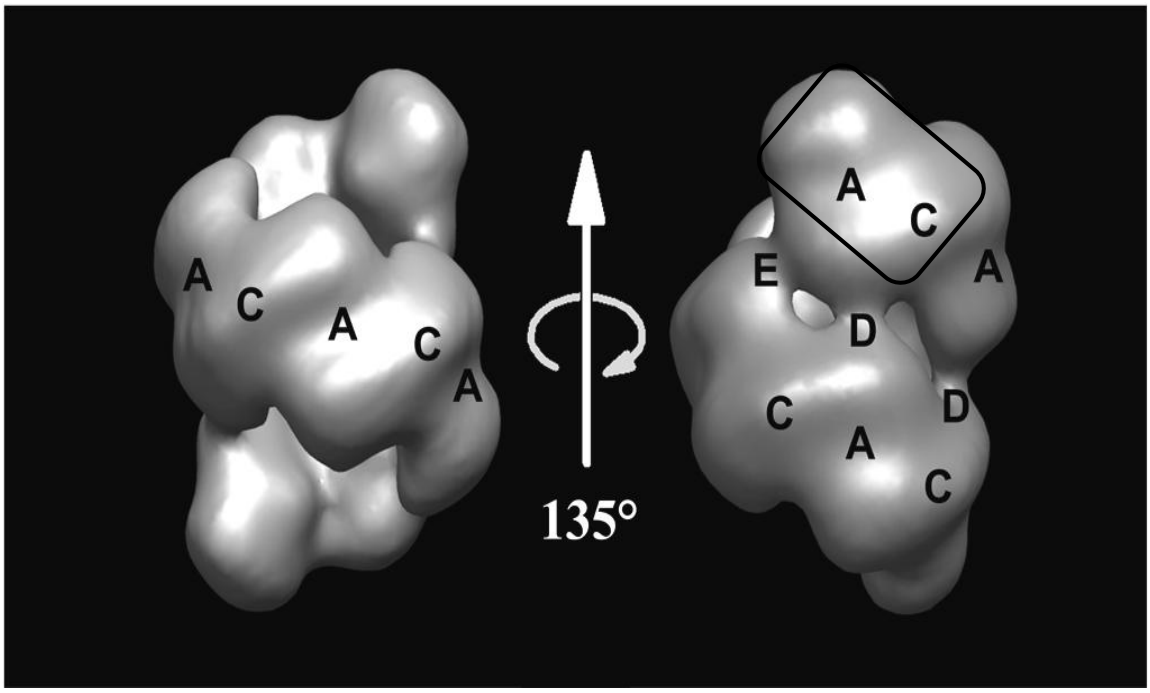

FIG.1.2. Oligomeric structure of $CynD_{stut}$. The enzyme forms a 14-subunit oligomer. One dimer is shown outlined in a box. The interaction at the A, C, D and E surfaces can be seen between the dimers forming the spiral. C surface interaction is seen between the dimers to elongate the oligomer. D surface occurs when one turn of the spiral completes one turn. E surface terminates the spiral (126).

The nitrilase reaction mechanism is not well established. However, mutational and structural studies yielded information on the enzyme's active site and reaction mechanism. The catalytic site is formed by cysteine, glutamate, glutamate and lysine. These residues are conserved in the nitrilase superfamily. Mutating cysteine at position 163 to a serine abolished the activity of $CynD_{stut}$ (147). Other nitrilases, in which this

cysteine was replaced with other amino acids also lost their catalytic activity. Substrate-bound crystal structure of *N*-carbamoyl-d-amino acid amidohydrolase (Dcase) from *Agrobacterium radiobacter* clearly shows that the CEK catalytic triad formed of Glu47, Lys127, and C172S interacts with the carbamoyl group of the substrate. The crystal structure of an inactive mutant C166S of *Helicobacter pylori* AmiF formamidase showed a substrate binding pocket formed of Cys166, Glu60 and Lys133 (58). Another conserved glutamate at position 141 was shown to bind the formamide substrate. This Glu141 superimposed with Glu146 of *N*-carbamoyl D-amino acid amidohydrolase. It is suggested that this residue is crucial for the stability of the CEK triad as well as facilitating the docking of the substrate (58). Thus, although the early literature suggests a catalytic triad, this essential glutamate makes it more accurate to describe the active site as a catalytic tetrad.

A comparative study of three recombinant cyanide degrading enzymes, $CynD_{stut}$, $CynD_{pum}$ and CHT_{sorghi} showed that all three enzymes had maximal activity in the range of pH 7-8 (63). The activity of both CynD decreased quickly as the pH rose above 7.8 or dropped below 7.0.

As for the kinetic analysis, both $CynD_{pum}$ and $CynD_{stut}$ had similar K_m and V_{max}, 7.3 mM and 0.097 mmol min^{-1} mg^{-1}, 5.9 mM and 0.1 mmol min^{-1} mg^{-1}, respectively. However, CHT_{sorghi} had K_m and V_{max} significantly higher than that of CynDs, 90 mM and 4.4 mmol min^{-1} mg^{-1} (63).

DIRECTED EVOLUTION AND ERROR-PRONE PCR

The application of enzymes in industrial products and processes has impacted our modern life. Taking advantage of the catalytic properties of enzymes allows for the replacement of high temperatures and harsh pH needed for chemical reactions while ameliorating the purity and specificity of the chemical reactions. Industrial enzymes are true green catalysts; they reduce the cost of the process and the environmental impact. It is estimated that the global biotechnology industry revenue will reach $228.6 billion in 2012.

Advancement in these industries is related to the improvement of the enzyme properties. Directed evolution and rational redesign are two strategies in protein engineering aiming to develop enzymes suitable for the desired applications.

Rational redesign requires a working knowledge of the protein's structure. Based on the structure and the predicted interactions within the protein, specific amino acids are chosen for substitution. This strategy was shown successful in engineering a faster superoxide dismutase (46). On the other hand, directed evolution does not require information about the protein structure since it relies on random mutagenesis methods such as error-prone PCR to create a mutant library (119). Mutants with improved properties are then identified using a selection or a high throughput screening.

Several techniques can be used to randomly mutagenize a gene. *In vivo* mutagenesis can be achieved using bacterial strains mutant in various DNA repair pathways (48). Also, chemical mutagens can be used *in vivo* and *in vitro* to increase the frequency of mutations (128). Error-prone PCR is an *in vitro* mutagenesis technique that

uses Taq DNA polymerase to amplify a gene and introduce random mutations. This polymerase has a low fidelity of DNA synthesis since it lacks 3' → 5' proofreading activity (137). Modifications of the PCR reaction conditions further lower the Taq polymerase fidelity; Mn^{2+} can be added, Mg^{2+} concentrations can be increased and unequal dNTP concentrations can be used in the reaction mixture (23). $MnCl_2$ is mutagenic for several DNA polymerases (39) and $MgCl_2$ increases the error rate by stabilizing noncomplementary pairs (38). Also the mutation rate is affected by the concentration of the DNA template and the number of PCR cycles.

SUMMARY AND PURPOSE

Cyanide, the simplest nitrile, is a powerful poison. Exposure to small amounts of it is lethal. Due to its high affinity to metals, cyanide is widely used in industry especially mining industries. Detoxifying the wastewaters from these industries is a major concern. Cyanide needs to be removed before wastewaters can be disposed in the environment. Several spills have occurred around the word in Europe, the United States and Africa. These spills are environmentally disastrous since the cyanide contaminated waters endanger human lives as well as ecosystems.

Several methods can be applied to treat cyanide. Most rely on chemical reactions for detoxification. These methods are expensive and sometimes produce other toxic pollutants. On the other hand, several organisms are known to produce and degrade cyanide. This triggered the investigation into using these organisms for bioremediation of cyanide waste. Several enzymes with the ability of degrading cyanide into less toxic

products have been characterized. For the majority of these enzymes, the specificity for cyanide is low and in some case additional substrate or cofactors are required for the reaction to take place. However, cyanide degrading nitrilases from the nitrilase superfamily, which do not require co-factors or secondary substrates, are possible candidates for industrial use in the cyanide detoxification.

The goal of this thesis work was to understand the structure and function of cyanide hydratases and cyanide dihydratases in order to engineer enzymes with improved stability, catalytic activity and specificity. To accomplish this goal, I rely on directed evolution and screening for mutants with improved characteristics since a protein crystal structure is still elusive. Mutants with new catalytic properties are often helpful to understand the role of specific residues in an enzyme. In the second chapter of this dissertation, I describe a simple and efficient method utilizing *in vivo* recombination to create recombinant libraries incorporating the products of PCR amplification. This *in vivo* cloning method will be useful for generating large pools of randomly mutagenized clones after error-prone PCR of cyanide dihydratase of *B. pumilus* C1. In the third chapter, I describe the isolation and characterization of 3 $CynD_{pum}$ variants with higher catalytic activity *in vivo*. I characterize the mutations and their location in the enzyme and I compare the kinetics, stability and pH profile of the purified proteins. These results lead me to investigate the role of the C-terminus of cyanide dihydratase of *B. pumilus* C1 and *P. stutzeri*. In the last chapters, I show the effects of C-terminal deletions and swapping in cyanide dihydratase of *B. pumilus* C1 and *P. stutzeri* and cyanide hydratase of *N. crassa* and their effects on the activity and stability of the enzymes. I describe a

hybrid CynD mutant, a *B. pumilus* and *P. stutzeri* hybrid that is several fold more stable than wild type enzymes. This hybrid is 100% active at pH 9, a pH where the wild-type enzyme is inactive.

CHAPTER II

RAPID GENERATION OF RANDOM MUTANT LIBRARIES*

OVERVIEW

Directed evolution is often used in protein engineering to improve the properties of several enzymes (119, 130). However, its success hinges on the ability to generate libraries of significant size and diversity. A variety of methods for mutagenesis and subsequent library construction have been previously described along with appropriate methods for screening or selection. Herein, we will describe a simple and streamlined approach to rapidly generate diverse randomly mutagenized libraries.

Error-prone PCR (EP-PCR) is a method of choice to generate random mutation throughout a gene or gene region without being limited by a size constraint (within the limits of conventional PCR). It relies on the use of *Taq* or similar DNA polymerase lacking proofreading activity so that mismatched bases are not removed (137). To further increase this mutation rate the addition of Mn^{2+} ions and/or changes in the Mg^{2+} ion concentration along with unbalancing the available nucleotide pool have all been shown effective (13, 23, 39). Amplification of the gene under these conditions leads to a population of molecules carrying random point mutations. The degree of mutagenesis can be controlled by varying those conditions or adjusting the number of amplification cycles allowing an easily manipulable choice of mutation rate.

---

* Reprinted with permission from "Rapid Generation of Random Mutant Libraries" by Mary Abou-Nader and Michael J. Benedik, 2010. *Bioengineered Bugs*, 1:5, 337-340, Copyright [2010] by Landes Biosciences

The rate limiting step is often cloning the DNA products generated from EP-PCR into a vector that will allow appropriate expression for screening. Screening a large population of mutants increases the likelihood of finding the one with the desired properties. However, the ease of construction and the size of the library depend on the methods employed. Most common is the use of restriction digestion and ligation with T4 DNA ligase, either using internal sites from the gene or by the use of primers with internal restriction sites (122), with subsequent ligation to an appropriately prepared vector. Alternately TA and TOPO cloning utilize a vector with a 5'-T overhangs that compliment the 3'-A overhangs generated by the *Taq* polymerase nontemplate-dependent terminal transferase activity (25).

Other non-ligase dependent approaches to build libraries involve *in vitro* site specific recombination. The Invitrogen Gateway system of recombinational cloning uses primers flanked by λ*attB* sites (55) incubated *in vitro* with a vector containing the target *attB* recombination site in the presence of bacteriophage λ integrase. Elledge *et al* (80) have proposed a different but elegant *in vivo* method to transfer a DNA fragments between vectors.

Transformation of *E. coli* with linear DNA is problematic due to its degradation by the RecBCD nuclease complex (131). The use of *recBCD* mutants has been exploited for allelic replacement in *E. coli* (121, 150) although these mutants are dramatically reduced in their overall rate of recombination. However the use of recombinational genes from bacteriophage λ has proven even more effective. Upon infection of *E. coli,* the phage expresses Gam (γ), a protein that specifically inhibits RecBCD and allows the

survival of rolling circle replicative DNA (138). Supplementing this with the Red α and β subunits a functional recombinase system is reconstituted that works effectively with linear DNA. This system has been exploited both for allelic replacement (95) and for *in vivo* cloning (103). The latter uses linearized vector to co-transform *E. coli* along with DNA fragments sharing flanking homology; the fragments can be generated either by a restriction digest or amplified by PCR. By using *E. coli* cells that transiently express the Red recombinase and Gam genes allows recombination to generate plasmids carrying the co-transformed insert.

Our work extends that method to the generation of highly complex libraries after EP-PCR. We have optimized *in vivo* recombinational cloning and to further reduce background have developed a "universal" positive selection vector carrying the F plasmid toxin gene *ccdB* that is replaced after recombination, which can readily be used for any gene cloned in any of the myriad blue/white screening vectors in use.

MATERIALS AND METHODS

DNA fragment preparation

The plasmid template used for PCR was pMB3504, derived from pBluescript II KS+ (Stratagene) containing the $cynD_{pum}$ gene encoding cyanide dihydratase from *Bacillus pumilus* (62) as a 1KB insert cloned with XbaI and XhoI.

PCR reactions were performed as 50 microliters reactions containing 25 microliters of Taq 2X Master Mix (New England Biolabs). The standard reactions from contained plasmid DNA concentration as listed and 100ng of each PCR primer with the

following reaction conditions for 30 cycles of 95^{o}C for 30 seconds, 55^{o}C for 1 minute and 72^{o}C for 1 minute. The PCR primers used were the M13 universal sequencing primers that can be used with most blue/white screening plasmids. Three different pairs of primers were the M13 universal sequencing primers -20 primer pair, the -60 primer pair and the -200 primer pair that can be used with most blue/white screening plasmids and are listed in TABLE 2.1.

TABLE 2.1 List of primers used in this work.

Primer	Sequence
-20M13F	(5'-CGCCA GGGTT TTCCC AGTCA CGAC
-20M13R	5'-GAGCG GATAA CAATT TCACA CAGGA
-60M13F	5'-GCGAA AGGGG GATGT GCTGC AAGG
-60M13R	5'-CACTT TATGC TTCCG GCTCG TATG
-200M13F	5'-CCATT CGCCA TTCAG GCTGC GCAAC
-200M13R	5'- CCCAA TACGC AAACC GCCTC TCCC

The PCR products were ethanol precipitated, resuspended in water and stored at -20^{o}C. The DNA concentration was determined by measuring the A_{260} using a Nanodrop spectrophotometer.

Vector preparation

The recipient plasmid used in this work was the chloramphenicol resistant pBC SK+ from Stratagene. The DNA was digested using EcoRI and BamHI enzymes at 37^{o}C for 2 hours. Dephosphorylation as indicated was done using Antarctic Shrimp Phosphatase followed by heat inactivation and ethanol precipitation. The DNA was resuspended in water and stored at -20^{o}C and the DNA concentration was measured at A_{260}.

Positive selection vector

The *ccdB* gene was amplified from F-carrying *E. coli* DNA using ccdB-F (5'-CAGAC TGCAG GAAGG GATGG CTGA) and ccdB-R (5'-CACTG CCGGT ACCAT GACTG CAGA) which introduced PstI sites at each end and thereby cloned into pBC SK+. The resultant plasmid pMB4105 was transformed into the F' strain MB1547 [*supE thi-1 Δ endA Δ(lac-proAB) Δ(mcrB-hsdSM)5 /* F' [*traD36 proAB*$^{+}$ *lacI*^{q} *lacZΔM15*]. For use in *in vivo* cloning, the vector was digested with EcoRI and BamHI, ethanol precipitated, resuspended in water and stored at -20^{o}C.

Transformation

The recipient strain MB4091 [DH10B (pKD46)] was used for *in vivo* recombination. The pKD46 plasmid (30) carries the λ *red* and *gam* genes expressed from the arabinose inducible *pBAD* promoter, confers resistance to ampicillin and is temperature sensitive for replication to allow plasmid loss after transformation (30). The

cells were grown in LB broth supplemented with 100 mg/L ampicillin at 30°C. Electroporation competent cells were made from cells grown in LB broth at 30°C to an O.D. (600 nm) = 0.3 with 0.1% arabinose added for specified times.

Electroporation was carried out using a Bio-Rad Micropulser and cells were allowed to recover in a 1ml volume on a shaker at 37°C for 1 hour unless otherwise stated. Aliquots of 0.1 ml were spread on plates with chloramphenicol (25 mg/L) and Xgal (40 mg/L) and incubated at 37°C. The number of transformants per ml are reported and the recombination rate was calculated by dividing the number of white colonies by the number of total colonies on the plate. Experiments were all performed in triplicate.

RESULTS

Preliminary experiments confirmed published results (95) that *in vivo* recombination using the λRed system was effective at creating recombinant clones. Vector DNA linearized by restriction digestion could be co-transformed with insert DNA containing terminal homology and recombinants generated with reasonable efficiency. Here we report experiments designed to investigate and optimize the parameters for this approach.

Effect of length of homology

One parameter likely to affect the efficiency with which recombinants are obtained is the length of the homology region. As a means of varying the homology region to test this, PCR products were generated using different primer pairs that yield

different lengths of homologous regions. The donor and recipient plasmid both carry the *lacOP-lacZα* region commonly found in blue/white screening vectors allowing us to utilize "universal" sequencing primers of varying distance from the polylinker, but within the *lac* region. MB4091 cells were co-transformed with linearized pBC plasmid as the recipient and DNA fragments generated by PCR from pMB3504, a pBluescript II (KS+) clone carrying the *cynD* gene of *B. pumilus*. Three different primer pairs were used to generate the PCR products: the -20M13 primer pair generates a fragment with 81 and 89 bp of homology, the -60M13 primer pair generates a fragment with 121 and 127 bp of homology, and the -200M13 primer pair generates a fragment with 194 and 269 bp of homology from each end of the 1kb insert respectively.

The percent recombinants were determined from the numbers of blue (nonrecombinant) and white (recombinant) colonies. All white colonies tested were shown to be true recombinants both by plasmid digestion profiling of about 20 colonies, as well as by measuring the ability to express CynD activity from about 95 colonies.

TABLE 2.2 Effect of length of homology region on recombination rate.

PCR primers	Vector (pmole)	PCR fragment (pmole)	30°C			37°C		
			Blue colonies	White colonies	Recombination rate	Blue colonies	White colonies	Recombination rate
	0.25	0				$4x10^4$	0	
	0	1				0	0	
-20M13	0.25	1	$1.3x10^4$	$2.2x10^3$	14 ±3%	$1.7x10^4$	$5.4x10^3$	24 ±2%
-60M13	0.25	1	$8.8x10^3$	$1.6x10^4$	64 ±6%	$1.6x10^4$	$3.4x10^4$	68±2%
-200M13	0.25	1	$1.5x10^4$	$4x10^4$	73±4%	$2x10^4$	$6.5x10^4$	76±4%

PCR fragments were generated using three primer pairs that confer different lengths of homology with the recipient plasmid. After transformation, the cells were left to recover at 30°C or 37°C. The recombination rate reflects the number of white colonies divided by the total number of colonies. Values are the average of 3 experiments.

As shown in TABLE 2.2, efficiency of recombination improved by nearly 3-fold when the length of homology between the plasmid and the PCR fragment increased from 81 bp to 121 bp. There was a small further increase with the -200 primer pairs. In both cases there was a concomitant increase both in the number of white colonies as well their percent of the total. The number of blue colonies, which represent non-recombinant plasmids, remained relatively similar. The presence or absence of the *red* genes post-transformation did not affect the recombination rate significantly as shown by similar values when transformants were recovered at the permissive (30^{o}C) or non-permissive (37^{o}C) temperatures for the pKD46 replication.

Vector preparation

To analyze what vector treatment was best for efficient recombination, therefore the recombination rate was determined using undigested plasmid, digested plasmid, and digested and dephosphorylated plasmid. The latter would be expected to decrease potential plasmid self-religation and possibly increase the opportunity for recombination with the PCR fragments.

Vector DNA prepared by each treatment was co-transformed into MB4091 with PCR fragments generated using -60M13 primer pairs. In a comparison of digested vector with digested and dephosphorylated vector the number of blue colonies decreased by about two-fold after dephosphorylation while the number of white colonies increased slightly, resulting in a higher recombination rate (TABLE 2.3). Dephosphorylation of the cloning vector decreased the background but had no significant affect on the recovery of

recombinants. On the other hand, the use of uncut vector yielded a very high rate of transformation with non-recombinant plasmid as might be expected and recombinants were not detected, likely masked by the high background.

TABLE 2.3 Effect of vector treatment.

Vector treatment	Blue colonies	White colonies	Recombination rate
Phosphorylated vector	$3.3x10^4$	$2.7x10^4$	45±2%
Dephosphorylated vector	$1.6x10^4$	$3.4x10^4$	68±2%
Uncut vector	$>1x10^5$	0	0

0.25 pmole of linear phosphorylated and dephosphorylated plasmid or 0.125 pmole of double stranded linearized plasmid were co-transformed into MB4091 cells with PCR products generated using -60M13 primers. The recombination rate reflects the number of white colonies divided by the total number of colonies. Values are the average of 3 experiments.

Effect of induction time

The expression of λRed recombinase carried by pKD46 is regulated by the arabinose inducible *pBAD* promoter. An analysis of optimal induction time by arabinose is shown in TABLE 2.4. The highest recombination rate and the highest yield of recombinants were observed when cells were induced for 30 to 60 minutes with 1% arabinose. The lack of recombinants without induction shows that Red expression was necessary.

TABLE 2.4 Effect of induction time.

Induction time (minutes)	Blue colonies	White colonies	Recombination rate
0	$2.4x10^4$	$1.8x10^2$	0.7±1%
30	$1.3x10^4$	$6.1x10^4$	82±3%
60	$1.1x10^4$	$5x10^4$	82±2%
90	$2.6x10^4$	$4.8x10^4$	65±2%

Cells were induced with 1% arabinose for the times listed before making competent. The cells were harvested at similar OD600 of around 0.3 and were similarly competent. 1 pmole of PCR fragment amplified using the primer pairs -60M13 and 0.25 pmole of digested vector were used in all the transformations. Values are the average of 3 experiments.

Ratio of fragment to vector

In TABLE 2.5 recombination rates are shown for a variety of different vector/insert ratios. The vector concentration was kept constant for these experiments with the quantity of insert as the variable. The recombination rate increased with increasing insert amount up to about a 4 to 1 ratio. Beyond that there was no significant further increase in recombination rate.

TABLE 2.5 The ratio of fragment to vector.

Ratio F/V	Blue colonies	White colonies	Recombination rate
1:1	$2x10^4$	$1.6x10^4$	44±4%
2:1	$1.8x10^4$	$2.7x10^4$	60±5 %
3:1	$1.5x10^4$	$2.1x10^4$	58±5 %
4:1	$1.4x10^4$	$3x10^4$	68±2 %
6:1	$1.5x10^4$	$3.7x10^4$	71±6 %
8:1	$1.2x10^4$	$2.4x10^4$	66±5 %

The vector concentration was kept constant at 0.25 pmoles of linearized vector co-transformed into MB4091 along with 0.25, 0.5, 0.75, 1.5 and 2 pmoles of PCR fragments to confer a ratio of 1:1, 2:1, 3:1, 4:1, 6:1, 8:1 respectively. The values are the average of 3 experiments.

Construction of a positive selection vector

Although we routinely achieved recombination rates above 60% we wanted to see if we could improve that to nearly 100% with the use of a positive selection vector where a toxic gene would be replaced through recombination by the insert of choice, yet still maintain the ability to use the universal primer pairs.

The *ccdA* and *ccdB* (cell controlled death) genes comprise a plasmid toxin/antitoxin system carried by the F plasmid to ensure the maintenance of the plasmid in *E. coli* daughter cells (102). The toxin CcdB (11.7 KDa) selectively targets DNA gyrase (28, 141) and the antitoxin CcdA (8.7 KDa) both represses the promoter of *ccd* operon inhibiting the expression of the toxin CcdB as well as forming a tight complex with CcdB thereby inhibiting its activity. The half-life of CcdA is shorter than that of CcdB (142), consequently daughter cells losing the F plasmid do not survive.

The *ccdB* gene was cloned into pBC SK+ to generate plasmid pMB4105 and the plasmid maintained in the F' strain MB1547. Co-transformation of this vector with insert DNA into a strain lacking F, in this case we used the same MB4091 strain, eliminated the background of non-recombinant plasmids to less than 1% while maintaining comparable numbers of recombinant white clones.

Vector digestion was also shown crucial for recombination even when using pMB4105. If the plasmid was not digested, no recombinant plasmids were observed hence no colonies.

DISCUSSION

In this chapter, we show that λRed recombinase system is an efficient tool to use for the generation of recombinant libraries of reasonable size and complexity in lieu of *in vitro* reactions, when appropriate inserts can be generated carrying homology. Combined with error-prone PCR mutagenesis, this method rapidly generates large pools of randomly mutagenized clones used in a selection or screening of proteins with improved or novel properties.

The length of the flanking homology was found to be important in the efficiency of generating recombinants. Increasing the homology from about 80 to 120 bps generated a 3-fold increase in the number of recombinants. Further increasing the length of homology yielded smaller increases in efficiency. The generation of recombinants was dependent on the presence of Red recombinase enzymes and required the use of linearized vector, recombinants were not detected when the recipient vector remained circular. Dephosphorylation of the digested vector did decrease the number of background colonies but the use of a positive selection vector virtually eliminated any background. This cloning technique is very simple, fast and only few pmoles of PCR fragments are sufficient to generate large libraries in less than one day.

We anticipate this approach could find use for routine subcloning although there are clearly restrictions on the source and target DNA's stemming from the requirement to have homology. Our use of *lac* region homology extends the potential utility to a wide variety of vector systems, we routinely move inserts between blue/white screening

plasmids in this manner. The method however is not limited to *lac* homology; any stretch of terminal homology (of about 100 bp) should be suitable.

Of perhaps greater interest is in the generation of random mutational libraries of high complexity generated by error prone PCR. Such libraries routinely find applications in directed evolution and protein engineering. We have applied this approach to build mutant libraries for a number of enzymes which commonly yield mutant alleles carrying multiple mutations. While no method can sample the entire sequence space of a protein, the complexity is sufficient to isolate mutants requiring multiple changes. The remarkable ease by which this method generates large libraries makes it our favorite approach for protein engineering applications.

CHAPTER III

CYANIDE DIHYDRATASE FROM *BACILLUS PUMILUS* MUTANT WITH HIGHER CATALYTIC ACTIVITY AT pH 7.7

OVERVIEW

Cyanide has been used for decades by the mining industry for the extraction of fine metals (77). Due to its high affinity for metals, cyanide binds and extracts metal ions from the ore by carrying them into solution. Environmental regulations restrict the discharge of cyanide-contaminated waste-waters into the environment because of its high toxicity. Removal or transformation of the cyanide is required to reduce its residual concentration to levels that meet the discharge requirements. The US Environmental Protection Agency has set the maximum contaminant level goals (MCLG) for cyanide in drinking water to 0.2 mg/L or 200 ppb (140).

Traditional decontamination methods consist of oxidation of cyanide via hydrogen peroxide, chlorine or sulfur dioxide (33, 70). Even though these methods are successful in lowering the concentration of cyanide, they have several disadvantages notably unfavorable byproducts, special chemical handling and high cost of reagents.

Interest has risen lately in the biodegradation of cyanide using microorganisms. The most successful is the biological treatment of cyanide solution at Homestake Mining Co. in South Dakota using rotating biological contactors (RBC). The wastewaters were supplemented with phosphoric acid as bacterial nutrient and the RBC was populated with a strain of *Pseudomonas paucimobilis* acclimated to the waste (11). Another

application of biological cyanide treatment was conducted by Pintail System Inc. at Yellow Pine Mine in Idaho for a heap leach pad treatment using a mixture of bacteria collected at the site (139). The bioremediation approach suggests cleaner and safer reactions and lower operational costs are possible.

Cyanide degrading nitrilases convert cyanide into nontoxic products. Cyanide dihydratases (CynD) catalyze cyanide into ammonia and formate while cyanide hydratases (CHT) transform it into formamide. Even though a variety of enzymes have been shown to react on cyanide, cyanide dihydratases and cyanide hydratases do not require cofactors or secondary substrates, favoring them for industrial applications. Organisms producing CynD include *Bacillus pumilus* and *Pseudomonas stutzeri* (87, 146) while many fungi like *Neurospora crassa* and *Gloeocercospora sorghi* produce CHT (10).

Industrial application of these enzymes requires improving their characteristics such as catalytic efficiency and stability to make them effective. The lack of a high resolution structure prevents rational design and calls for isolating or screening for mutants showing an enhancement in enzyme properties. Such mutants may also prove helpful to understand the role of specific residues in an enzyme, especially in the absence of a protein crystal structure.

Numerous reports describing the successful improvement of enzymes have been published in the last ten years, as have the number of patents describing the biotechnological applications of these improved enzymes (61). Among these, one report on nitrilases catalyzing the hydrolysis of diverse nitriles to corresponding carboxylic

acids is of special interest (32). These biocatalyst enzymes are extremely useful for pharmaceutical applications to produce precursors of several drugs. For example, the production of the precursor to Lipitor drug, (*R*)-4-cyano-3-hydroxybutyric acid, from 3-hydroxyglutaryl nitrile is carried out by such a nitrilase (32). Mutant nitrilases were selected for improved biotechnological relevant characteristic such as stability, substrate specificity, pH dependant activity and especially enantioselectivity. The selection of improved enzyme characteristics utilized various mutagenesis techniques, including directed evolution, followed by high-through put screening.

A successful example of this approach was demonstrated in a prior study in our lab where $CynD_{pum}$ pH tolerant mutants were isolated following error-prone PCR, a random mutagenesis technique followed by extensive screening (144). The parent enzyme had an optimal activity at pH 7.7 but rapidly lost activity at pH 9 (63). The purified variants exhibited an increase in stability relative to the wild type and degraded cyanide at pH 10 *in vivo*.

In this study my aim is to screen for $CynD_{pum}$ mutants with higher catalytic activity. Such higher performance variants could be useful in the bioremediation of cyanide, making the process more efficient than with wild type enzyme. I predict that such mutants should fall into three general categories. The first category would include mutants with a higher specific activity for cyanide, meaning a higher rate at which the substrate will be converted to product once bound to the enzyme (higher K_{cat}). The second category consists of variants with higher stability. The third category includes mutants with a higher expression of the enzyme. For example, a mutation in the

promoter could render it stronger at expressing the gene or a mutation affecting the stability of the mRNA would cause the mRNA to be translated for a longer time. These mutants would produce more per cell similarly giving the impression of a higher activity. Such stability and expression variants can be excluded when the protein is purified and similar amounts of enzyme are compared. Of these categories, the first two are of primary interest, resulting in an enzyme with higher specific activity or higher stability. Both have potential benefits when it comes to application of the enzyme in the real world.

Here I describe the isolation of 3 $CynD_{pum}$ mutants using error-prone PCR for random mutagenesis, *in vivo* cloning for mutant library construction and colorimetric detection with picric acid in a microplate format for the screening. Three of these mutants showed higher catalytic activity *in vivo* when compared to the parent enzyme.

Furthermore, I characterized the effect of the mutation(s) on the kinetics, stability and pH activity of each purified enzyme. Two point mutations, K93R and D172N increased the enzyme's thermostability by several fold whereas E327K mutation had a lesser effect on improving stability. The D172N variant also increased the affinity of the enzyme for its substrate at pH 7.7 suggesting an involvement of that amino acid in the active site but lower its K_{cat}. However the A202T mutation is located in the dimerization or the A surface and rendered the enzyme inactive by destabilizing it. No significant effect on activity at alkaline pH was observed for any of the purified mutants.

MATERIALS AND METHODS

Culture media and reagents

All strains were grown in LB broth. Antibiotics were used at concentrations of 100 ug/ml of ampicillin, 25 ug/ml of kanamycin or 25 ug/ml of chloramphenicol as needed.

Bacterial strains and plasmids

E.coli strain MB3436 [Δ*endA thiA hsdR17 supE44 lacI*^{q}*ZΔM15*] was used as host strain for DNA manipulations. *E.coli* strain MB1837 [BL21 (DE3) pLysS] was used for protein expression. The *E. coli* strain MB4091 [DH10B (pKD46)] was used as the recipient for *in vivo* recombination. *E. coli* strain MB4105 [*supE thi-1 Δ endA Δ(lac-proAB) Δ(mcrB-hsdSM)5 /* F' [*traD36 proAB*$^{+}$ *lacI*^{q} *lacZΔM15*] was used as host for the positive selection vector p4105 (2). The plasmids used are described in TABLE 3.1.

Error-prone PCR

The plasmid template used for error prone PCR was p3980, derived from pBluescript II KS+ (Stratagene) containing the *cynD*$_{\text{pum}}$ C1 gene encoding cyanide dihydratase from *Bacillus pumilus* with an N-terminal his-tag. PCR reactions were performed as 50 ul reactions containing 25 ul of Taq 2X Master Mix (New England Biolabs). In addition, 150 ng of DNA template, 100 ng of each PCR primer, 0.2 mM $MnCl_2$ and 2.5 mM $MgCl_2$ were added to the reaction mixture and adjusted to 50 ul with MQH_2O. The reaction conditions were as following: 25 cycles of 95^{o}C for 30 sec, 55^{o}C

for 60 sec and 72°C for 90 sec. The PCR primers used were the -60M13 universal sequencing primers with the following sequences: -60M13F (5'-GCGAA AGGGG GATGT GCTGC AAGG); -60M13R (5'-CACTT TATGC TTCCG GCTCG TATG). The PCR products were ethanol precipitated, resuspended in water and stored at -20°C. DNA concentration was determined by measuring the absorbance at 260 nm using a Nanodrop ND-1000 spectrophotometer.

PCR fragment cloning

In vivo cloning (2) as described in chapter II was used to clone PCR fragments generated from EP-PCR into a positive selection vector p4105. 1pmole of PCR fragments were mixed with 0.25 pmole of linearized vector and transformed into electro-competent cells MB4091[DH10B (pKD46)] made from cells grown in LB broth at 30°C to an O.D. (600 nm) of 0.3 with 0.1% arabinose added for the final 1 hour following the protocol described in Abou-Nader and Benedik. (2). After the electroporation, 1 ml of LB broth was added and cells were incubated for 30 min at 37°C on a roller drum for recovery. 100 ul of cells were then spread on LB plates supplemented with 25 μg/ml chloramphenicol and incubated at 37°C overnight.

TABLE 3.1 Plasmids used and constructed carrying various CynD$_{pum}$ alleles.

Plasmids	Description	Reference
pBS (KS+)	*E. coli* cloning cloning vector (Amp-r)	Stratagene
pBC (SK+)	*E. coli* cloning cloning vector (Cam-r)	Stratagene
pEt26b	*E. coli* T7 expression vector (Kan-r)	Novagen
pEt28a	*E. coli* T7 expression vector (Kan-r)	Novagen
p3980	pBS carrying CynD$_{pum}$ with N-terminal His-tag	Wang *et al.* 2011
P4105	pBC *ccdB*	Abou-Nader and Benedik 2010
p4165	P4105 carrying CynD$_{pum}$ CD12	This work
p4240	P4105 carrying CynD$_{pum}$ 7G8with N-terminal His-tag	This work
p4606	P4105 carrying CynD$_{pum}$ DD3 with N-terminal His-tag	This work
p4257	pEt26b carrying CynD$_{pum}$ CD12 with N-terminal His-tag	This work
p4265	pEt26b carrying CynD$_{pum}$ 7G8 with N-terminal His-tag	This work
p4631	pEt28a carrying CynD$_{pum}$ DD3 with N-terminal His-tag	This work
p4406	CynD$_{pum}$ from p3980 in pET28a	This work
p5466	p4406 E327K	This work
p5471	p4406 K93R	This work
p5557	p4406 D172N	This work
p5472	p4406 A202T	This work
p5591	p4406 D172N A202T	This work
p5496	p4406 K93R E327K	This work
p5593	p4406 K93R D172N E327K	This work
p5630	p4406 E327K A202T	This work
p5631	p4406 K93R A202T	This work

Screening for higher activity mutants

Single colonies were picked and inoculated into 96-well plates containing 150 µl LB supplemented with 25 µg/ml of chloramphenicol and cultured at 37°C overnight. 20 µl of culture from each well was transferred into the corresponding well of a new 96-well plate. 80 µl of MOPS buffer (100 mM, pH 7.7) containing 5 mM KCN were added to each well and the plates were sealed with parafilm and incubated in a fume hood at room temperature for 20 min. The reaction was stopped by the addition of 100 µl picric acid (0.6% picric acid in 250 mM sodium carbonate) and plates were left at 60^{o}C for 20 min. Under these conditions, cells carrying the wild-type *cynD*$_{pum}$ do not completely degrade all the cyanide present and the well retains a red or dark orange color. Any mutant with increased cyanide degrading activity was picked if the cyanide in the well was completely degraded; in this case, the well had a bright yellow color.

Construction of single, double and triple mutants

Alleles of CynD$_{pum}$ carrying single or double mutations were constructed by site-directed mutagenesis. The mutagenesis reactions were carried out using 25ul Phusion High-Fidelity PCR Master Mix with HF Buffer (New England Biolabs), 150 ng dsDNA template and 100ng of each of the forward and reverse primers. MQH$_2$O was added to the reaction mixture for a total volume of 50ul. Each reaction was run for 18 cycles at 93^{o}C for 30 sec, primer's annealing temperature for 1 min and 72^{o}C for 5 min. The mutagenic primers are listed in TABLE 3.2. The mutations were confirmed by DNA sequencing.

TABLE 3.2 Primer sequences used in site-directed mutagenesis.

Primer	Sequence
K93R	ATAAGTGAGGCAGCGCGCAGAAATGAAACGTAC
D172N	CAAGTCCCACTTAATCTTATGGCGATGAAT
A202T	CAAGTAGATATTATACTATAGCGACACAGAC
E327K	ATCAACATGGTATACTTAAGGAAAAAGTTTAA

Forward primers sequence. The underlined nucleotides indicate the substituted site.

SDS-PAGE and western blot

Overnight cultures were diluted 1:100 in 3ml LB kanamycin and grown to an OD600 of 0.3 at 37^{o}C. 1 mM IPTG was added for 3-4 hours and induction continued at 30^{o}C. Cells from 3 ml of induced culture were then pelleted by centrifugation at 3750 rpm for 10 min and were washed two times with 0.1 M MOPS pH 7.7. The cells pellet was resuspended in 300 ul of 0.1 M MOPS pH 7.7 and sonicated on ice 10 times for 10 sec each. Cells debris was centrifuged and the supernatant was recovered and transferred to a different tube. The cell debris was also resuspended in 300 ul of 0.1 M MOPS pH 7.7. 10 ul of the supernatant or the resuspended cell debris were mixed with 3 ul of Amresco 4X Next Gel Sample Loading Buffer, boiled for 10 min and run on an Amresco Pro-Pur Next Gel 10% polyacrylamide gel along with Ez-Run Prestained *Rec* Protein Ladder (Fisher Bioreagents). The gel was then electroblotted to a nitrocellulose membrane from Whatman and nitrilase polyclonal antiserum was used as primary

antiserum (1:3000) and HRP conjugated goat anti-rabbit IgG as the secondary antibody. SuperSignal West Pico rabbit IgG Chemiluminescent detection kit (Thermoscientific) was used to visualize the protein bands.

Protein expression and purification

Wild type $CynD_{pum}$ and variants were cloned into the expression vector pET28a using NdeI and XhoI restriction sites and transformed into MB1837 (BL21 pLysS) cells. Proteins were expressed as described in the previous section. The pellet was then stored at -20^{o}C overnight. Cells were then thawed and lysed at room temperature with B-PER II Protein Extraction Reagent (Thermo Scientific). 2mL of B-PER II reagent per gram of cell pellet was used supplemented with 0.5 mg/ml lysozyme, 10ug/ml DNase and 1X EDTA-free protease inhibitors as recommended by the manufacturer. The cell lysate was centrifuged at 13,000 rpm for 15 min at 4^{o}C. Purification of hexahistidine-tagged proteins was performed at 4^{o}C using the *HisPur Cobalt purification kit (*Thermo Scientific). Desalting of the purified protein at 4^{o}C used Zeba Spin Desalting Columns (Thermo Scientific) and the protein was resuspended in 0.1 M MOPS pH 7.7. Protein concentration was determined using the NanoDrop ND-1000 at 280 nm using the predicted his-tagged protein extinction coefficient of 58,790 cm^{-1} M^{-1} and molecular weight of 39,654 g/mol. SDS-PAGE confirmed the purity of the protein. Purified proteins were stored in aliquots at -80^{o}C.

Kinetic measurement

3.9 ug of enzyme was used for kinetics analysis of wild type and $CynD_{pum}$ variants in total volume of 1 ml. The enzymes tested were purified from strains carrying p4406, p4257, p4265, p463, p5557 and p5593 plasmids. A stock solution of 1 M of cyanide was prepared in a 1 M MOPS pH 7.7. Reactions were done at room temperature in 50 mM MOPS at pH 7.7 at different concentrations of cyanide. Each reaction was run for 5 min and time points were taken every 1 min. The reaction rates over the first 5 min were linear and $V_{initial}$ was calculated by monitoring ammonia production using 100ul of reaction mixed with 100 ul of diluted Nessler reagent (100) (1:3 in MQ H_2O) and using a 96-well plate reader (Bio-Rad) the absorbance was determined at 420 nm to determine the concentration of ammonia generated. Lineweaver-Burk plots were then used to estimate K_m and V_{max}. For each enzyme, the final K_m and V_{max} values are averages from 3 separate protein preps. V_{max} was used to calculate K_{cat}. All enzymes were considered as 18 subunits oligomers with molecular weight of 713,772 g/mol.

pH activity measurement

5.5 ug of enzyme was used for pH activity analysis of the wild type enzyme and $CynD_{pum}$ variants in total volume of 1 ml. The enzymes tested were purified from strains carrying p4406, p4257, p4265, p4631, p5557, p5496 and p5593 plasmids. Three cyanide stock solutions were prepared: 1 M citric acid/Na_2HPO_4 at pH 5.5, 1 M MOPS pH 7.7 and 1 M CAPS at pH 9.5. Reactions were done at room temperature in a fume hood at a final concentration of cyanide of 4 mM. The activity of the purified enzyme was

measured over pH range 4-10. Buffers used are as follow: 50 mM citric acid/ Na_2HPO_4 (pH 4, 5 and 6), 50 mM MOPS (pH 7), 50 mM Tris-HCl (pH 8) and 50 mM glycine/NaOH (pH 9 and 9.5). The activity was monitored for the first 5 min and time points were taken every min. Ammonia production was measured as described above. Final values are averages from 3 separate protein preps.

Enzyme stability

The thermostability of the enzyme was determined by incubating 80 ug of purified enzyme in a total volume of 8 ml of 50 mM MOPS pH 7.7 in a water bath at 42^{o}C. The enzymes tested were purified from strains carrying p4406, p4257, p4265, p4631, p5557, p5496 and p5593 plasmids. At different times, 0.5 ml of mixture was taken out of 42^{o}C into a new 1.5 ml Eppendorf tube and left at room temperature for 3 min before adding cyanide in 1 M MOPS pH 7.7 to a final concentration of 4 mM. The reaction continued at room temperature and the activity was monitored for the first 5 min with time points taken every minute to measure ammonia production as described above. The reaction rate was calculated using the zero time value considered as 100% and the relative activity of the enzyme at the different incubation times was then calculated. Final values are averages from 3 separate protein preps.

RESULTS

Screening for variants with higher cyanide degrading activity at pH 7.7

A previous study from our lab was successful in isolating CynD$_{pum}$ mutants that allowed the degradation of cyanide at pH 10 *in vivo*, a pH where the wild-type enzyme is inactive (144). The aim of this work was to isolate additional CynD$_{pum}$ variants with improved degrading activity at pH7.7, the enzyme's optimum pH. In the absence of a high resolution structure, a directed evolution strategy was used. Randomly mutagenized *cynD*$_{pum}$ DNA was generated by error-prone PCR. This was followed by *in vivo* cloning to create the mutant library. Using 96-well plates and a colorimetric assay to measure cyanide, approximately 5000 highly mutagenized clones were screened. The condition for the screen was chosen as half the reaction time needed for cells expressing wild-type CynD$_{pum}$ to completely degrade the cyanide, visualized by a color change from red to yellow in the picric acid assay (FIG.3.1) (43). Putative mutants would show a yellow color in the well due to the absence to cyanide whereas the wild-type parent remains red due to the remaining substrate. To eliminate false positives, a verification of the putative positive clones was done by repeating the test in a microcentrifuge tube.

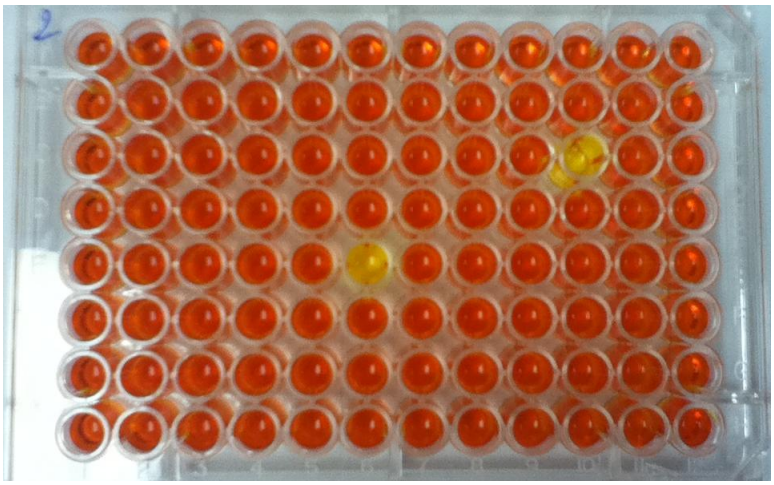

FIG.3.1. 96-well screening plate using picric acid assay for cyanide detection. Two putative mutants (yellow wells) are shown. Red color indicates the presence of cyanide in the well whereas yellow color indicates its absence (43).

Characterization of CynD$_{pum}$ mutants

Three candidate mutants were found that had higher catalytic activity at pH 7.7. Each mutant was isolated from an independent screen and they were named CD12, DD3 and 7G8. DNA sequencing of the plasmids carrying these *cynD*$_{pum}$ alleles revealed the nucleotide changes for each mutant (FIG.3.2).

CD12 had one mutation resulting in the amino acid change E327K and 2 silent mutations (T849C and T957A). DD3 had one mutation resulting in the amino acid change K93R and one silent mutation (A867G). 7G8 had two mutations resulting in the amino acid changes D172N and A202T and one silent mutation (T570C). Single amino

acid change as well as double and triple mutants were reconstructed using site-directed mutagenesis and their cyanide degrading activity was tested *in vivo* (TABLE 3.3).

TABLE 3.3 Cyanide degrading activity at pH 7.7 of $CynD_{pum}$ mutants.

$CynD_{pum}$ mutant	*In vivo* activity at pH 7.7
K93R (DD3)	Active
D172N	Active
A202T	Inactive
E327K (CD12)	Active
K93R E327K	Active
D172N A202T (7G8)	Active
K93R A202T	Inactive
E327K A202T	Inactive
K93R D172N E327K	Active

Proteins were expressed from pEt26b expression constructs and induced in BL21 (DE3) cells. The cyanide degrading activity of the mutants was tested using 4mM cyanide in 0.1M MOPS at pH 7.7 at room temperature for 30 min. Cyanide degradation was measured using picric acid to detect the remaining cyanide.

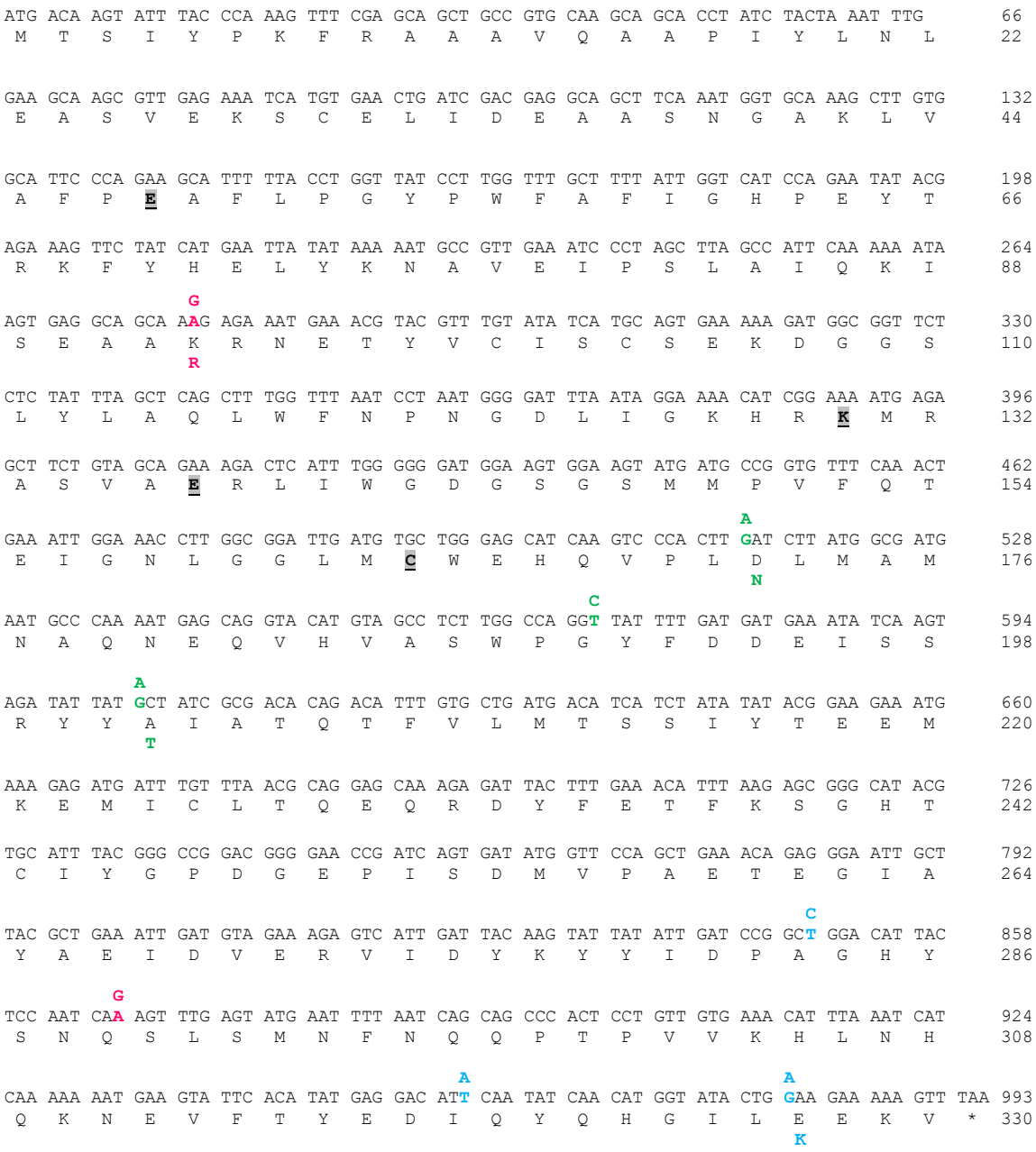

FIG.3.2. DNA and amino acid changes of mutants CD12, 7G8 and DD3. Residues in blue, green and pink show the nucleotides and amino acid changes of mutants CD12, 7G8 and DD3 respectively. Conserved catalytic tetrad is underlined and highlighted in grey.

Protein expression

Cells carrying the parental and mutant allele plasmids were induced, activity was tested and the protein expression was confirmed by a western blot. The A202T mutant was inactive as were the other double mutants carrying A202T, K93R/A202T and E323K/A202T, with the exception of D172N/A202T which retained activity (TABLE 3.3) Thus, it was important to demonstrate the inactive proteins were being expressed. Likewise for the active mutants, a comparison of their level of expression to the wild-type enzyme might suggest whether the mutations affect proteins levels or not. Therefore, soluble cell extracts from induced cultures grown to similar ODs was separated by SDS-PAGE and western blot was used to detect the CynD protein as described in materials and methods (FIG.3.3).

The 37 kDa $CynD_{pum}$ protein can be readily detected on the blot and is absent in the negative control lane**.** All mutant proteins had similar levels of expression compared to parent enzyme except the A202T single mutant (FIG.3.3). A202T was barely detectable in the soluble cell lysate (FIG.3.3 lane 6). This low level of A202T soluble protein might be due to an aggregation of the protein in the cell debris. Therefore, a sample from A202T cell pellet was separated on SDS-PAGE and blotted. Similarly, the inactive double mutants E327K/A202T and K93R/A202T were also analyzed and their solubility was compared to that of the A202T single mutant and D172N/A202T (FIG.3.4).

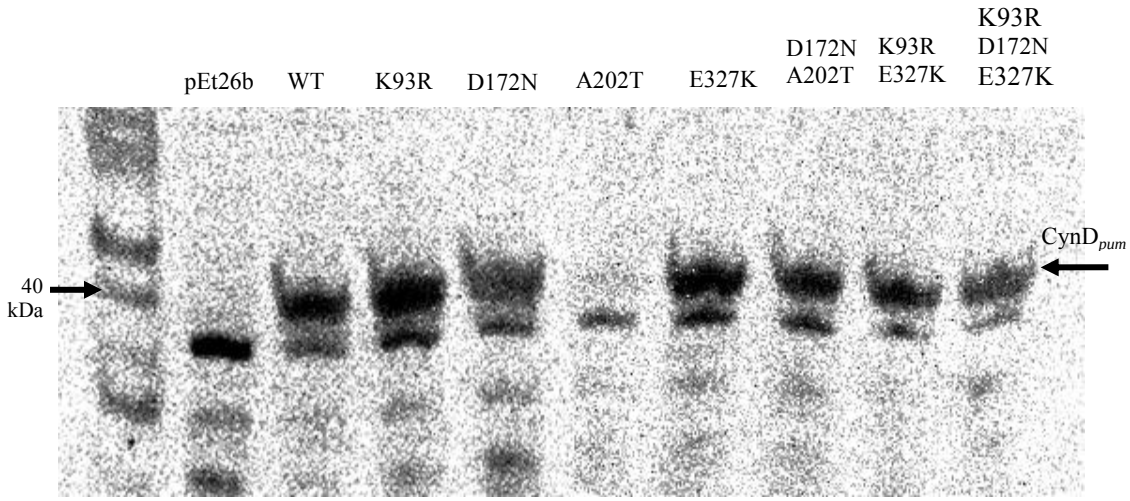

FIG.3.3. Western blot showing the expression of CynD$_{pum}$ wild-type and mutants in soluble cell extracts. Plasmids were expressed in BL21 cells with 1mM IPTG for induction. Lane1: EZ-Run Prestained *Rec* Protein Ladder. Lane 2: pEt26b empty vector (negative control). Lane 3: wild-type CynD$_{pum}$. Lane 4: K93R. Lane 5: D172N. Lane 6: A202T. Lane 7: E327K. Lane 8: D172N/A202T. Lane 9: K93R/E327K . Lane 10: K93R/D172N/E327K .

The inactive double mutants E327K/A202T and K93R/A202T had a similar profile as the A202T single mutant (FIG.3.4). The protein was several-fold less abundant than the wild-type in the soluble cell lysate (lanes 3, 5 and 6), the majority of the protein was primarily found as aggregates in the pellet (FIG.3.4 lane 8, 9 and 10).

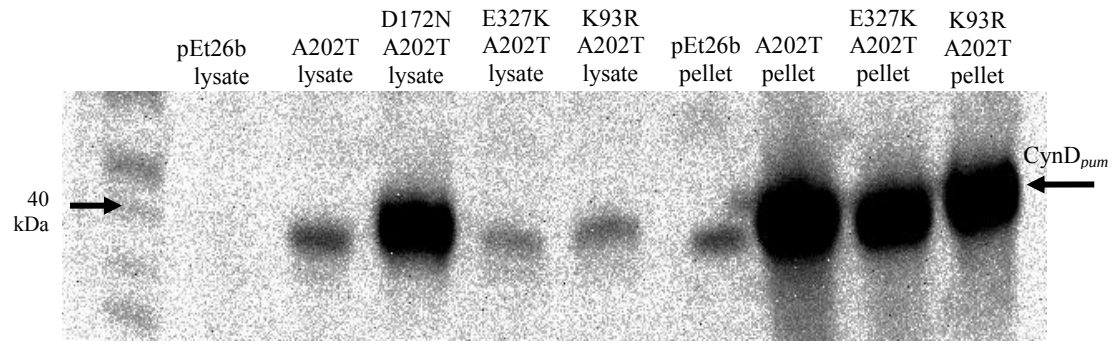

FIG.3.4. Expression and solubility of CynD variants carrying the A202T mutation. Lane1: EZ-Run Prestained *Rec* Protein Ladder. Lane 2: supernatant of pEt26b empty vector (negative control). Lane 3: A202T supernatant. Lane 4: D172N/A202T supernatant. Lane 5: E327K/A202T supernatant. Lane 6: K93R/A202T supernatant. Lane 7: pEt26b pellet. Lane 8: A202T pellet. Lane 9: E327K/A202T pellet. Lane 10: K93R/A202T pellet.

The presence of A202T protein in these insoluble aggregates or inclusion bodies likely explains its low activity. This phenotype seemed to be rescued when A202T mutation was combined along with D172N (FIG.3.3, lane 8) and both activity as well as soluble protein levels were rescued.

Kinetic measurement

To test whether any of the mutants show difference in their affinity to cyanide or changes in their maximal velocity compared to parent enzyme, wild type CynD$_{pum}$ along

with the mutants K93R, D172N, E327K, D172N/A202T, and K93R/D172N/E327K were expressed with a his-tag and purified. Kinetic measurements were performed at room temperature (23^{o}C) in 1 ml of 50 mM MOPS pH 7.7 with 3.9 ug of purified enzyme. The cyanide concentration ranged from 1 mM to 8 mM. The rate for ammonia production was determined during the first 5 min of the reaction where the initial rate of reaction was linear (100).

TABLE 3.4 summarizes the K_m and V_{max} values found for each allele (the A202T single mutant was not active). In FIG.3.5, the Lineweaver-Burk plot used to determine the kinetic values is shown. Each mutant had diverse kinetic parameters.

E327K and K93R had similar enzyme kinetics (TABLE 3.4) and showed a slight increase in V_{max} compared to wild type but their affinity for the substrate decreased by a factor of 2.

D172N had higher affinity for cyanide with a 3-fold decrease in K_m compared to wild type but its maximal velocity was reduced by nearly 2-fold. The D172N/A202T allele had a similar phenotype to D172N. Its K_m and V_{max} values were lower than wild-type and of E327K and K93R. This suggests that A202T mutation contributes little or nothing to the phenotype of the double mutant.

The triple mutant K93R/D172N/E327K combined the effects of the single mutants. Its K_m is the average value of the single mutants K_m making it similar to that of the parent enzyme. However, its maximal velocity was lower than the wild-type resembling the V_{max} of the single mutant D172N (TABLE 3.4).

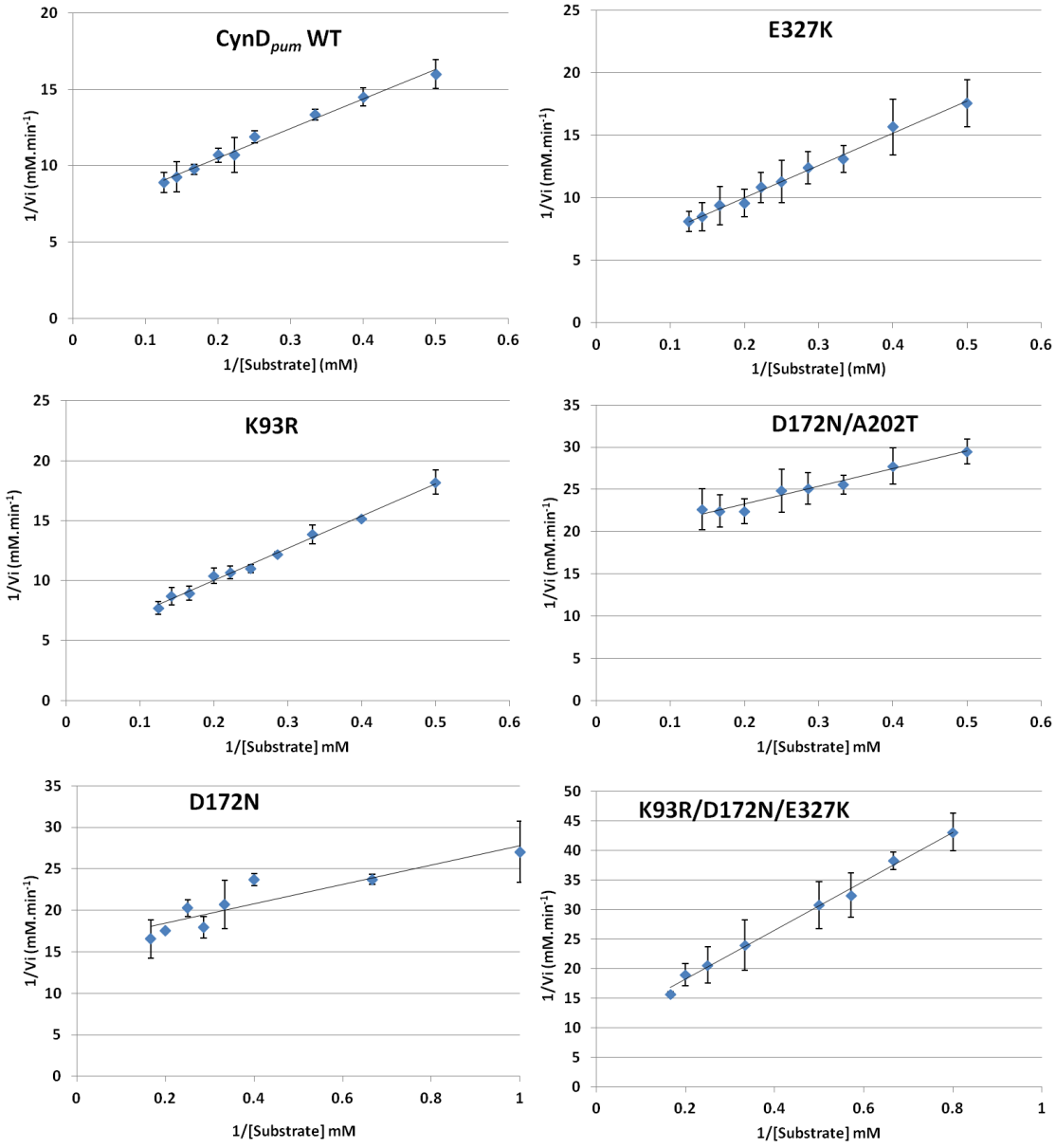

FIG.3.5. Lineweaver-Burk plots for WT CynD$_{pum}$ and the mutants. Error bars indicate the standard deviation of the average from three separate protein preps.

TABLE 3.4 Kinetic parameters for wild type CynD$_{pum}$ and mutants.

Enzyme	K_m (mM)	V_{max} (mmole/min.mg)	K_{cat} (min^{-1})
WT CynD$_{pum}$	2.9 ±0.5	0.038 ±0.004	2.63 x10^4
K93R	5.88 ±0.3	0.056 ±0.004	3.79 x10^4
D172N	0.72 ±0.4	0.016 ±0.001	1.13 x10^4
A202T	N/A	N/A	N/A
E327K	5.31 ±0.3	0.053 ±0.006	3.7 x10^4
D172N/A202T	1.09 ± 0.4	0.013 ± 0.002	0.95 x10^4
K93R/D172N/E327K	4.2 ±1.2	0.026 ±0.006	2.02 x10^4

The K_m and V_{max} values represent the average and the standard deviation of the average from three separate protein preps. All enzymes were assumed to be 18 -subunit spirals with a molecular weight of 713,772 g/mole.

Thermal stability

To test if any mutants had an increase in stability, their thermostability was compared to that of the wild type enzyme. In a prior study (63), the stability of CynD and CHT was tested by incubation at different temperatures; 23°C, 37°C, 42°C and 55°C. Extended incubation at 42°C was found to be a suitable criterion for enzyme stability. Therefore, each enzyme was incubated in a water bath at 42^{o}C and at different time points aliquots were removed and the residual activity was measured at room

temperature. The cyanide degrading activity calculated before incubation at 42^{o}C was taken as 100% (FIG.3.6).

The effect of the mutations on enzyme stability varied. All three single mutations increased the stability of the enzyme. D172N and K93R (DD3) mutations had the highest effect on the enzyme stability (FIG.3.6). After 2 hours incubation at 42^{o}C, K93R, D172N and E327K mutants retained 60%, 45% and 30% of their residual activity respectively compared wild type enzyme which had only 10% of its activity remaining. The K93R/E327K double mutant retained its activity slightly longer than the single mutants, although its rate of loss was comparable at earlier times.

The triple mutant K93R/D172N/E327K was the most stable. It kept 90% of its activity after 2 hours incubation at 42^{o}C whereas the wild-type had only 10% of its activity. This additive effect of the single mutations suggests a synergistic interaction. Thus, the various mutations are likely to stabilize different aspects of the enzyme.

On the other hand, the double mutant D172N/A202T (the 7G8 mutant) had an unanticipated phenotype. It was less stable than the wild-type and the D172N single mutant. This can be explained by the fact that single mutation A202T rendered the enzyme inactive. As shown previously on the western blot (FIG.3.4), A202T was insoluble and formed inclusion bodies or aggregates. Thus, it can be suggested that when the highly stable D172N mutant is combined with single mutation A202T (the 7G8 mutant), it repairs the inactivity of A202T mutant by compensating for the decrease in stability thereby restoring the catalytic activity to the enzyme.

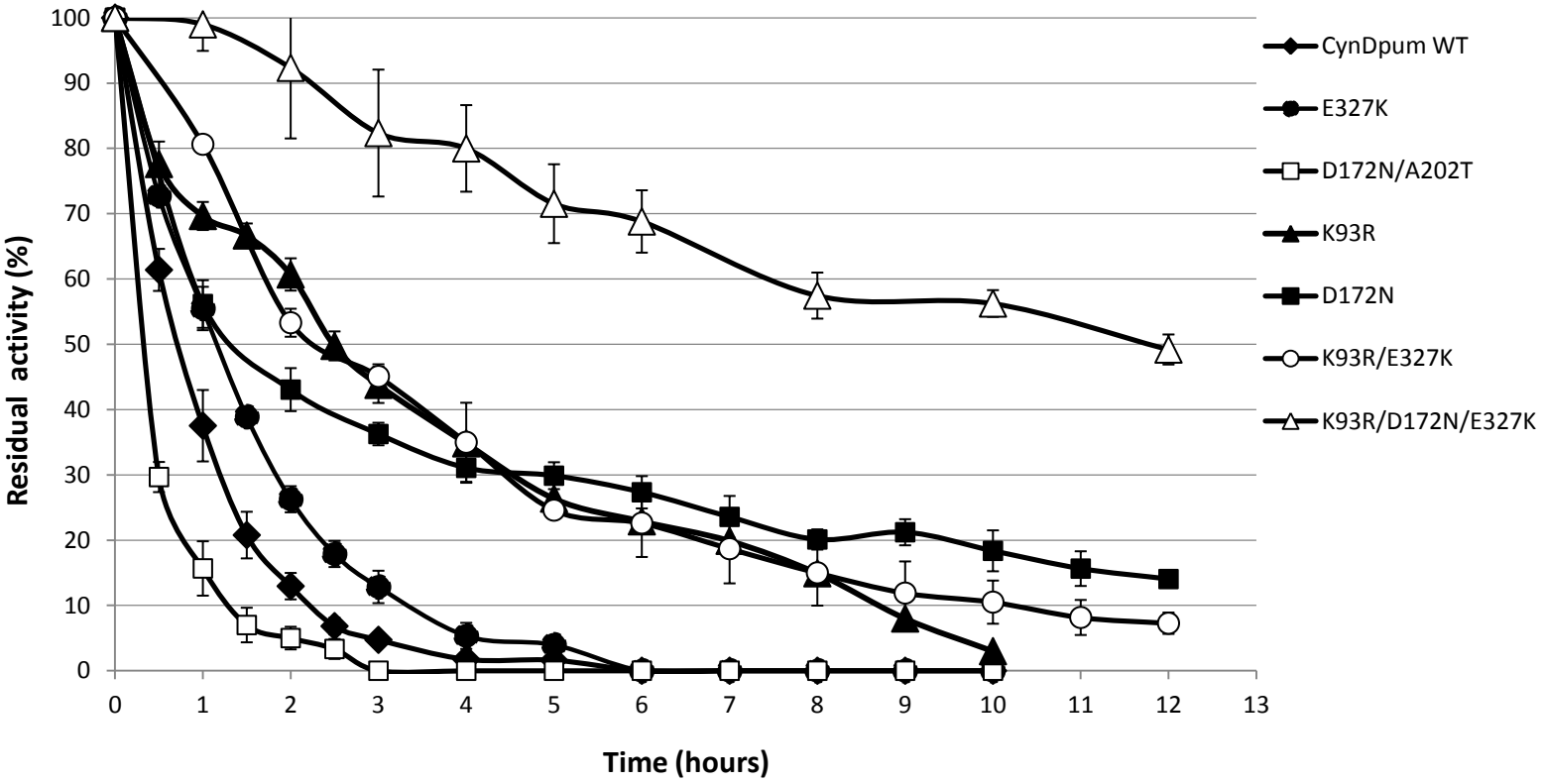

FIG.3.6. Thermostability of $CynD_{pum}$ and mutants. Purified enzymes were incubated at 42^{o}C. Residual activity was tested at room temperature. Error bars indicate the standard deviation of the average from experiments conducted with three separate protein preps.

pH activity profile

Wild-type CynD$_{pum}$ had a maximal activity in the pH range of 7-8 with the peak at pH 7.7. At higher pH, the enzyme sharply lost its activity. However, in acidic solution, its activity diminished gradually (63). Previously, our lab identified higher stability mutants that showed an increase in cyanide degrading activity at pH 9 (144). Since the mutants isolated in this study show an increase in thermostability, their effect on the pH activity profile of the enzyme was similarly tested.

No significant increase in activity at pH 9 was observed for any of the purified enzymes compared to the wild-type CynD$_{pum}$ (FIG.3.7). The increased thermal stability of the enzyme did not compensate for its lack of activity *in vitro* at alkaline pH. None of the mutants had any activity when tested at pH 9.5.

The activity of the enzyme at different pHs was plotted two different ways in order to clearly show the effect of the mutations. FIG.3.7 shows the initial reaction rate expressed in terms of absorbance of the product measured at 420 nm generated per minute. This graph allows for a comparison of the actual activity of the enzymes at various pH while FIG.3.8 shows the percentage of activity for each enzyme at each pH relative to its activity at pH 8.

Single mutants E327K and K93R as well as the double mutant K93R/E327K exhibited a similar pH activity profile to the wild-type. The maximal activity was around pH 8 but it diminished gradually at more acidic pHs.

On the other hand, D172N, D172N/A202T and K93R/D172N/A202T showed lower activity than wild type at pH 7 and pH 8 (FIG.3.7). Mutants carrying D172N had a

lower V_{max} than wild-type at pH 7.7 (TABLE 3.3). Thus, the decrease in activity seen can be the result of the decrease in V_{max} value and is likely the contribution of the common D172N change.

Since the wild-type showed a maximal activity at pH 8, the relative activity of each enzyme was plotted with the initial reaction rate at pH 8 taken as 100% activity (FIG. 3.8). It is clear that enzymes carrying the D172N mutation exhibited a shift in their optimal activity from pH 8 to pH 7. The D172N/A202T double mutant and D172N single mutant exhibited very similar pH activity profiles which support the idea that A202T has little or no effect. Nearly a 30% increase was noted in their activity at pH 7 compared to pH 8 and only 34% decrease at pH 6 whereas the wild-type enzyme lost more than 60% of its activity at pH 6.

Wild-type and E327K lost 20% of their activity when the pH shifted from 8 to 7 (FIG.3.8). Nevertheless, K93R and double mutant K93R/E327K lost 12 % and 6 % of their activity respectively. At lower pHs, their activity declined similarly.

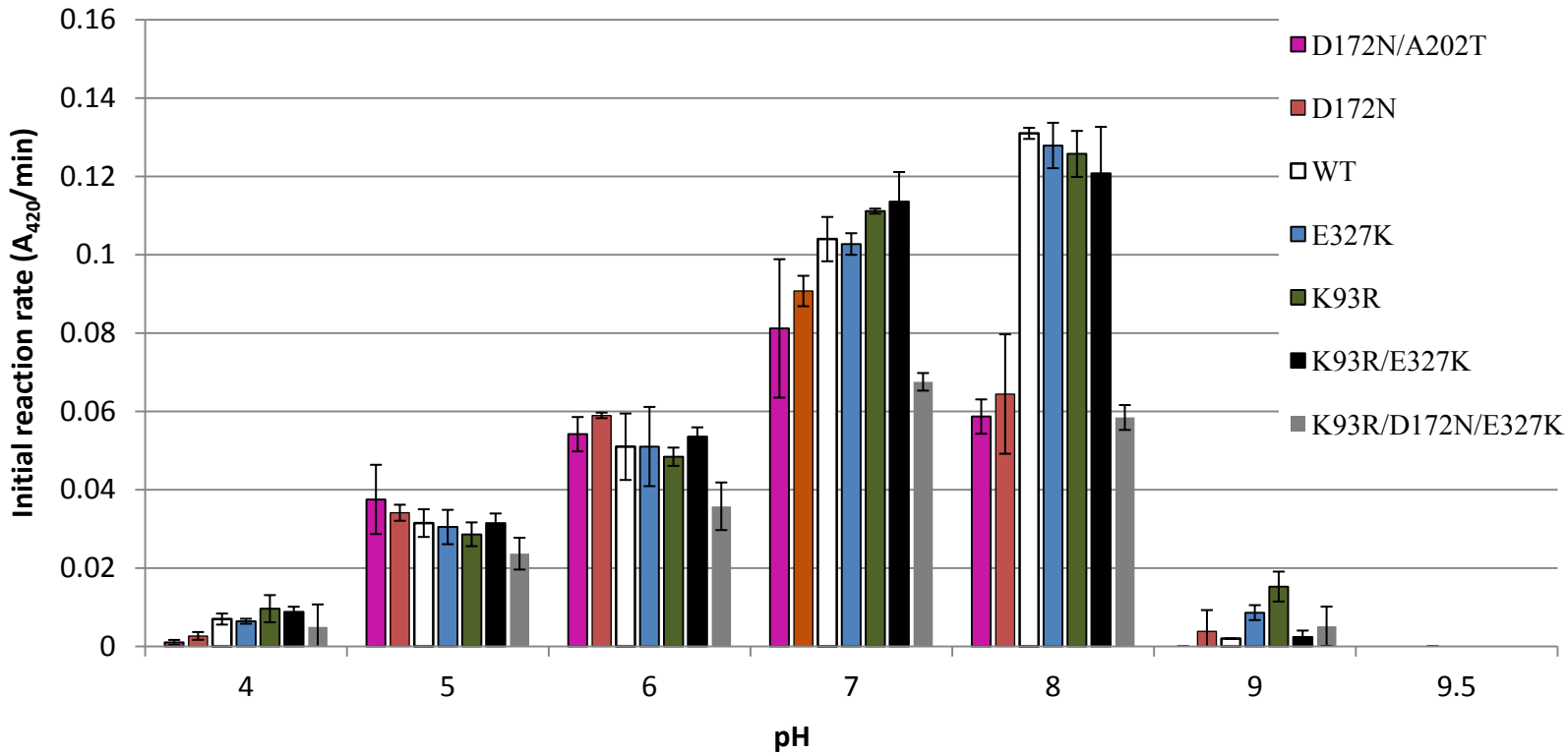

FIG.3.7. Comparison of pH activity profile. 5.5ug/ml of enzyme was tested with 4 mM cyanide and activity was measured at each pH. Initial reaction rate is represented by absorbance of product at 420 nm generated per minute. All mutants were inactive at pH 9.5. Error bars indicate the standard deviation of the average from experiments conducted with three separate protein preps.

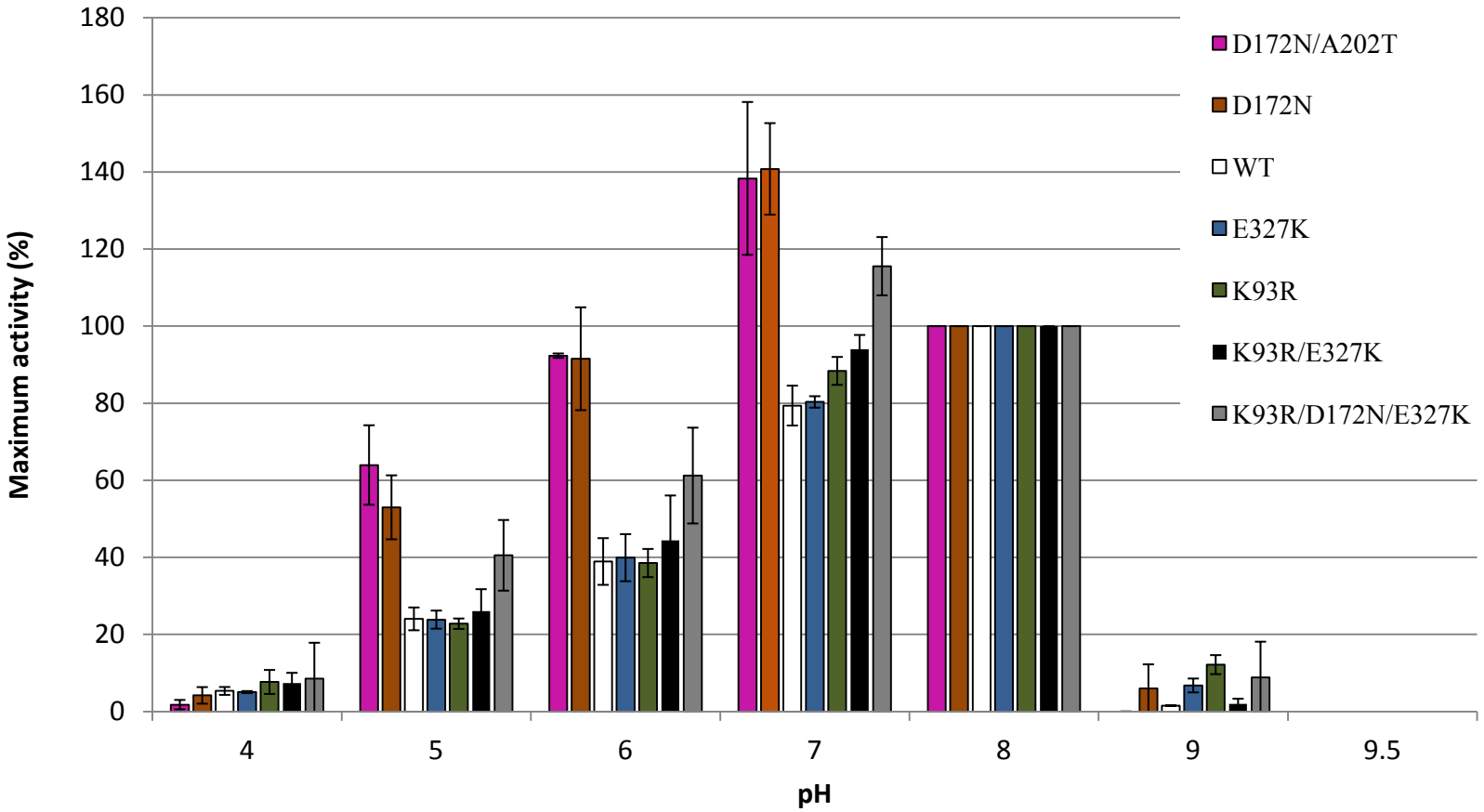

FIG.3.8. Percentage of activity at each pH relative to the activity at pH 8. The initial reaction rate at pH 8 of each enzyme was taken as 100%. All mutants were inactive at pH 9.5. Error bars indicate the standard deviation of the average from experiments conducted with three separate protein preps.

DISCUSSION

Using random mutagenesis followed by high throughput screening, I identified three $CynD_{pum}$ mutants with a higher catalytic activity at pH 7.7. The mutants CD12 and DD3 had one amino acid change each, E327K and K93R respectively while 7G8 had two mutations D172N and A202T (FIG.3.2). Kinetics measurements, thermostability and pH activity profiles were used to characterize the effect of these mutations on enzyme activity and stability. These results in combination with structural modeling of the location of the residues help us hypothesize as to the role of these residues and better understand the cyanide dihydratase structure.

A structural model of $CynD_{pum}$ has been published based on a low resolution cryo-electron microscopy along with modeling of its sequence to those of related crystallographically determined structures (62, 126). The building block of the helix is a dimer and each monomer is a 37 KDa subunit (62). At pH 8, the enzyme formed an 18-subunit spiral with 2-fold symmetry. Five surfaces, A,C,D, E and the C-terminus are predicted to be involved in interfacial interactions and have been proposed to play a role in the protein oligomerization (126, 135) (FIG.3.9). It is notable that the residues identified in this study K93R, D172N, A202T and E327K are located on these important surfaces and their putative role is discussed below (FIG.3.10).

Surface B is formed of β-sheets which harbor the active site and none of my mutations map there.

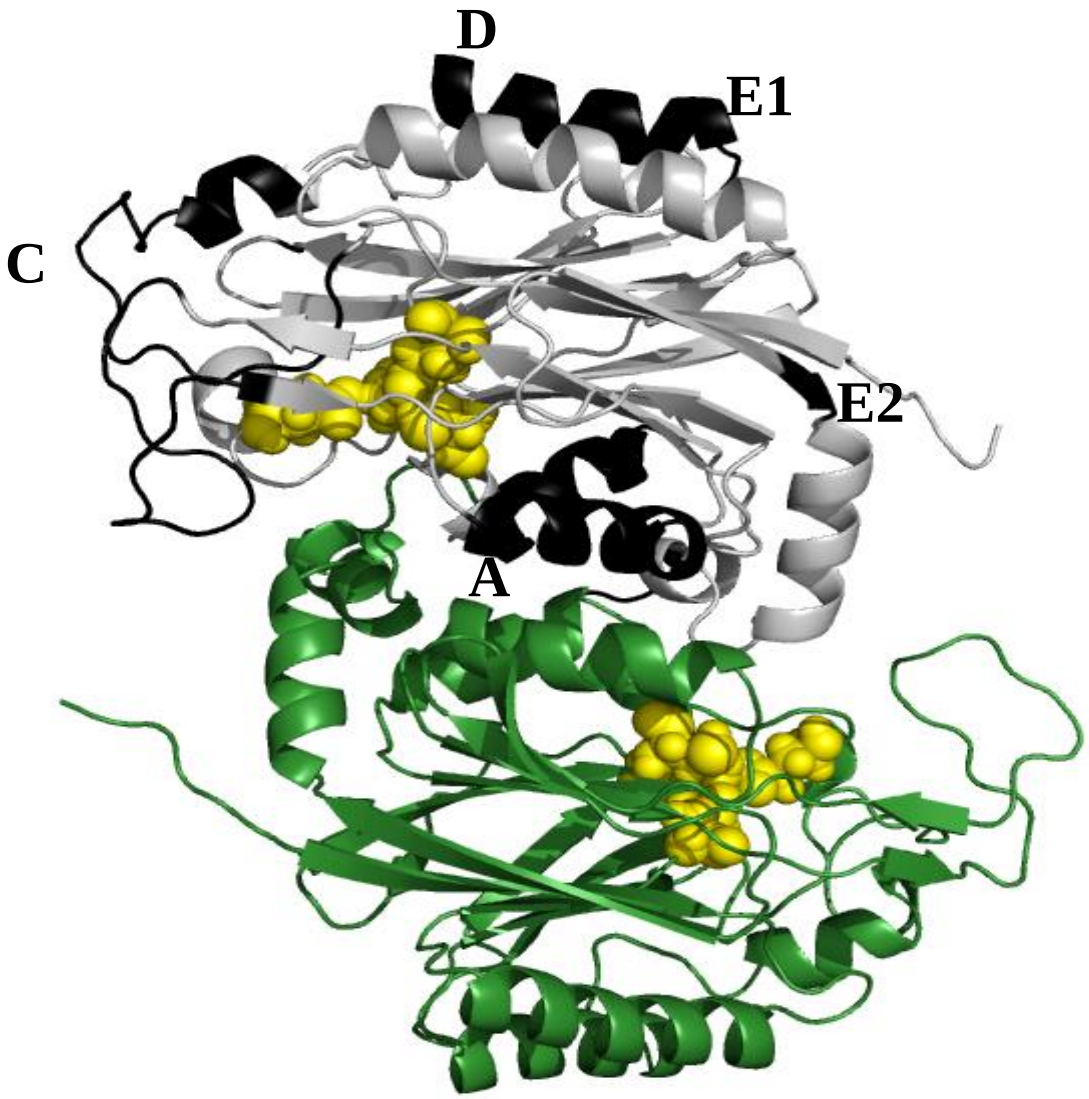

FIG.3.9. Dimer model of $CynD_{pum}$. Figure was constructed using PyMOL (Accession No AAN77004) using the model from Jandhyala *et al*. (62). One monomer is represented in gray and the second in green. Residues involved in the A, C, D and E surfaces are colored in black. The catalytic tetrad E48, K130, E137 and C164 side chains are shown as spheres colored in yellow. The extended C-terminal region could not be modeled and therefore it is not shown.

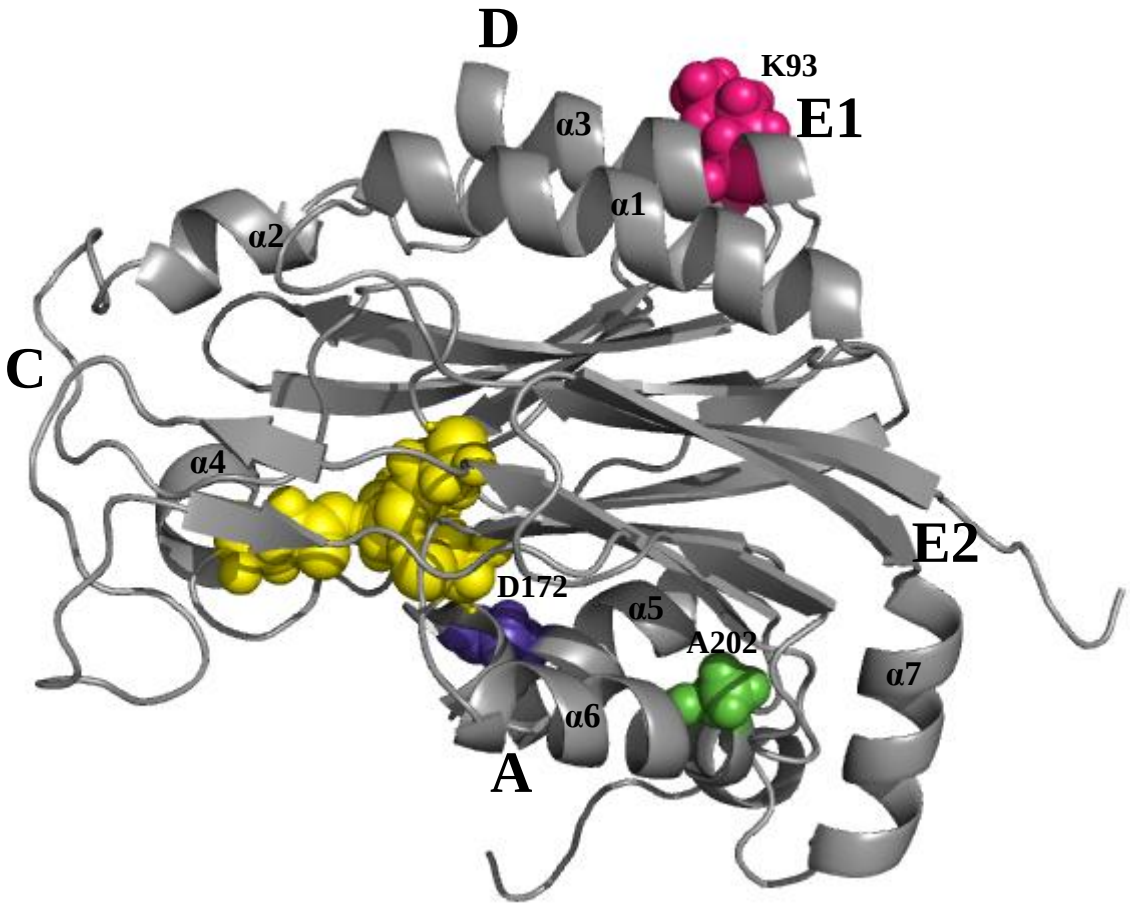

FIG.3.10. Monomer model of $CynD_{pum}$ showing residues K93, D172 and A202. Figure was constructed using PyMOL (Accession No AAN77004) based on the coordinates from Jandhyala *et al*. (62). The catalytic tetrad is shown in yellow, K93 in pink, D172 in purple and A202 in green. E327 is not represented due to the lack of structure of the C-terminal region.

A surface mutants: D172N and A202T

The proposed model of $CynD_{pum}$ suggests that the elongation of the spiral arises from the interactions at the A, dimerization surface and C, oligomerization surface. The A surface is the dimerization surface, formed by two α helices, α5 and α6. The interactions across this surface are important for connecting the monomer subunits together. It was also suggested that they are important for positioning the catalytic residue C164 in the active site (74). Mutations at this interface lead to loss of activity of the enzyme (126). D172N and A202T are located on these α5 and α6 helices respectively (FIG.3.10) but their effect on enzyme activity differs.

A202 is highly conserved in the nitrilase superfamily. The A202T mutant is inactive, a phenotype similar to another α6 A surface mutation, Y201D/A204D and a deletion of residues 219-233 (126). The majority of the A202T protein was found aggregated in the pellet indicating the mutant is not folded normally (FIG.3.4). If α6 is crucial for dimerization and A202 has a crucial role on this surface, a threonine at this position may disrupt critical interactions and destabilize the protein. This idea is supported by the restoration of activity when A202T was introduced with D172N, a mutant with increased stability (FIG.3.6). D172N, also at the A surface, stabilized to some degree A202T but did not quite restore wild-type stability. The other stability mutants K93R and E327K did not restore function to the A202T mutant (FIG.3.4). However, these residues are not at the A surface and for that reason are perhaps unable to suppress the A202T defect.

On the other hand, D172N retained full activity. Its affinity for the substrate at pH 7.7 was 2-fold higher than the native enzyme but its maximal velocity was only 50% (TABLE 3.3 and FIG.3.7). This activity was higher at pH 7 than pH 8 by about 35% whereas the wild-type activity at this pH decreased by 20% (FIG.3.8)

D172 is located on the α5 helix of the A surface and D172N mutation had the opposite effect on stability than A202T (FIG.3.7). It increased the enzyme stability compared to wild-type. It was not surprising that the mutation affected the stability of the enzyme since the A surface is important for the dimerization of the subunits. On the other hand, D172N led to some changes in the enzyme's kinetics as well and, based on the proposed model for $CynD_{pum}$, D172 is in proximity of the active site (FIG.3.11).

Previously, it was suggested that residues on α5 helps position the catalytic cysteine in the active site through strong hydrogen bonds (74). This raises the possibility that D172N mutation modified the affinity and the reaction rate by affecting the positioning of C164 residue, or other catalytic residues, in the active site.

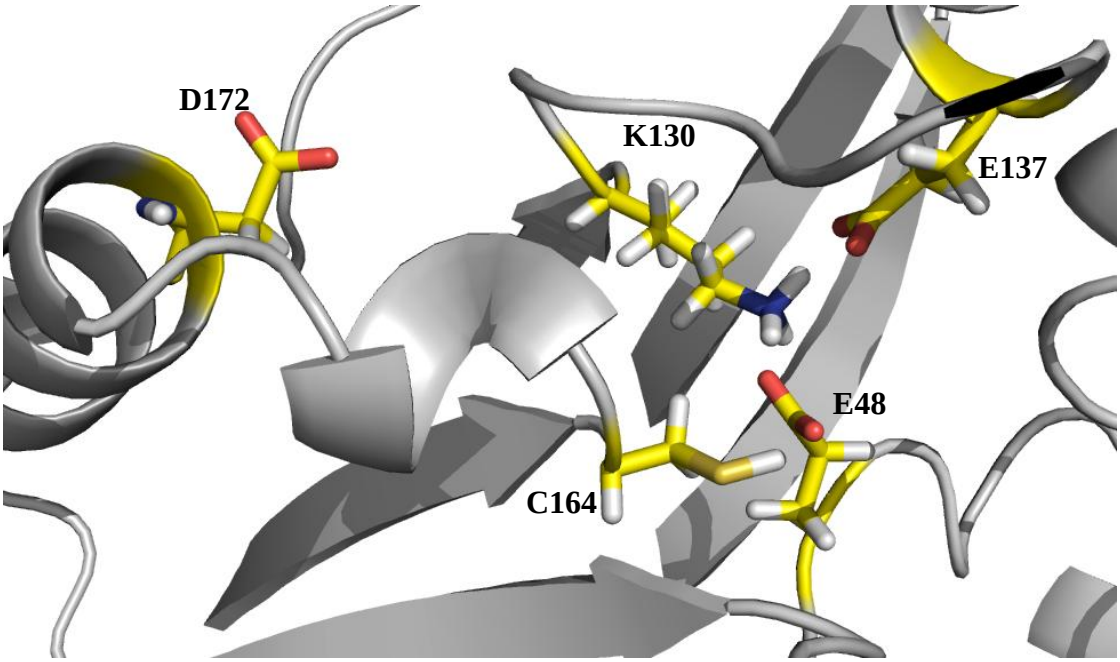

FIG.3.11. A close-up view of the catalytic tetrad and D172 on α5 helix of $CynD_{pum}$. Figure was constructed using PyMOL (Accession No AAN77004) (62). The active site is comprised of E48, K130, E137 and C164.

D/E surface mutant: K93R

Based on the model for $CynD_{pum}$ (62), K93 is proposed to be involved in the interactions at the E surface (Fig.3.10). Unlike the interactions at A and C surfaces that elongate the spiral, interactions at the E surface are thought to terminate the helix by tilting the last dimer and reducing the diameter of the spiral and thus prevent additional dimers from adding (126) (FIG.3.12 and FIG.3.13).

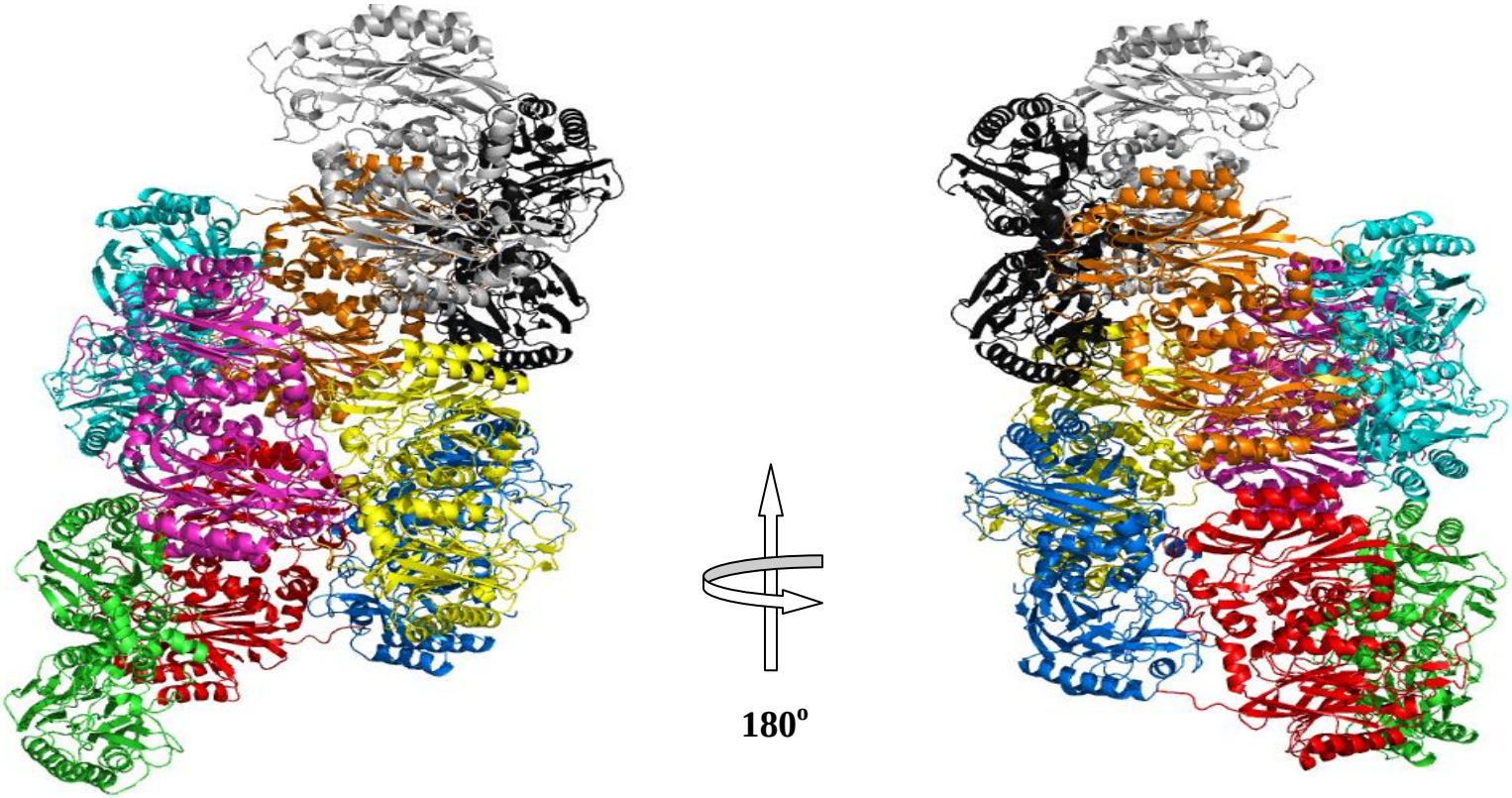

FIG.3.12. The 18-subunit oligomeric structure of $CynD_{pum}$ (Accession No AAN77004) (62). Dimers are colored differently with first dimer shown in green and last dimer in gray. The E surface putative interactions occur due to the tilting of the terminal dimers (grey and green).

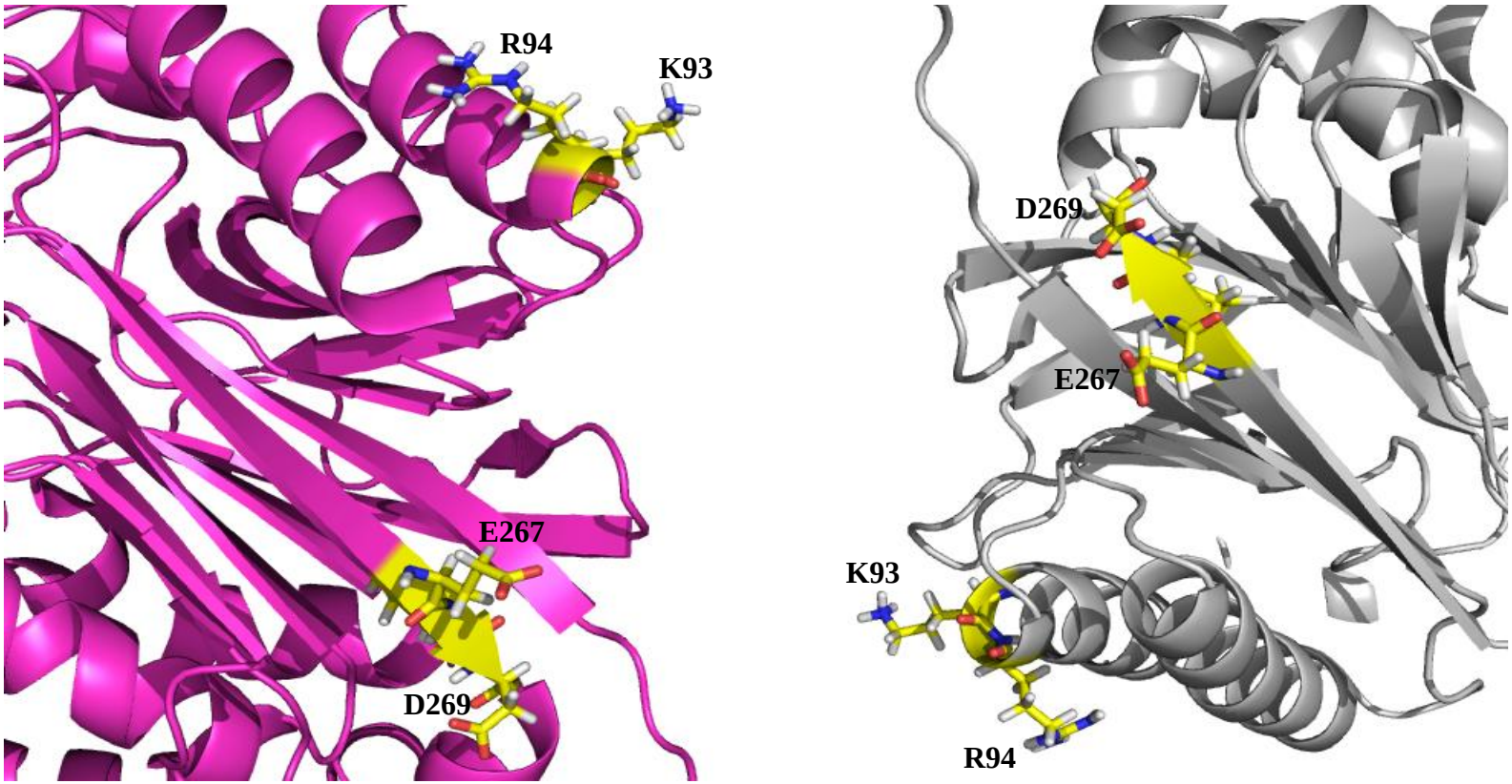

FIG.3.13. A close-up view of the putative E surface of two dimers. The model is based on the low resolution structure of $CynD_{pum}$ (Accession No AAN77004). Interactions between the positively charged residues 93KR94 and negatively charged E267 and D269 are thought to cause the termination of the 18-subunit spiral.

Nitrilases that occur as long spirals such as *R. rhodochrous* J1 nitrilase (136) and $CynD_{pum}$ at pH 5.5 (62) might have structural changes in the C-terminal region disrupting the E surface. At pH 5.4, $CynD_{pum}$ exists as long fibers (62). This effect was reversible and pH dependant implicating the involvement of three histidines in the carboxy-region which become protonated at pH 6. The protonated histidines are proposed to cause a repulsion of the C-terminus of the different subunits located in the center of the spiral leading to an expansion of the diameter and disruption of the E surface. Thus, additional subunits can now be added to the oligomer extending the spiral without termination.

The putative residues involved in this E surface interaction are the highly conserved negative charged residues of the E2 region 267EID269 at the end of strand β14 and the positive charged residues of the E1 region 93KR94 on the carboxy-terminal end of α3 (FIG.3.13). It is speculated that these two regions interact to form the E surface. The highly similar $CynD_{stut}$ and more distant CHT_{sorghi} and CHT_{crassa} all have an arginine at position 93. Even though lysine and arginine are both positively charged, changing one for the other can have big impact on the protein. Lysine has a single amino group which limits the number of hydrogen bonds it can form with the negatively charged E2 surface. However, due to its guanidinium group, arginine makes multiple hydrogen bonds. Thus the K93R mutation might be strengthening the interactions at the E surface and stabilizing the spiral through increasing the hydrogen bonds at that surface.

Another hypothesis for the effect of K93R can be based on the phenotype of a different mutant, Q86R (144). Q86 is part of the D surface which is formed by α1 and α3 (FIG.3.14). Positively and negatively charged residues are found on this surface and the electrostatic interactions between charged residues at this surface occur when the spiral completes one turn.

Wang *et al*. showed that Q86R created a more stable enzyme than the wild-type. At pH 9, the mutant formed elongated helices similar to the ones seen at pH 5.5 (144). The wild-type enzyme forms elongated helices at pH 5.5 but short spirals at pH 9 as described earlier. It was suggested that Q86R mutation is stabilizing the D surface thus increasing the stability of the protein.

Thuku *et al*. also suggested that in the nitrilase of *Rhodococcus rhodochrous* J1, residue R94 which correspond to K93 in $CynD_{pum}$ forms a salt bridge with residue D91 (E90 in $CynD_{pum}$) across the D surface (136). Similar to the Q86 mutant, *Rhodococcus rhodochrous* J1nitrilase forms elongated helices. This transition from inactive dimers to helical oligomer is permitted after 39 amino acids in the C-terminus are post-translationally auto-catalytically cleaved. This auto-cleavage of part of the C-terminal region is required for the activity of the enzyme. Only the oligomeric structure of the nitrilase is active. The steric obstruction caused by the last 39 amino acids might prohibit interactions necessary for helix formation. It is thought that the extension of the carboxy-region interferes with the A and C surface blocking the dimers from oligomerizing.

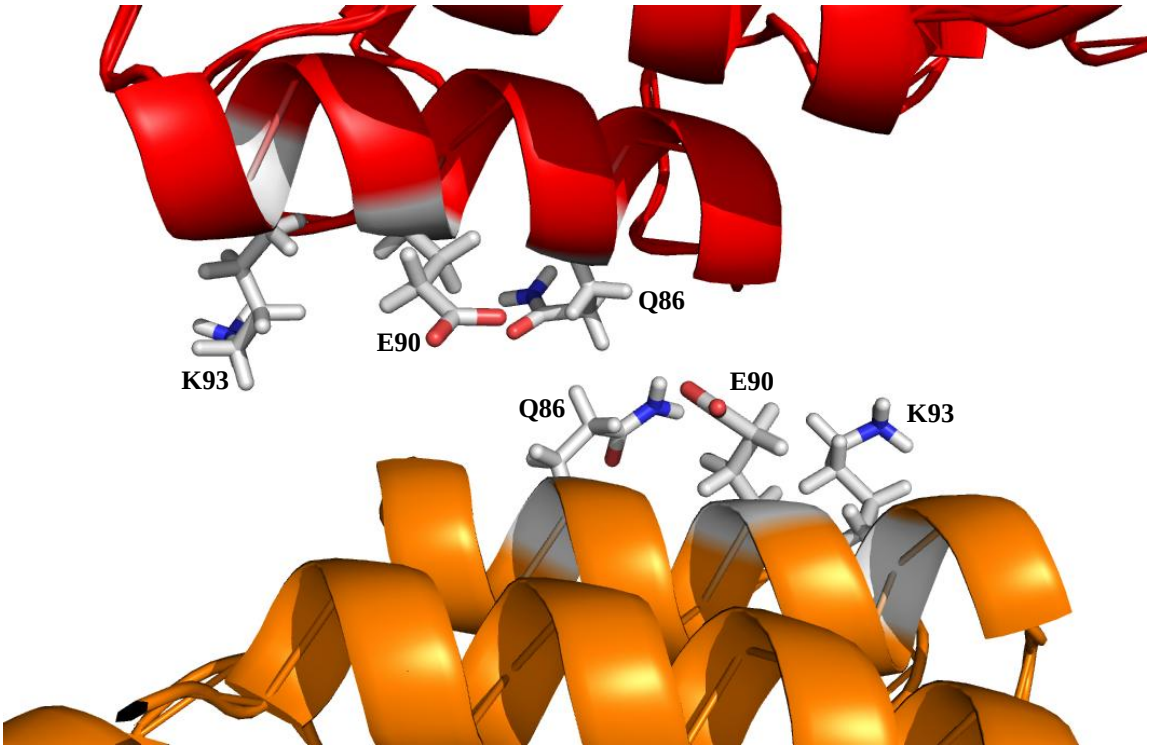

FIG.3.14. Model of D surface showing Q86, E90 and K93 residues on α3 helix of $CynD_{pum}$. The image was reconstructed using PyMOL based on the structure model of $CynD_{pum}$ (Accession No AAN77004) from Jandhyala *et al*. (62).

Based on the interactions across the D surface described in *Rhodococcus rhodochrous* J1, it might be possible, in the case of the Q86R and K93R mutants, that the arginine is responsible for creating stronger salt bridges across the D surface with the negatively charged residues found on the opposite α3 helix (FIG.3.14). This interaction might be disrupting of the E surface interactions between K93R and region 267EID269 by tilting the α3 helix and pulling K93R residue away from the E surface and closer to the D surface interface.

Thus the K93R mutation might actually be stabilizing the D surface with arginine increasing the hydrogen bonding with E90 and other negatively charged amino acids found at this surface. It will be interesting to see if K93R forms long helices at pH 9 similar to Q86R mutant and *Rhodococcus rhodochrous* J1 nitrilase.

C-terminal region mutant: E327K

E327 is located in the carboxy-terminal region. In the microbial nitrilases, this surface is an extension of 30 to 60 amino acids. No structural data of this region is available due to lack of sequence identity with related crystallographically determined structure but it is thought to be formed by 4 α helices, α8-α11 (135). The nitrilases in the superfamily used for the protein docking lacked this extension and the low resolution cryo-electron microscopy failed to show clear detail. However, due to electron densities observed in the 3D reconstruction models, it was speculated that it is located in the center of the spiral. Studying the effects of various C-terminal truncations has led to clues on the role and location of this extension. Deletion of more than 28 amino acids from the $CynD_{pum}$ C-terminus disrupted its activity but shorter deletions remained active *in vivo* (126).

The same result was seen in the *R. rhodochrous* J1 nitrilase which lost activity when 55 C-terminal residues were deleted. However, the enzyme performs an auto-cleavage of 39 amino acids from its tail in order to form active oligomers (136). Thus, it was speculated that this region might be interacting with the A and C surface and was important for the oligomerization of the protein.

Another interesting role of the C-terminus is seen in the elongation of the spiral. As mentioned earlier, the nitrilase C-terminus is thought to be located in the center of the spiral. $CynD_{pum}$ at pH 8 formed short 18-subunit helices. However at pH 5.5 extended spirals were seen and this effect was reversible. It is believed that changes in side chain charges of histidines found in the carboxy-terminus lead to an increase in helix length. At pH 5.5, three histidines, H305, H308 and H323 are protonated and would cause the tails to repulse disrupting the E surface and elongating the spiral. Lysine substitution of these histidines residues increased the stability of wild-type (personal communication of unpublished data from Dr. Sewell). H323K which is in proximity to E327 increased the stability. Based on the model, both residues H323 and E327 are located on the α11 helix. This indicates that E327 might be acting at the same surface, either A or C just like H323. The positive charge that the lysine brings stabilizes the surface similarly whether it is at position 323 or 327.

E327K mutation increased the stability of the enzyme. However, its effect on stability was modest compared to that of K93R and D172N. E327 residue was also identified in a previous study for a mutant E327G increasing the pH tolerance of the nitrilase *in vivo* (144). In that case, the change was from glutamic acid, a negatively charged amino acid to glycine, a hydrophobic residue. This pH tolerance is thought to be a result of the enzyme's stabilization at this alkaline pH. A similar phenotype was noted for E327K *in vivo* where it degraded cyanide at pH 9. The role of the C-terminus will be further discussed in Chapter IV.

CONCLUSION

In this study, I characterized the K93R, D172N, A202T and E327K mutations of $CynD_{pum}$ and described their effects on the enzyme's characteristics from increasing the affinity to the substrate to increasing the V_{max} as well as on stability. From the results, it is clear that interactions at the D/E and A surfaces as well as the C-terminal extension are important for enzyme stability. An accurate structure of $CynD_{pum}$ would enlighten the mechanism of this phenotype, but that remains elusive.

CHAPTER IV

IDENTIFICATION OF C-TERMINAL RESIDUES REQUIRED FOR $CynD_{stut}$ ACTIVITY

OVERVIEW

Nitrilase enzymes are members of the nitrilase superfamily that include amidases, biotinidases, NAD synthetases, carbamylases and N-acyltransferases. There is significant interest in them due to their potential commercial use. Nitrilases hydrolyze organic nitriles to carboxylic acids and ammonia under mild acidic or basic reaction conditions and low temperatures. Thus, biocatalysis using nitrilases has become an important tool in industrial and pharmaceutical applications, a prominent example being the hydrolysis of racemic mandelonitrile to R-mandelic acid, a precursor of various drugs, by an *Alcaligenes* nitrilases (153). However, most of the nitrilases show a low degree of enantioselectivity and stability, important qualities for industrial enzymes (124), and directed evolution has been used to ameliorate the deficiency reaction specificity of these enzymes (32, 152).

Currently, there are no crystal structures available for any member of the nitrilase branch of the nitrilase superfamily. Other members of the superfamily do have solved structures such as a Dcase (N-carbamoyl-D-amino acid amidohydrolase) from *Agrobacterium* sp. strain KNK712 (98), a NitFhit (nit-fragile histidine triad fusion) protein from *Caenorhabditis elegans* (105), a putative cyanide hydrolase from *Saccharomyces cerevisiae* (74) and several amidases (3, 58). Based on low resolution

electro-microscopy and alignment of sequences of related crystallographically determined structures, a model has been predicted for several members of the branch (62, 125).

All nitrilases possess a similar structure to that of Dcase and NitFhit with minor differences. The monomers fold in an αββα structure and then form αββα-αββα dimers which are the building blocks for the oligomeric structure. An important difference found between the nitrilases and the known crystal structures was in the carboxy-terminal region. Microbial nitrilases from *Bacillus pumilus* (62), *Pseudomonas stutzeri* (125), *Neurospora crassa*, *Gloeocercospora sorghi* and other microbes (10) and the crystalline amidases from *Helicobacter pylori* (58), *Geobacillus pallidus* (3) and *Pseudomonas aeruginosa* (6) all show an extension of the C-terminal region. This extension varies in length between the members of the superfamily.

Secondary structure predictions for this region were different for all the superfamily enzymes due to the highly variable sequences (135). Thus, no predictions of structural data exist for the C-terminal domain in the proposed models for nitrilases and interactions of this region with the other surfaces remain elusive.

Several studies have been conducted to understand the role of the C-terminus. The effects of mutations, deletions and swapping of this region were different for each nitrilase. The nitrilase from *Rhodococcus rhodochrous* J1 is normally found as inactive dimers. Following post-translational deletion of 39 C-terminal amino acids, the enzyme formed stable active helices (136). This natural process is thought to be an autoproteolysis and deletion of more or fewer residues led to formation of inactive “c”

shaped aggregates. This suggests that residues of this region are important for the oligomerization and activity of the enzyme.

A similar phenotype was seen with C-terminal deletions of an arylacetonitrilase from *Pseudomonas fluorescens* EBC191 (69). This enzyme transforms different phenylacetonitriles with some enantioselectivity to the corresponding carboxylic acids. With longer deletions, the enzyme's nitrilase activity, stability and enantioselectivity were reduced. Mutants with up to 32 C-terminal amino acids deleted had similar properties to the wild-type. However, mutants with 47 to 67 C-terminal amino acids removed demonstrated a decrease in activity; only 10% of the activity remained compared to wild-type (69). The stability and enantioselectivity also decrease combined with increase in amide formation. Longer C-terminal deletions abolished the activity of the arylacetonitrilase. However, when up to 59 amino acids in the C-terminal region were swapped with that of other nitrilases from *Rhodococcus rhodochrous* or *Alcaligenes faecalis*, the enzyme was active and had similar enantioselectivity and amide formation in comparison to the wild-type (69).

The cyanide dihydratase from *B. pumilus* and *P. stutzeri* also show significant difference in sequence and behavior of their C-terminus. Alignment of $CynD_{pum}$ and $CynD_{stut}$ amino acid sequences reveals an overall 76% identity with significant divergence at the C-terminus. A conserved motif D-(P/S)-X-G-H-Y was detected when C-terminus sequences from bacterial, fungal and plant nitrilases were aligned (69, 135). Other members of the superfamily do not show this motif suggesting a functional significance for the nitrilases. Beyond this conserved motif, the C-terminus sequences

diverge and show very little conservation. In the case of CynD$_{pum}$ and CynD$_{stut}$, the motif is found at position 281-286. CynD$_{pum}$ and CynD$_{stut}$ are 330 and 334 amino acid proteins respectively, followed by a further conserved 11 amino acids. However, beyond residue 297, only 30% identity is observed between the two C-termini.

A series of C-terminal truncations were generated and analyzed (126). CynD$_{pum}$ deleted for the majority of the C-terminus (CynD$_{pum}$ Δ 303) had full activity *in vivo* suggesting no role of the C-terminal on the enzyme activity. But further deletion of CynD$_{pum}$ to residue 293 had partial activity. Deletion beyond that point, the enzyme was inactive. On the other hand, deletion of CynD$_{stut}$ only to residue 310 rendered the enzyme inactive as did any further deletions.

Hybrid enzymes were also constructed (126). The CynD$_{pum}$ C-terminus was replaced by that of CynD$_{stut}$ after the conserved motif D-P-X-G-H-Y and the hybrid remained fully active. However, when the CynD$_{stut}$ C-terminus was replaced with the CynD$_{pum}$ C-terminus, the enzyme had no activity. These results emphasized the importance of this highly variable region especially on the activity of CynD$_{stut}$ yet did little to clarify its role.

In addition, the C-terminus is thought to have some effects on the oligomerization of the enzyme. At pH 8, CynD$_{pum}$ formed 18-subunits spirals. However at pH 5.4, the enzyme was found as long spirals (62). This effect was reversible and pH dependant suggesting the possible involvement of three histidines found in the C-terminus of CynD$_{pum}$ C1which would become protonated at pH 6. Another *Bacillus pumilus* strain, strain 8A3 contains a CynD highly similar to that of C1 (97% identical)

with only 10 different amino acids out of 330 residues (62). When compared to CynD$_{pum}$ C1, 7 out of the 10 different residues were found in the C-terminus of CynD$_{pum}$ 8A3. CynD$_{pum}$ 8A3 does not have any histidines in the C-terminus nor does it form long spirals at pH 5.4. Thus, it was suggested at pH 5.4 the protonated histidines cause a repulsion of the C-termini of the different subunits located in the center of the spiral leading to an expansion of the diameter and disruption of the E surface, the spiral terminating surface, and elongation of the spiral (135).

A slight increase in specific activity was also detected at pH 5.4 with CynD$_{pum}$ (63). Oligomerization is thought to be required for catalytic activity by helping position the catalytic residues, especially E137 (in the case of CynD$_{pum}$ C1), in the active site. Thus, the increase in specific activity at pH 5.4 was proposed to be the result of activation of the terminal monomers of the short spiral due to the formation of significantly longer oligomers, resulting in fewer terminal monomers.

Even though CynD$_{pum}$ is tolerant to changes and deletions in its C-terminus, mutations at residue 327 of CynD$_{pum}$ resulted in a more stable variant as described in chapter III and by Wang *et al*. (144). Mutations at this residue were selected in 2 independent screens for improved enzyme activity, the first at pH 10 and the second at pH 7.7.

This study aims to better understand the role of the C-terminus in determining the stability and the activity of the dihydratase and the hydratase enzymes and to better explain the results of the C-terminus swap hybrids. Measurements of activity and stability were performed for CynD$_{pum}$, CynD$_{stut}$ and CHT$_{crassa}$ C-terminus deletions and

the activity of several hybrids was also tested. Comparison of non-conserved residues led to the identification of residues in $CynD_{stut}$ C-terminus necessary for the activity of the enzyme but missing in $CynD_{pum}$.

MATERIALS AND METHODS

Culture media and reagents

All strains were grown in LB broth. Antibiotics were used at concentrations of 100 ug/ml of ampicillin, 25 ug/ml of kanamycin or 25 ug/ml of chloramphenicol.

Bacterial strains and plasmids

E.coli strain MB3436 [Δ*endA thiA hsdR17 supE44 lacI*^{q}*ZΔM15*] was used as the host strain for DNA manipulations. *E.coli* strain MB1837 [BL21 (DE3) pLysS] was used to express the proteins. A synthetic gene encoding the *P. stutzeri* cyanide dihydratase was used instead of the original bacterial gene. The synthetic gene contains *E. coli* optimized codons and additional restriction sites but encodes the same $CynD_{stut}$ protein as the wild-type gene. The plasmids used are described in TABLE 4.1.

TABLE 4.1 List of plasmids used in this study.

Plasmids	Description	Reference
p4276	pEt26b carrying synthetic *P. stutzeri cynD*	This work
p5277	pEt28a p4276	This work
p2890	pEt26b carrying *B. pumilus* C1 *cynD*	Jandhyala *et al.* 2003
p4406	pEt28a carryimg p2890	this work
p3418	pBS carrying *N. crassa cht*	Basile *et al.* 2008
P4951	p3418 BstBI	This work
p3460	pEt26b carrying *N. crassa cht*	Basile *et al.* 2008
Tail deletions		
p3326	p2890 Δ279	Sewell *et al.* 2005
p3052	p2890 Δ293	Sewell *et al.* 2005
p3319	p2890 Δ303	Sewell *et al.* 2005
p4948	p3460 Δ307	This work
p4949	p3460 Δ323	This work
p4950	p3460 Δ339	This work
p3328	pEt26b carrying *P.stutzeri* cynD Δ302	Sewell *et al.* 2005
p5067	p4276 Δ310	This work
p4959	p4276 Δ330	This work
Hybrids		
p3407	pEt26b carrying Stut-Pum	Sewell *et al.* 2005
p3411	pEt26b carrying Pum-Stut	Sewell *et al.* 2005
p4956	pEt26b carrying Crassa-Stut	This work
p4972	pEt26b carrying Stut-Crassa	This work
p4993	pEt26b carrying Pum-Crassa	This work
p5026	pEt26b carrying Crassa-Pum	This work
p5389	pEt28a carrying Pum-Stut	This work
p5383	5389 K93R	This work

TABLE 4.1 Continued.

Plasmids	Description	Reference
P. stutzeri CynD alanine scanning		
p5158	p4276 G306A	This work
p5159	p4276 E306A	This work
p5160	p4276 R306A	This work
p5161	p4276 D306A	This work
p5162	p4276 S306A	This work
p5163	p4276 T306A	This work
C-terminal mutants		
p5042	p3407 322HGILto 322VSDE	This work
p5044	p5042 306NHQKNE to 306GERDST	This work
p5046	p3407 306NHQKNE to 306GERDST	This work
p5100	p3407 H307D Q308K K309E	This work
p5182	p3407 N306G Q308R E311T	This work
p5214	p3407 N306G K309D	This work
p5244	p3407 N306G H307E	This work
p5249	p4972 306VDRNGG to 306GERDST	This work
p5250	p5046 306GERDST to 306 NHQKNE	This work
p5253	p3407 H307E	This work
p5365	p5046 320YQHGILEEK to 320LSVSDEEPV	This work
p5367	p3407 320YQHGILEEK to 320LSVSDEEPV	This work

C-terminal amino acids deletion

Nitrilase alleles with deletions in their C-termini were constructed using Phusion High-Fidelity PCR Master Mix with HF Buffer (New England Biolabs) and the primers are listed in TABLE 4.2. The primers were designed to add a stop codon at the desired position with deletion of the remaining gene in order to avoid any readthrough expression of the wild-type protein. The mutations were confirmed by DNA sequencing. The enzymes were expressed in the cells and activity was tested using whole cells mixed with 4 mM HCN in 1 M MOPS pH 7.7 for 30 min at room temperature. Picric acid was added to detect remaining cyanide.

TABLE 4.2 Primers used for C-terminal deletions.

Primers	Sequence
N. crassa BstBI'F	5'-CTTTGCTGGACACTATTCGAACCCGGATCTCATTCG TCT
N. cras d307 R	5'- AAGTGAAGCTTAGAGATCCGGCCGCATGTAG
N. cras d323 R	5'- AAGTGAAGCTTACACCTCGGTGACGAGCTC
N. cras d339 R	5'- AAGTGAAGCTTAGCCCAAGCGCTCGCGC
P. stut d310 R	5'-CTAATCGTCTCGAGTTAATCGCGTTCACCGATTTTGCG
P. stut d330 R	5'- CATAATGAGCTCACACAACAGGTTCCTCATCAG

Hybrid constructs

The BstBI restriction site was introduced in cht_{crassa}, $cynD_{pum}$ and $cynD_{stut}$ at nucleotides position 903, 858, 855 respectively which represents the same residue in the protein. C-terminal swaps were constructed using this BstBI site and a XhoI site at the end of each gene. $CynD_{pum\text{-}stut}$ hybrid (N-terminal $CynD_{pum}$ and C-terminal $CynD_{stut}$) constructs were described in Sewell *et al.* 2005.

$CynD_{stut\text{-}pum}$ and $CynD_{stut\text{-}crassa}$ mutagenesis

In order to introduce different mutation in the C-terminal region of the $CynD_{stut\text{-}pum}$ and the $CynD_{stut\text{-}crassa}$ hybrids, the C-terminal sequence was divided into 3 parts starting from the BstBI restriction site at nucleotide position 855 in the $cynD_{stut}$ gene. Then three sets of overlapping primers were annealed to reconstitute the C-terminal domain. A list describing the DNA primers and their sequences is shown in TABLE 4.3.

TABLE 4.3 Primers used for C-terminal mutagenesis.

Overlapping Primers	Sequence
Pum tailA F	5'- CGAATCAAAGTTTGAGTATGAATTTTA ATCAGCAGCCCACTCCTGTTGTGAAA
Pum tailA R	5'- CTGCTGATTAAAATTCATACTCAAACTTTGATT
Pum tailB F	5'- CATTTAAATCATCAAAAAAATGAAGTATTCACcTATGA GGACATT
Pum tailB R	5'- TACTTCATTTTTTTGATGATTTAAATGTTTCACAACAGGA GTGGG
Pum tailC F	5'- CAATATCAACATGGTATACTGGAAGAAAAAGTTTAAGAA TTCc
Pum tailC R	5'- TCGAGGAATTCTTAAACTTTTTCTTC CAGTATACCATGTTGATATTGAATGTCCTCATAGGTGAA
$CynD_{pum}$ 307NHQKNE to 307GERDST	
muttailB F	5'- CATTTAGGTGAACGCGATAGCACCGTATTCACcTATGAG GACATT
muttailB R	5'- TACGGTGCTATCGCGTTCACCTAAATGTTTCACAACAGGA GTGGG
$CynD_{pum}$ 323HGIL to 323VSDE	
muttailC F	5'- CAATATCAAGTTTCTGATGAGGAAGAAAAAGTTTAAGA ATTCC
muttailC R	5'- TCGAGGAATTCTTAAACTTTTTCTTCCTCATCAGAAACTT GATATTGAATGTCCTCATAGGTGAA
$CynD_{pum}$ 320YQHGILEEK to 320LSVSDEEPV	
tailC mut2 F	5'- CAATTGTCGGTTTCTGATGAGGAACCAGTCGTTTAAGAAT TCC
tailC mut2 R	5'- TCGAGGAATTCTTAAACGACTGGTTCCTCATCAGAAACCG ACAATTGAATGTCCTCATAGGTGAA
CHT_{crassa} 322VDRNGG to 322GERDST	
muttail B F	5'- CGCAAGGAGCTCGTCACCGAGGGTGAACGCGATAGCACG ATCGTGCAGTACTCGACGCGC
muttail B R	5'-GCGCGTCGAGTACTGCACGATCGTGCTATCGCGTTCACCC TCGGTGACGAGCTCCTTGCG

Site directed mutagenesis

The mutagenesis reactions were carried out using 25ul Phusion High-Fidelity PCR Master Mix with HF Buffer (New England Biolabs), 150 ng dsDNA template and 100ng of each of the forward and reverse primers. MQH_2O was added to the reaction mixture for a total volume of 50ul. Each reaction was run for 18 cycles. The mutagenic primers are listed in TABLE 4.4. The mutations were confirmed by DNA sequencing.

TABLE 4.4 Site directed mutagenesis primers.

Primers	Sequence
Pum 308DKE F	5'- GTTGTGAAACATTTAAATGATAAAGAAAATGAAGTATT CACGTATGAGGACATTCAATAT
Pum 308DKE R	5'- ATATTGAATGTCCTCATACGTGAATACTTCATTTTCTTT ATCATTTAAATGTTTCACAAC
Pum N307G K310D F	5'- TGTTGTGAAACATTTAGGTCATCAAGACAATGAAGTA TTCACGTATGAGGACATTCAATA
Pum N307G K310D R	5'- TATTGAATGTCCTCATACGTGAATACTTCATTGTCTTG ATGACCTAAATGTTTCACAACA
Pum N307G Q309R E312T F	5'- CTGTTGTGAAACATTTAGGTCATCGAAAAAATACAG TATTCACtTATGAGGACATTCA

TABLE 4.4 Continued.

Primers	Sequence
Pum N307G Q309R E312T R	5'- TGAATGTCCTCATAAGTGAATACTGTATTTTTTCGATGA CCTAAATGTTTCACAACAG
Pum N307G H308E F	5'- GTTGTGAAACATTTAGGTGAGCAAAAAAATGAAGTATT CACGTATGAGGACATTCAA
Pum N307G H308E F	5'- TTGAATGTCCTCATACGTGAATACTTCATTTTTTTGCTCA CCTAAATGTTTCACAAC
Pum H308E F	5'- GTGAAACATTTAAATGAGCAAAAAAATGAAGTATTCAC CTATGAGGACATTCAA
Pum H308E R	5'- TTGAATGTCCTCATAGGTGAATACTTCATTTTTTTGCTC ATTTAAATGTTTCAC

CynD$_{stut}$ 306GERDST domain alanine scanning

Overlapping primers were used to reconstitute the CynD$_{stut}$ C-terminus with mutations G306A, E307A, R308A, D309A, S310S or T311A. The different primers and their sequences are listed in TABLE 4.5.

TABLE 4.5 Overlapping primers used for $CynD_{stut}$ C-terminus alanine scanning.

Overlapping primers	Sequence
Stut tailA F	5'- CGAACCAGTCTCTGTCCATGAACTTTAACCAATCTCCGA ACCCGGTTGTTCGCAAAATC
Stut tailA R	5'- GGTTCGGAGATTGGTTAAAGTTCATGGACAGAGACTGGTT
Stut tailC F	5'- AGGAACCTGTTGTGCGTTCCCTGCGTAAATGACCATGGA AGCTTGCTATTGC
Stut tailC R	5'- GCAATAGCAAGCTTCCATGGTCATTTACGCAGGGAACGC ACAACAGGTTCCTCATCAGAAACGGACAGG
G306A F	5'- GCCGAACGCGATAGCACCGTATTCACTTACGACGACCT GAACCTGTCCGTTTCTGATG
G306A R	5'- TTCAGGTCGTCGTAAGTGAATACGGTGCTATCGCGTTCG GCGATTTTGCGAACAACCG
E307A F	5'- GGTGCCCGCGATAGCACCGTATTCACTTACGACGACCT GAACCTGTCCGTTTCTGATG
E307A R	5'- TTCAGGTCGTCGTAAGTGAATACGGTGCTATCGCGGGCA CCGATTTTGCGAACAACCG
R308A F	5'- GGTGAAGCCGATAGCACCGTATTCACTTACGACGACCT GAACCTGTCCGTTTCTGATG
R308A R	5'- TTCAGGTCGTCGTAAGTGAATACGGTGCTATCGGCTTC ACCGATTTTGCGAACAACCG
D309A F	5'- GGTGAACGCGCCAGCACCGTATTCACTTACGACGACCT GAACCTGTCCGTTTCTGATG
D309A R	5'- TTCAGGTCGTCGTAAGTGAATACGGTGCTGGCGCGTTCAC CGATTTTGCGAACAACCG

TABLE 4.5 Continued.

Overlapping primers	Sequence
S310A F	5'- GGTGAACGCGATGCCACCGTATTCACTTACGACGA CCTGAACCTGTCCGTTTCTGATG
S310A R	5'- TTCAGGTCGTCGTAAGTGAATACGGTGGCATCGCGTT CACCGATTTTGCGAACAACCG
T311A F	5'- GGTGAACGCGATAGCGCCGTATTCACTTACGACGAC CTGAACCTGTCCGTTTCTGATG
T311A R	5'- TTCAGGTCGTCGTAAGTGAATACGGCGCTATCGCGTT CACCGATTTTGCGAACAACCG

Activity and stability measurements of deletion mutants

Overnight cultures of BL21 (DE3) cells transformed with each expression plasmid were induced with IPTG as described previously in Chapter III. The induction continued at 37^{o}C for 3 hours. 1 ml of cells carrying wild-type and variant genes was adjusted to a similar OD600 of 0.3. 200ul of cells were added to 800 ul of 50 mM MOPS pH 7.7. 4mM of cyanide was added and the reaction was carried out at room temperature. 100ul of the mixture was removed every 2 min and the reaction was terminated by adding 100ul of picric acid reagent (0.5% picric acid in 0.25 M sodium carbonate). The mixture was incubated in a 100^{o}C heat block for 5 min to allow color development and the absorbance was measured at 540 nm.

To test stability, the cells were lysed as described in Chapter III. 80 ul of each cell lysate were resuspended in 4 ml 50 mM MOPS pH 7.7 and tubes were left in a water bath at 38^{o}C (CynD) or 42^{o}C (CHT). The stability test was done as described in Chapter III. Nessler reagent was used to measure ammonia production of CynD$_{pum}$, CynD$_{pum}$Δ303, CynD$_{stut}$ and CynD$_{stut}$Δ330 whereas picric acid was used to measure cyanide degradation by the cyanide hydratases CHT$_{crassa}$ and CHT$_{crassa}$Δ339, which do not produce ammonia.

Activity and stability measurements of CynD$_{stut}$ alanine mutants

Wild-type CynD$_{stut}$ along with the alanine mutants were grown in LB kanamycin and induced as described previously in Chapter III. Cells were adjusted to a similar OD600 of 0.3 and 200ul were added to 800 ul of 50mM MOPS pH 7.7. 4 mM cyanide was added to the solution and the reaction was done at room temperature. At different times 100ul of the reaction was combined in a 1.5 ml Eppendorf tube with 100ul picric acid and then placed on heat block at 100^{o}C for 5 min to allow color development. 100 ul of the mixture was then transferred into 96-wells plate and absorbance was determined at OD540 nm using the microplate reader Benchmark Plus from BioRad. The reaction rate of the mutants was then compared to wild-type CynD$_{stut}$. The stability test was performed as described above using clear cell lysates. 80 ul of lysate was added to 4 ml of 0.1 M MOPS pH 7.7 and placed in a water bath at 39^{o}C. At different times, 500ul of the mixture was mixed with 4 mM cyanide and ammonia production was monitored using Nessler reagent (100) by measuring absorbance at 420 nm.

RESULTS

Effect of C-terminal deletions on nitrilase activity

A previous study from our lab looked at the effect of mutating interfacial residues on the nitrilase activity, including deletions in the C-terminal region of two cyanide dihydratases, $CynD_{pum}$ and $CynD_{stut}$ (126). Even though these two bacterial cyanide nitrilases share a high similarity in their amino acid sequence (FIG.4.1), it was clear from the results that $CynD_{pum}$ was more tolerant to deletions than $CynD_{stut}$. *In vivo*, $CynD_{pum}$ Δ303, with 28 amino acids deleted was fully active. With 38 amino acids removed, $CynD_{pum}$ Δ293 was partially active. Larger deletions left the enzyme inactive ($CynD_{pum}$ Δ279). As for $CynD_{stut}$ carboxy-terminal deletions, the results were different. $CynD_{stut}$ Δ310 (25 amino acids removed) and $CynD_{stut}$ Δ302 (33 amino acids deleted) were both inactive.

To extend this study of C-terminal deletions to the cyanide hydratases (CHT), I chose to create similar deletions in CHT_{crassa}. Three different deletions were constructed; CHT_{crassa} Δ339, CHT_{crassa} Δ323 and CHT_{crassa} Δ307. Residue 307 is the position where the alignment with the bacterial CynDs diverged. Thus CHT_{crassa} Δ307 would be similar to $CynD_{pum}$ Δ293 (FIG.4.1). At residue 323, the C-terminal amino acid sequence alignment begins to diverge from other cyanide hydratases such as CHT_{sorghi} (FIG.4.1). One further shorter deletion was also chosen randomly at residue 339.

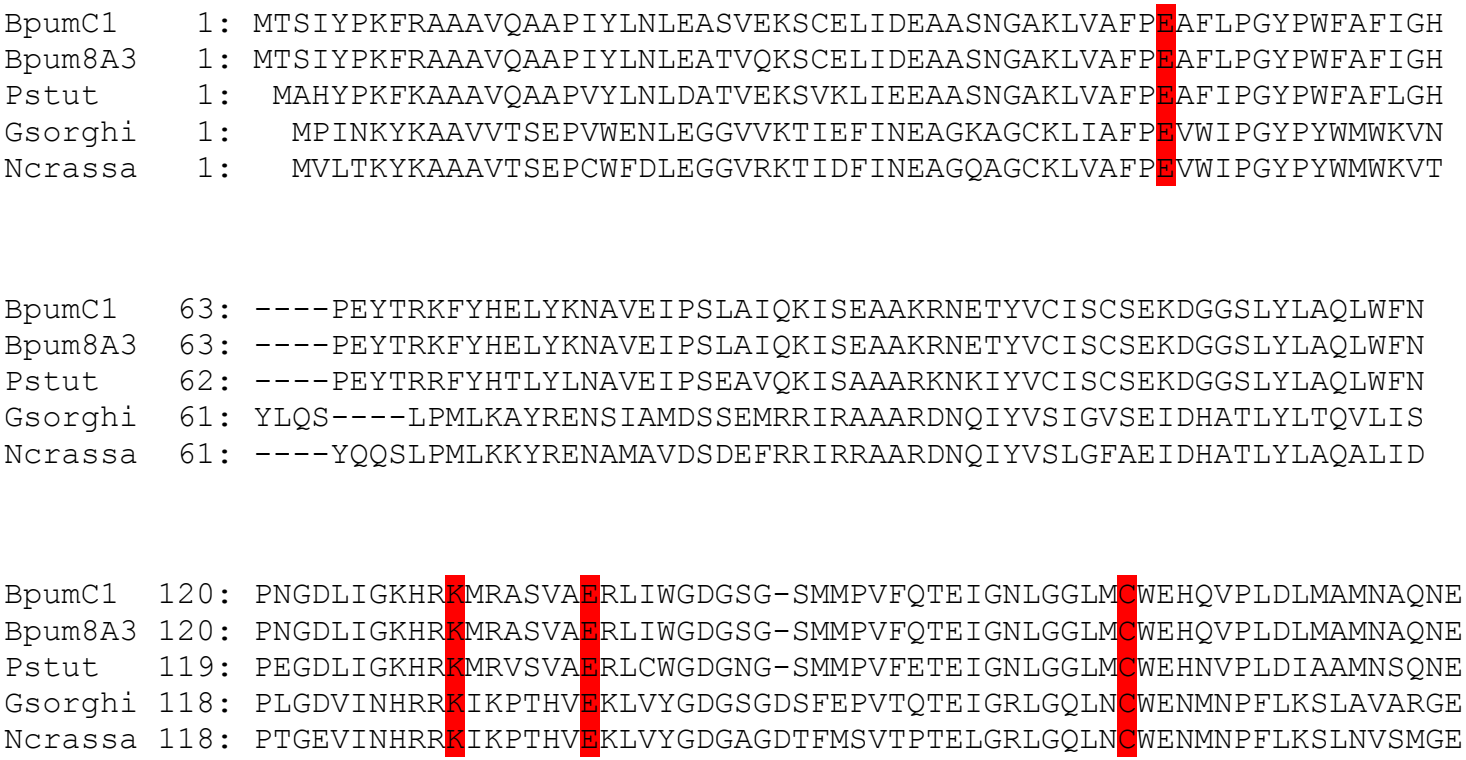

FIG.4.1. Multiple alignments of the sequences of the microbial cyanide nitrilases. The sequences represent nitrilases from $CynD_{pum}$ C1 (BpumC1), $CynD_{pum}$ 8A3 (Bpum8A3), $CynD_{stut}$ (Pstut), CHT_{sorghi} (Gsorghi) and CHT_{crassa} (Ncrassa). The C-terminus region used for the swaps starts at the BstBI site and is shown in grey. Colored in green are the positions of the C-termini deletions. The catalytic tetrad residues are shown in red. Underlined is the conserved sequence D-P-X-G-H-Y region.

FIG.4.1. Continued.

```
BpumC1   182: QVHVASWPGY-----------------FDDEISSRYYAIATQTFVLMTSSIYTEEMKEM
Bpum8A3  182: QVHVASWPGY-----------------FDDEISSRYYAIATQTFVLMTSSIYTEEMKEM
Pstut    181: QVHVAAWPGF-----------------FDDETASSHYAICNQAFVLMTSSIYSEEMKDM
Gsorghi  181: QIHVAAWPVYPDLSKQVHPDPATNYADPASDLVTPAYAIETGTWVLAPFQRISVEGLKR
Ncrassa  181: QIHIAAWPIYPGKETLKYPDPATNVADPASDLVTPAYAIETGTWTLAPFQRLSVEGLKK

BpumC1   224: ICLTQEQRDYFETFKSGHTCIYGPDGEPISDMVPAETEGIAYAEIDVERVIDYKYYIDPAGHY
Bpum8A3  224: ICLTQEQRDYFETFKSGHTCIYGPDGEPISDMVPAETEGIAYADIDVERVIDYKYYIDPAGHY
Pstut    223: LCETQEERDYFNTFKSGHTRIYGPDGEPISDLVPAETEGIAYAEIDIEKIIDFKYYIDPVGHY
Gsorghi  240: HTPPGVEPETDATPYNGHARIFRPDGSLYAKPAV-DFDGLMYVDIDLNESHLTKALADFAGHY
Ncrassa  240: NTPEGVEPETDPSTYNGHARIYRPDGSLVVRPDK-DFDGLLFVDIDLNECHLTKALADFAGHY

BpumC1   287: SNQSLSMNFNQQPTPVVKHLNHQKNEVFTYEDIQYQHGILEEKV
Bpum8A3  287: SNQSLSMNFNQQPTPVVKQLNDNKNEVLTYEAIQYQNGMLEEKV
Pstut    286: SNQSLSMNFNQSPNPVVRKIGERDSTVFTYDDLNLSVSDEEPVVRSLRK
Gsorghi  302: MRPDLIRLLVDTRRKELVTEVGGGDNGGIQSYSTMARLGLDRPLEEEDYRQGTDAGETEKASSNGHA
Ncrassa  302: MRPDLIRLLVDTSRKELVTEVDRNGGIVQYSTRERLGLNTPLENDKEGKK
```

.

Two additional C-terminal deletions were also constructed in the *P. stutzeri* gene; $CynD_{stut}$ Δ330 and $CynD_{stut}$ Δ310. $CynD_{stut}$ is a 334 amino acids and its C-terminus has 5 additional amino acids compared to $CynD_{pum}$ (FIG.4.1). The deletion of these five amino acids was tested with $CynD_{stut}$ Δ330. Even though $CynD_{stut}$ Δ310 was characterized in a previous study (126), the deletion was reconstructed by adding a stop codon and deleting the rest of the gene to avoid readthrough or suppression of the stop codon.

A similar pattern was found for all three enzymes. With increasing number of amino acids deleted, the activity of the enzyme declined (TABLE 4.6).

The rate of cyanide degradation of $CynD_{pum}$ Δ303 was 87 % of the wild-type. This rate decreased to 27% when 39 amino acids were deleted ($CynD_{pum}$ Δ293). No cyanide degradation activity was detected for larger deletion ($CynD_{pum}$ Δ279).

Deletions of $CynD_{stut}$ C-terminus also affected the activity of the enzyme (TABLE 4.6). $CynD_{stut}$ Δ330 was as active as the wild-type. However with larger deletions of 26 amino acids, the reaction rate of $CynD_{stut}$ Δ310 was only 13% of the wild-type. Similarly, with larger deletions the cyanide degrading activity was undetectable. This result was similar to previously published results for $CynD_{stut}$ Δ310 (126) except they observed no activity and I was able to detect a low level of activity.

The reaction rate of CHT_{crassa} decreased by 50% when 13 amino acids were deleted from its C-terminus. When the deletion was increased to 29 amino acids, the reaction rate decreased to 22 % of the wild-type (TABLE 4.6).

TABLE 4.6 Cyanide degrading activity of C-terminal deletion mutants.

Mutant	Length of deletion (amino acids)	Reaction rate compared to wild-type (%)
B. pumilus		
Δ303	28	87 ± 5
Δ293	38	27 ± 2
Δ279	52	Undetectable
P. stutzeri		
Δ330	5	97 ± 3
Δ310	26	13 ± 5
Δ302	33	Undetectable
N. crassa		
Δ339	13	46 ± 8
Δ323	29	22 ± 5
Δ307	45	Undetectable

Proteins were expressed from pEt26b expression constructs and induced in BL21 (DE3) cells. The cyanide degrading activity of these mutants *in vivo* was tested using 4mM cyanide in 0.1M MOPS at pH 7.7 at room temperature for 30 min. Cyanide degradation was measured using picric acid to detect the remaining cyanide and the reaction rate of the mutants was compared to wild-type. The reaction rate values represent the average and the standard deviation of the average from three separate experiments.

Effect of C-terminal deletions on nitrilase stability

In a previous study, the CynD$_{pum}$ C-terminal region was implicated in the stability of the enzyme (144). Likewise in the Chapter III, a mutation in that region, E327K increased the stability of the enzyme. Therefore, the stability of the C-terminal deletion variants with the highest reaction rate was compared to the stability of the parent enzymes.

Even though the deletion of 28 amino acids in CynD$_{pum}$ did not significantly change the activity of the enzyme *in vivo*, the stability of CynD$_{pum}$ Δ303 was greatly altered. The enzyme was very unstable losing 85% of its activity after 15 min incubation at 38^{o}C (FIG.4.2), conditions where the wild type retained 100 % of its activity.

Similar results were seen in CynD$_{stut}$ Δ330; however the destabilization of the enzyme was not as sharp. After 90 min incubation at 38^{o}C, the enzyme's activity was reduced about 50% (FIG.4.2) where the wild type only lost 5 % of its activity.

CHT$_{crassa}$ Δ339, whose activity was altered by the deletion of the amino acids, seemed to be more stable than the bacterial nitrilases, losing its activity at a slower rate. 40% of the activity was lost only after 3h incubation at 42^{o}C (FIG.4.3).

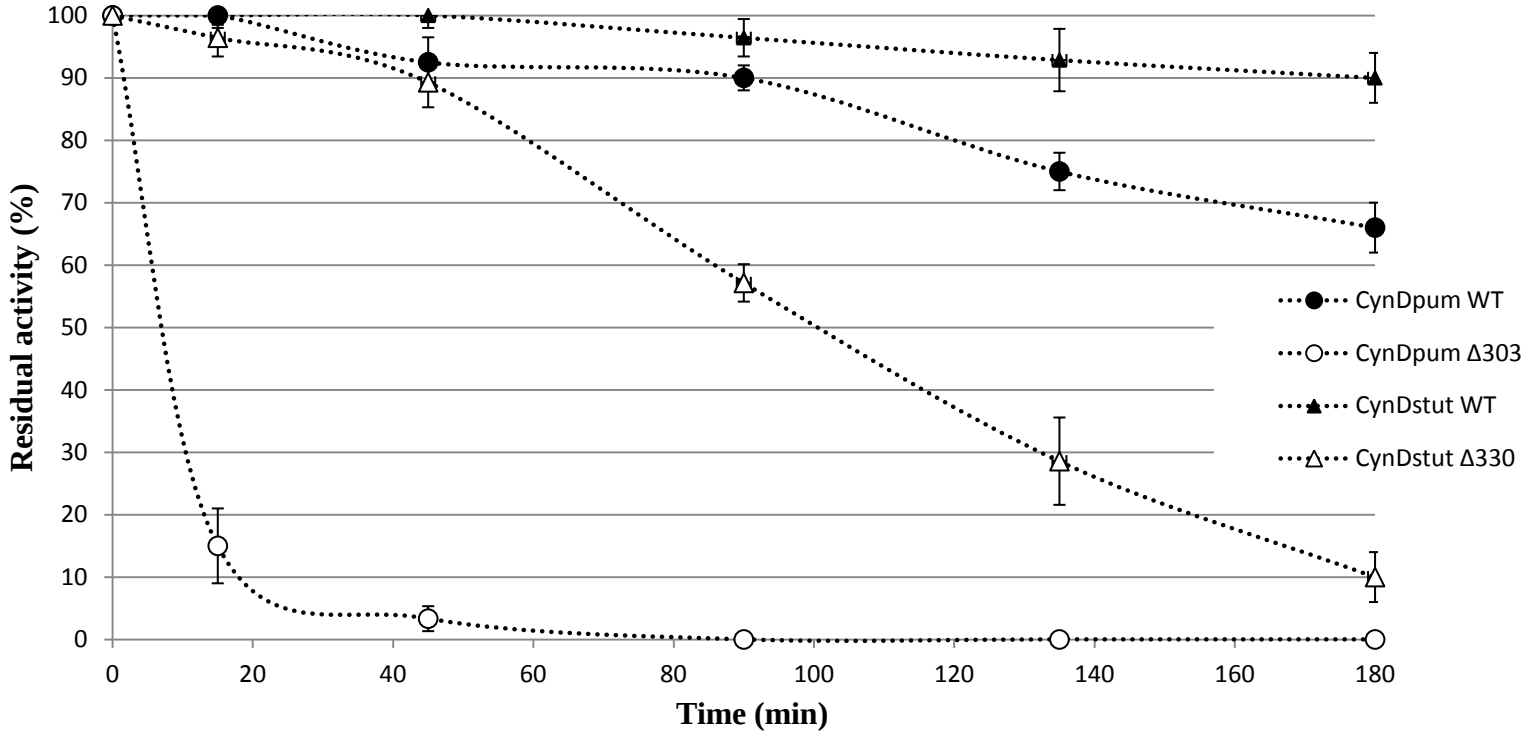

FIG.4.2. Effect of C-terminal deletions on stability of $CynD_{pum}$ and $CynD_{stut}$. Clear cell lysates were incubated in a water bath and 38^{o}C and at different times the residual degrading activity was calculated. Error bars indicate the standard deviation of the average from three separate experiments.

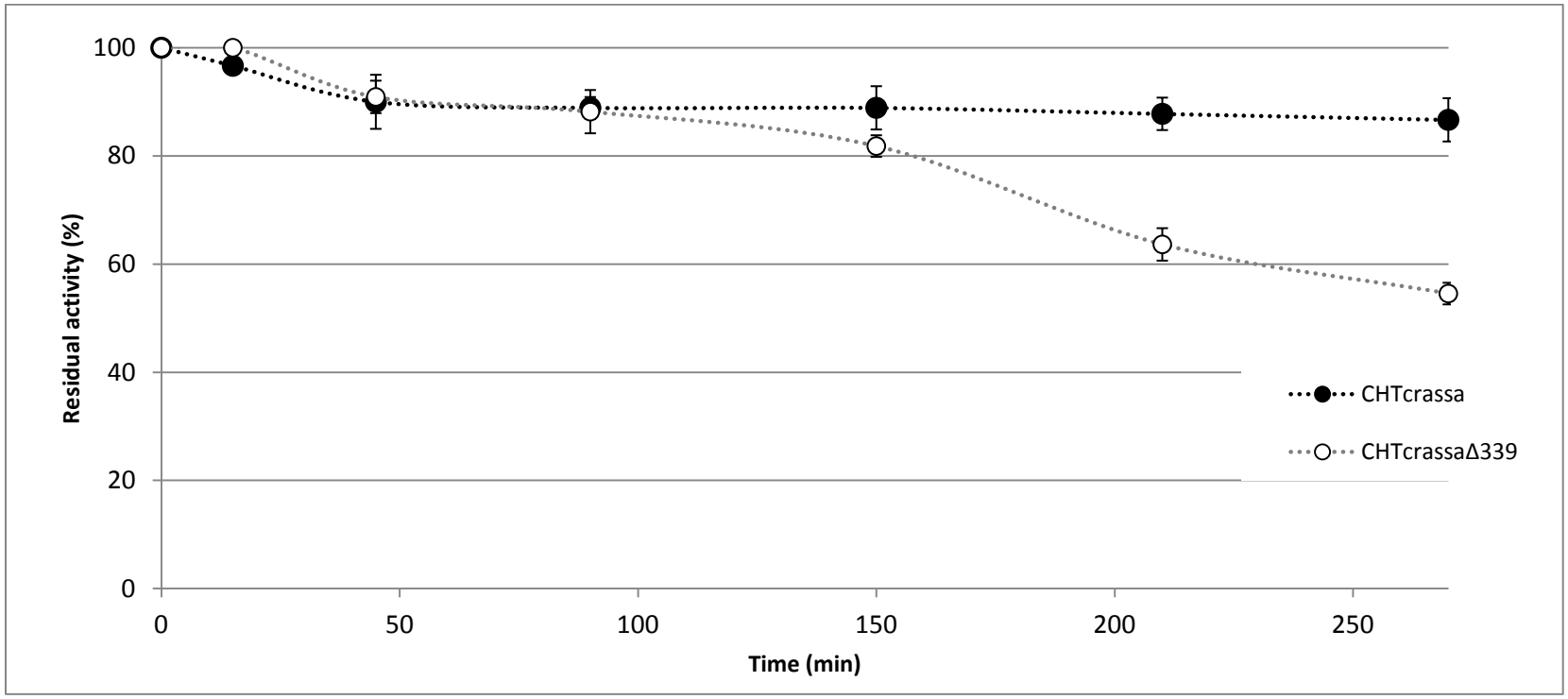

FIG.4.3. Effect of C-terminal amino acid deletions on stability of CHT_{crassa}. Residual activity was tested at room temperature after clear cell lysates were incubated at 42^{o}C for the designated times. Error bars indicate the standard deviation of the average from three separate experiments.

Effect of C-terminal swap on nitrilase activity

Sewell *et al*. (126) described CynD hybrids between $CynD_{pum}$ and $CynD_{stut}$. The $CynD_{pum\text{-}stut}$ hybrid was active whereas the $CynD_{stut\text{-}pum}$ had no detectable activity. These results emphasized the robustness of $CynD_{pum}$ which activity was not altered regardless of the carboxy region it carried, and the sensitivity of $CynD_{stut}$ which does not readily tolerate changes to its C-terminus.

To extend this study, additional CynD and CHT hybrids were constructed and the activity was tested with 4 mM cyanide in 50 mM MOPS pH 7.7 at room temperature for 30 min (TABLE 4.7).

$CynD_{stut}$ lost its activity when its C-terminal was exchanged with that from *N. crassa* as it did with the *B. pumilus*. A similar effect on activity was seen in cyanide hydratase from *N. crassa* when its C-terminus was swapped with that of *P. stutzeri* and *B. pumilus.*

On the other hand, $CynD_{pum}$ showed a tolerance to changes in its C-terminal domain. The hybrids $CynD_{pum\text{-}stut}$ and $CynD_{pum\text{-}crassa}$ both retained activity *in vivo*. $CynD_{pum\text{-}stut}$ was 100% active compared to wild-type $CynD_{pum}$ whereas $CynD_{pum\text{-}crassa}$ had only 60% activity (TABLE 4.7).

TABLE 4.7 Cyanide degrading activity of hybrid nitrilases.

Hybrid	Residues	Reaction rate (%) compared to corresponding wild-type
$CynD_{pum\text{-}stut}$	Residues1-286 from *B. pumilus*, 287-end from *P. stutzeri*	103 ± 3
$CynD_{pum\text{-}crassa}$	Residues1-286 from *B. pumilus*, 287-end from *N. crassa*	59 ± 2
$CynD_{stut\text{-}pum}$	Residues 1-287 from *P. stutzeri*, 288-end from *B. pumilus*	Undetectable
$CynD_{stut\text{-}crassa}$	Residues 1-287 from *P. stutzeri*, 288-end from *N. crassa*	Undetectable
$CHT_{crassa\text{-}stut}$	Residues 1-303 from *N. crassa*, 304-end from *P. stutzeri*	Undetectable
$CHT_{crassa\text{-}pum}$	Residues 1-303 from *N. crassa*, 304-end from *B. pumilus*	Undetectable

The cyanide degradation of the hybrids was tested using whole cells mixed with 4mM cyanide in 0.1M MOPS at pH 7.7. The reaction was done at room temperature for 30 min. Cyanide degradation was measured using picric acid to detect the remaining cyanide and the reaction rate of the mutants was compared to wild-type. The reaction rate values represent the average and the standard deviation of the average from three separate experiments.

C-terminal residues required for CynD$_{stut}$ activity

Alignment of CynD$_{stut}$ and CynD$_{pum}$ show that these nitrilases from two very distant organisms share a high percentage of amino acid identity (76%) and similarity (86%), excluding the C-terminus the identity rises to 83 %. However, this high similarity is not conserved between CynD and CHT. For example, alignment of CynD$_{pum}$ and CHT$_{crassa}$ show only 29% identity and 48% similarity.

Even though they are highly similar, CynD$_{pum}$ and CynD$_{stut}$ did not respond the same way to deletions or changes in their C-terminal region (TABLE 4.6 and TABLE 4.7). The inactivity of CynD$_{stut\text{-}pum}$ hybrid suggests that specific residues in the CynD$_{stut}$ C-terminus are necessary for the enzyme's activity but are missing and not necessary in CynD$_{pum}$. 40% of the divergent amino acids between these two enzymes are located in this C-terminal region. Two regions especially stand out when the C-termini are aligned and the amino acid side chain properties are compared (FIG.4.4). The two regions are 306GERDST and 320LSVSDEEPV found in the *P. stutzeri* enzyme but missing in that of *B. pumilus*.

The inactive CynD$_{stut\text{-}pum}$ hybrid was used as a platform to identify the critical residues of the CynD$_{stut}$ C-terminus that could restore activity. The domain GERDST was tested at position 306 to 311, residues VSDE at position 322 to 325, and residues LSVSDEEPV at position 320 to 328. The cyanide degrading activity of CynD$_{stut\text{-}pum}$ carrying each was then tested with 4 mM CN in 0.1 M MOPS pH 7.7 (TABLE 4.8).

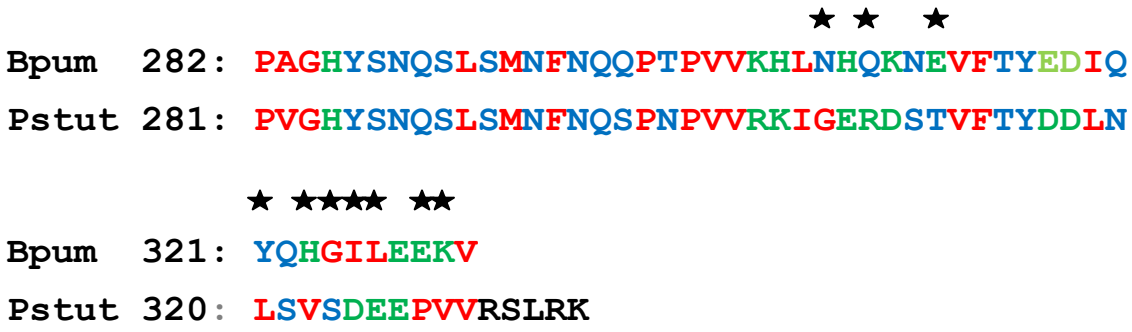

FIG.4.4. Alignment of CynD$_{pum}$ and CynD$_{stut}$ C-termini. Neutral non-polar amino acids are highlighted in red, neutral polar in blue and charged amino acids in green. Stars indicate residues that differed in polarity or charge. Black amino acids represent the extension of the CynD$_{stut}$ C-terminus not found in CynD$_{pum}$.

Restoring amino acids 306GERDST311 to the CynD$_{stut\text{-}pum}$ hybrid partially rescued the activity of the enzyme. The enzyme had 30% activity compared to wild-type CynD$_{stut}$ (FIG.4.5). However, neither 322VSDE325 nor 320LSVSDEEPV328 was able to restore the activity.

In addition, the presence of amino acids 322VSDE325 did not improve the activity of CynD$_{stut\text{-}pum}$ 306GERDST311; the relative activity of CynD$_{stut\text{-}pum}$ 306GERDST311/322VSDE325 was similar to CynD$_{stut\text{-}pum}$ 306GERDST311 (FIG.4.5). When the GERDST domain in the active CynD$_{stut\text{-}pum}$ 306GERDST311 was restored back to NHQKNE as a control, the protein lost its activity once again (TABLE 4.8).

TABLE 4.8 $CynD_{stut\text{-}pum}$ hybrids activity.

Hybrid	Mutation	Activity *in vivo*
$CynD_{stut\text{-}pum}$		Undetectable
$CynD_{stut\text{-}pum}$ GERDST	306NHQKNE → 306GERDST	Active
$CynD_{stut\text{-}pum}$ VSDE	322HGIL → 322VSDE	Undetectable
$CynD_{stut\text{-}pum}$ LSVSDEEPV	320YQHGILEEK → 320LSVSDEEP	Undetectable
$CynD_{stut\text{-}pum}$ NHQKNE	306GERDST → 306NHQKNE	Undetectable

Whole cells were tested for cyanide degradation using 4 mM CN with 0.1 M MOPS pH 7.7. The reaction was done at room temperature and was carried on for 30 minutes. Picric acid was used to detect the remaining cyanide.

These results indicate that the region 306GERDST is required for the activity of $CynD_{stut\text{-}pum}$ hybrid but is missing in the C-terminus of $CynD_{pum}$ which explains the inactivity of $CynD_{stut\text{-}pum}$ hybrid. However, restoration of this domain was not sufficient to fully restore the activity to that of wild type $CynD_{stut}$.

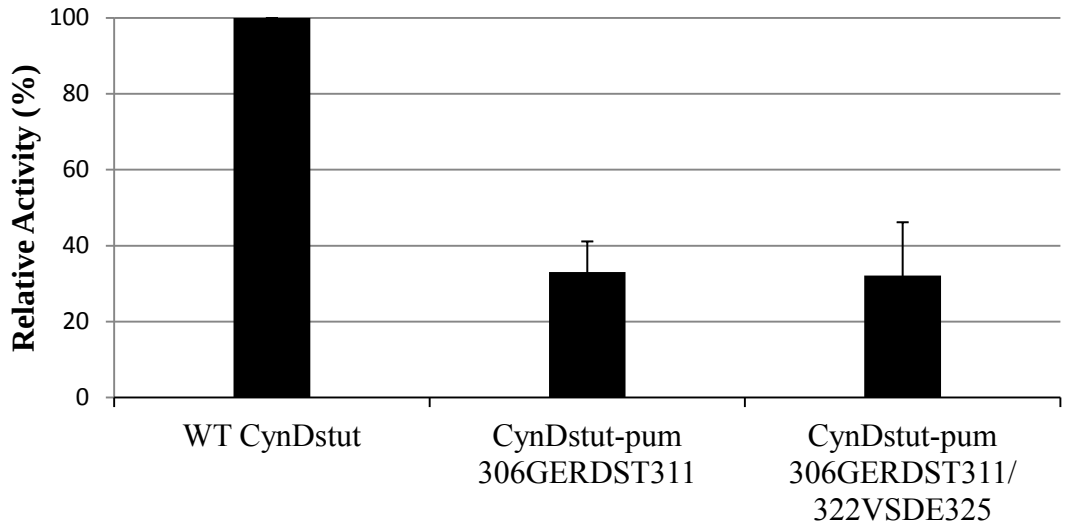

FIG.4.5. Comparison of cyanide degrading activity of $CynD_{stut\text{-}pum}$ 306GERDST and $CynD_{stut\text{-}pum}$ 306GERDST/322VSDE to wild-type $CynD_{stut}$. Cells were adjusted to similar OD600 of 0.3 and the cyanide degradation was monitored using picric acid and measuring absorbance at A_{540} nm. The $CynD_{stut}$ wild type reaction rate was taken as 100% and the relative activity of the mutants was then calculated. Error bars indicate the standard deviation of the average from three experiments.

These results were obtained by measuring enzyme activity in whole cells; on the other hand, neither mutant had any detectable activity in cell lysates. This might indicate a fast unfolding or aggregation of the mutant hybrids once the cells are lysed caused by their instability, or less likely increased susceptibility to proteolysis.

Alanine scanning of CynD$_{stut}$ GERDST region

Alanine scanning through the GERDST region in the wild type CynD$_{stut}$ was performed and the activity of the mutants was tested. Surprisingly, all mutants were active in whole cells when tested with 4 mM HCN at pH 7.7 for 30 min at room temperature. The reaction rate of the mutants and their stability was then calculated and compared to that of the parent enzyme.

Even though all 6 mutants were still active, their reaction rates noticeably differed (FIG.4.6). CynD$_{stut}$ G306A and D309A had the lowest activity, about 45-50 % of wild type. CynD$_{stut}$ R308A retained about 60% activity. The other 3 mutants, E307A, S310A and T311A had only a slight decrease in reaction rate, retaining more than 80% of the wild type activity.

In addition to changes to activity, the stability of these mutants also changed. Cell lysates were incubated in 50 mM MOPS pH 7.7 in a water bath at 39^{o}C and at different times the remaining activity was calculated (FIG.4.7). CynD$_{stut}$ G306A was highly unstable. It was completely inactivated within few minutes. Similarly, CynD$_{stut}$ R308A, CynD$_{stut}$ D309A and CynD$_{stut}$ T311A had a dramatic decrease in their stability. In less than 45 min of incubation at 39^{o}C, all three mutants lost 90% of their activity. CynD$_{stut}$ E307A lost 50% of its activity after 1h incubation at 39^{o}C while the wild-type CynD$_{stut}$ lost 30% of its activity. On the other hand, the stability of CynD$_{stut}$ S310A was not noticeably altered. Its activity rate loss of was similar to that of wild-type CynD$_{stut}$.

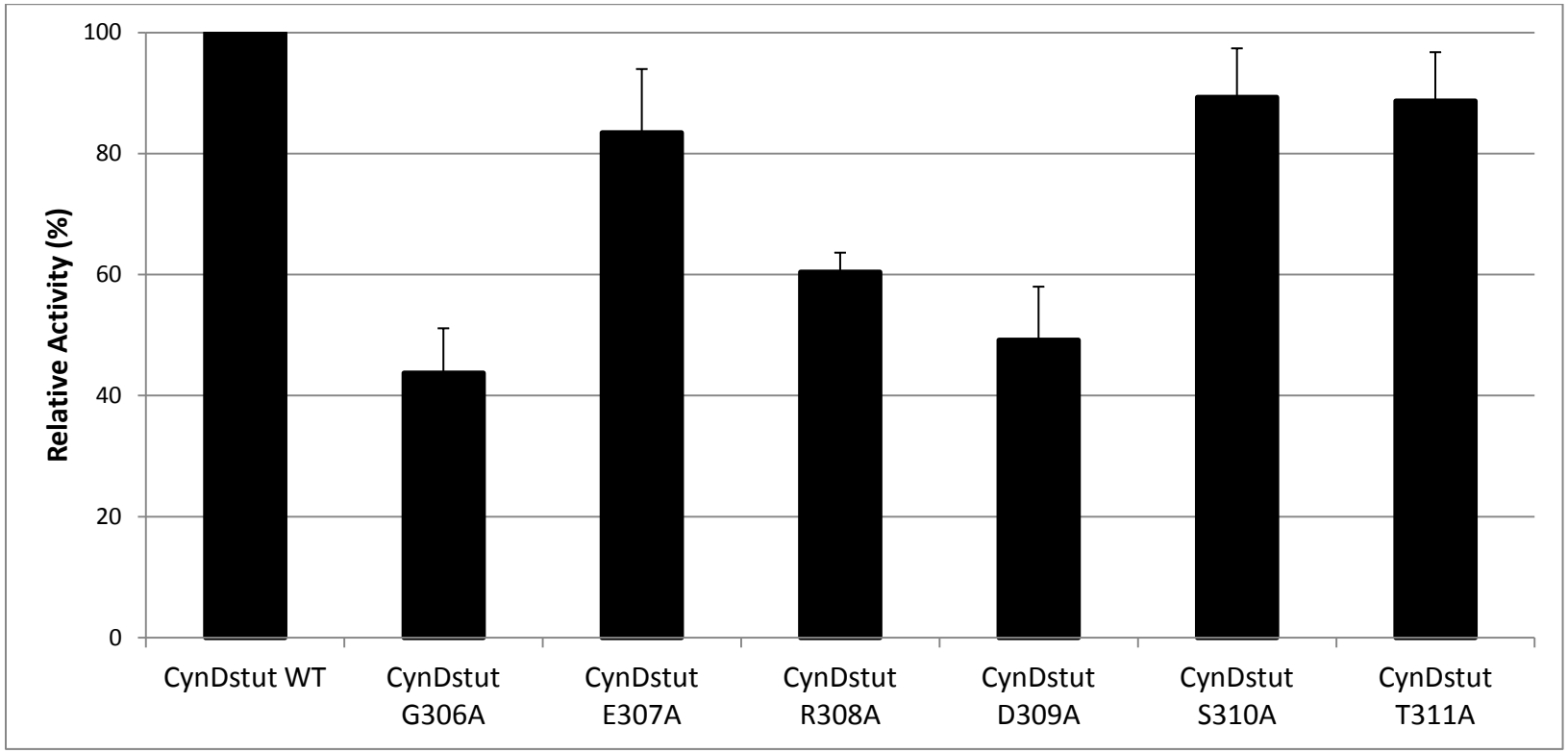

FIG.4.6. Comparison of cyanide degrading activity of $CynD_{stut}$ alanine mutants to the wild type enzyme. Induced cells were adjusted to similar OD of 0.3 and the cyanide degradation was monitored using picric acid absorbance at A_{540} nm. $CynD_{stut}$ wild-type reaction rate was considered 100% and the relative activity of the mutants was then calculated. Error bars indicate the standard deviation of the average from three repeats.

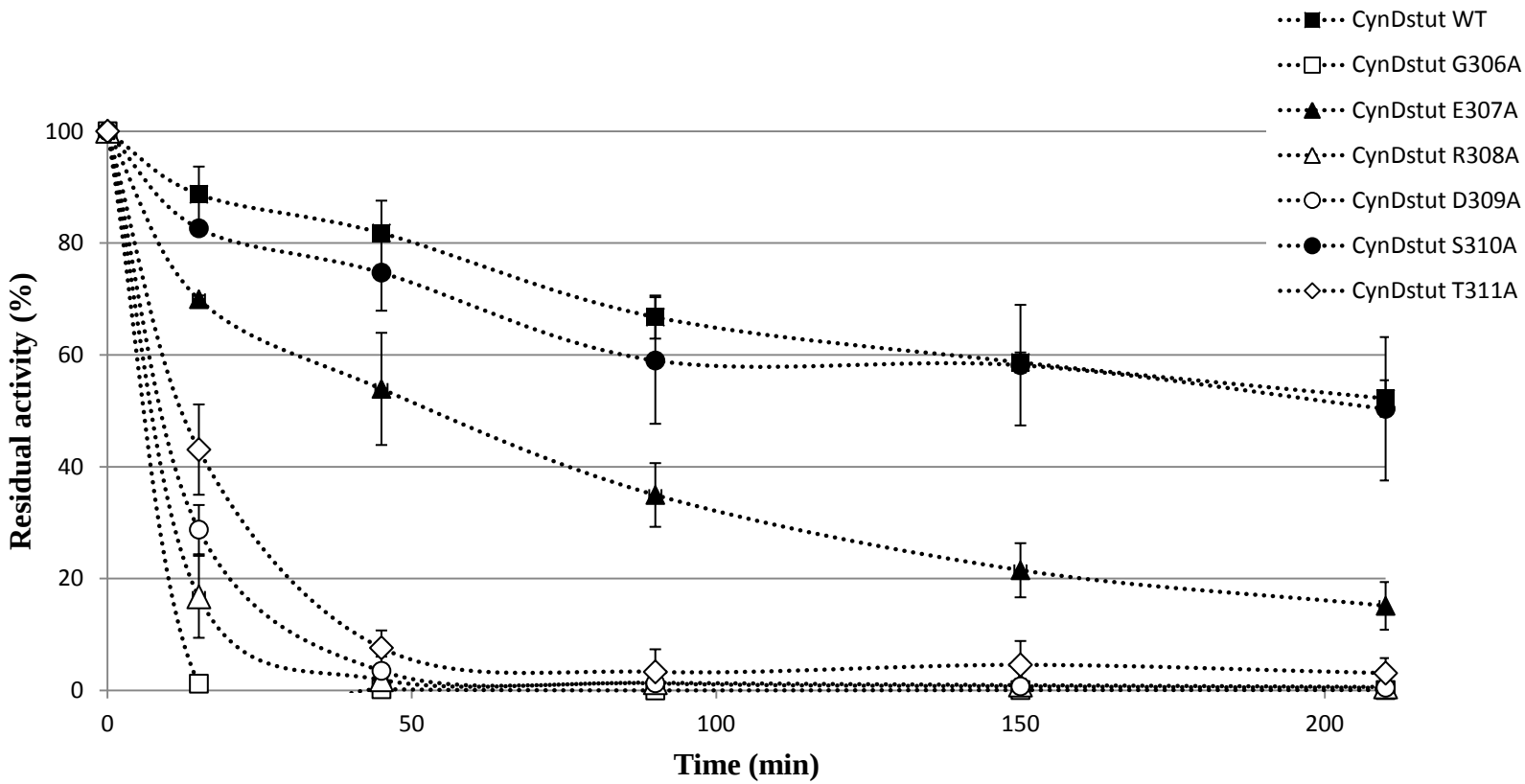

FIG.4.7. Thermostability of CynD$_{stut}$ alanine mutants. Cell lysates were incubated at 39^{o}C in a water bath and the residual activity was tested at different time using Nessler reagent and the absorbance measured at 420 nm. Activity at time 0 was considered 100%. Error bars indicate the standard deviation of the average from three repeats.

Restoring the activity of CynD$_{stut\text{-}pum}$ hybrid

The previous results narrowed the essential region for CynD$_{stut}$ activation to a six residues region, GERDST. To further narrow the target, site directed mutagenesis was performed to identify the residues that restore the activity to the dead CynD$_{stut\text{-}pum}$ hybrid. Several changes were made and the activity of the mutant hybrid was tested with 4 mM HCN at pH7.7 (TABLE 4.9).

TABLE 4.9 Site directed mutagenesis of CynD$_{stut\text{-}pum}$ GERDST domain.

Mutant	Amino acid change	Activity in cells
CynD$_{stut\text{-}pum}$ (NHQKNE)	306GERDST311→306NHQKNE311	Inactive
CynD$_{stut\text{-}pum}$ N<u>DKE</u>NE	H307D Q308K K309E	Inactive
CynD$_{stut\text{-}pum}$ <u>G</u>H<u>R</u>KN<u>T</u>	N306G Q308R E311T	Inactive
CynD$_{stut\text{-}pum}$ <u>G</u>HQ<u>D</u>NE	N306G K309D	Inactive
CynD$_{stut\text{-}pum}$ <u>GE</u>QKNE	N306G H307E	Active
CynD$_{stut\text{-}pum}$ N<u>E</u>QKNE	H307E	Inactive

Changes made to the parent sequence NHQKNE in CynD$_{stut\text{-}pum}$ are underlined. Cyanide degrading activity was tested using whole cells mixed with 4 mM CN and 0.1 M MOPS pH 7.7. Picric acid was used to detect the remaining cyanide.

Comparing the side chain charges of CynD$_{stut}$ and CynD$_{pum}$ at position 307, 308 and 309 showed opposite charges. CynD$_{stut}$ has a negative residue (E307) followed by a positive (R308) then a negative residue (D309). However, CynD$_{pum}$ has a positive residue (H307) then a neutral (Q308) and a positive residue (K309). If CynD$_{stut\text{-}pum}$ hybrid was inactive due to this inversion of charges in this important region, then mutationally reinstating the negative-positive-negative amino acids should restore the activity. This proved not to be the case; CynD$_{stut\text{-}pum}$ 306NDKENE was inactive (TABLE 4.9).

Shifting the focus to other residues in the essential 306GERDST region, the G306A mutation greatly altered the activity and stability of CynD$_{stut}$ suggesting it is a target for the site directed mutagenesis. The same effect was seen for R308A, D309A and somewhat for T311A. Therefore the restoration of these residues in CynD$_{stut\text{-}pum}$ was conducted in the presence of residue G306. The activity of CynD$_{stut\text{-}pum}$ GHRKNT and CynD$_{stut\text{-}pum}$ GHQDNE was then tested *in vivo*. Restoring these amino acids at the C-terminus did not restore the activity of CynD$_{stut\text{-}pum}$ hybrid; both mutants CynD$_{stut\text{-}pum}$ GHRKNT and CynD$_{stut\text{-}pum}$ GHQDNE were inactive (TABLE 4.9).

Another residue, E307 also altered the stability CynD$_{stut}$ when it was replaced by an alanine (FIG.4.7) even though it had similar activity to wild-type. Therefore, CynD$_{stut\text{-}pum}$ GEQKNE was constructed. This mutant was active at about 15% of the reaction rate of wild type CynD$_{stut}$ (FIG.4.8), and only 2-fold less than CynD$_{stut\text{-}pum}$ GERDST indicating a partial rescue of the activity. However, mutation H307E was unable to restore activity to the hybrid.

These results indicate the importance of two residues in the CynD$_{stut}$ C-terminus, G306 and E307. However, other residues in the domain are also required to restore the activity to the CynD$_{stut\text{-}pum}$ hybrid.

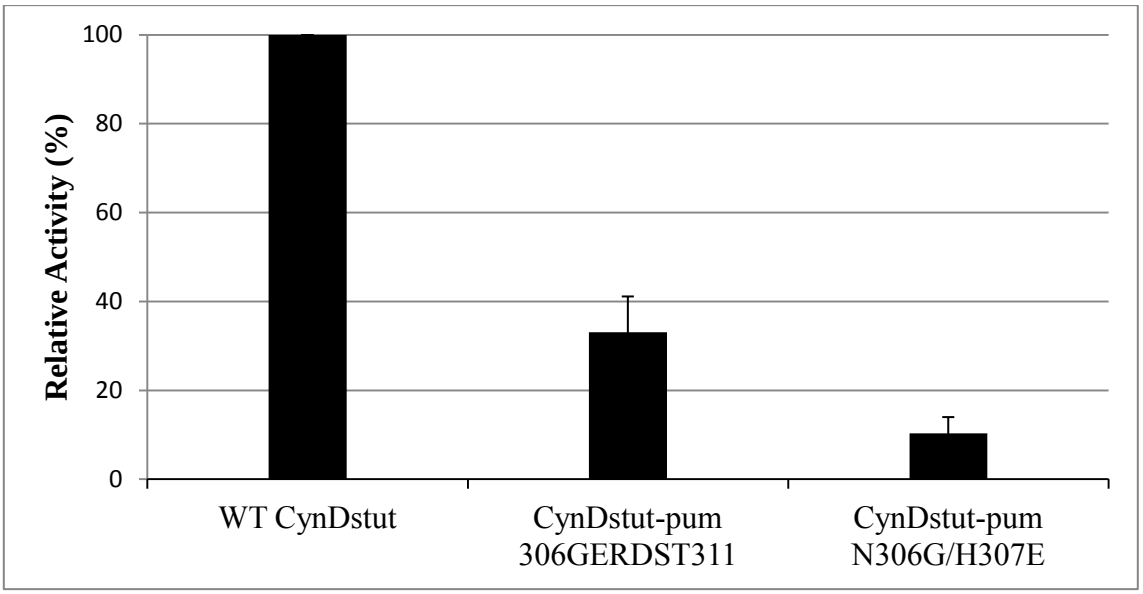

FIG.4.8. Reaction rate comparison of CynD$_{stut\text{-}pum}$ active mutants. Induced cells were adjusted to similar OD of 0.3 and the cyanide degradation was monitored using picric acid and measuring absorbance at 540 nm. The CynD$_{stut}$ wild-type reaction rate was considered 100% and the relative activity of the mutants was then calculated. Error bars indicate the standard deviation of the average from three reps.

DISCUSSION

Cyanide dihydratases from *B. pumilus* and *P. stutzeri* share a high level of similarity in their amino acid sequence. This is also seen in cyanide hydratases from *N. crassa* and *G. sorghi*. However, the C-termini seem to diverge among all the members. Only 30% identity was observed between the C-termini of $CynD_{stut}$ and $CynD_{pum}$. Even thought CHT_{crassa} and CHT_{sorghi} have a 78% identity, residues in the C-terminus are also not conserved (10). CHT_{sorghi} has an extension of 10 carboxy-terminal amino acid compared to CHT_{crassa}. Another example of the divergence is seen in two CynDs isolated from two *B. pumilus* strains; C1 and 8A3 which have 10 non-conserved amino acids within their whole sequence. 7 out of these 10 amino acids are found in their C-terminal domain (62).

This divergence is translated into differences in the properties of the enzyme. For example, $CynD_{pum}$ C1 formed long spirals at pH 5.5 instead of the 18-subunit short helix found at neutral pH (62). However, $CynD_{pum}$ 8A3 did not (123). $CynD_{pum}$ C1 has 3 histidines in its C-terminus, H305, H308 and H323 whereas $CynD_{pum}$ 8A3 has none (62). This reversible and pH dependent structural change is thought to be the result of histidines protonation at pH 5.5. The positive charge on the histidines is proposed to leads to repulsion of the monomer C-terminus, expansion of the spiral's diameter and elongation of the spiral.

CHT_{crassa} and $CynD_{stut}$ do not show structural changes with pH change keeping the same extended oligomers of variable length or 14-subunits respectively (31, 125). Another significant difference is seen in enzyme activity following truncation of the C-

terminus. CynD$_{pum}$ is more tolerant to deletions than CynD$_{stut}$ and CHT$_{crassa}$ (TABLE 4.6). With 28 carboxy-terminal amino acids deleted, CynD$_{pum}$ Δ303 had a reaction rate comparable to wild type (TABLE. 4.6), whereas CynD$_{stut}$ and CHT$_{crassa}$ were inactivated by a similar deletion. This activity decreased as larger regions are deleted. Similarly, the reaction rate of CynD$_{stut}$ and CHT$_{crassa}$ decreased with larger deletions. Even though CynD$_{pum}$ seems to be more tolerant of deletions than the other two enzymes, its stability was affected. The C-terminus seems to help stabilize the oligomeric structure of the enzyme. Thus with larger deletion, the activity of the enzyme might be decreasing because of the instability of its structure.

The localization of the C-terminus is not yet clear. No structural data for this region is available due to lack of sequence identity with related crystallographically determined structures but it is believed that this domain is found in the center of the helix. Structural information from known crystal structures of amidase helped predict the interfaces where the C-terminus might be interacting. Based on the visible C-terminal region of the amidase from *Geobacillus pallidus* (68), Dent *el al*. have suggested that in *Neurospora crassa* the C-terminus interacts with the C surface and then reaches across to the A surface (31). The A surface is the dimerization surface where monomers interact to form dimers. The C surface is the oligomerization surface where interactions between the dimers lead to the subunit oligomerization. Both these surface are essential for the activity of the nitrilase thus the importance of the C-terminus may be at these interfaces.

Based on the localization of C-terminus proposed in Dent *et al*. (31), the effect of the different constructs and mutations created in this study on the activity and stability of can be proposed.

C-terminus interaction with the A surface

The A surface is the dimerization surface. It is formed by two α helices, α5 and α6. Mutations at the A surface have been shown to alter the stability of the enzyme and render it inactive. Such was the case of the $CynD_{pum}$ A202T mutant described in chapter III.

Some C-terminal deletions such as $CynD_{pum}$ Δ303 and $CynD_{stut}$ Δ330 did not show a decrease in activity compared to the parent enzyme. This suggests that this last domain of the C-terminus is not required for activity and is not involved in the active site. However, the stability of these deletion mutants was greatly altered (TABLE 4.6 and FIG.4.2 and 4.3). Deletion of only 5 amino acids from $CynD_{stut}$ was enough to destabilize the enzyme. Enzymes with larger deletions such as $CynD_{pum}$ Δ293 and $CynD_{stut}$ Δ310 lost 70% to 90% of their activity respectively *in vivo* and no activity was detected in cell lysates.

This phenotype is very similar to $CynD_{stut\text{-}pum}$ GERDST and $CynD_{stut\text{-}pum}$ GEQKNE. These two mutants had 30% and 15% of activity respectively compared to $CynD_{stut}$ but no activity was detected when cells were lysed. The decrease in activity *in vivo* and lack of activity *in vitro* are probably due to a decrease in the stability of the enzyme which can cause unfolding or aggregation of the protein. However, the low

activity detected *in vivo* might be due to stabilization of the enzyme by chaperon proteins, or merely an effect of higher monomer concentration inside the cells.

Thus, the last domain of the C-terminus might be involved in interactions with the A surface helping stabilize the dimerization interface. The absence of the C-terminus thus could weaken the interactions across the A surface between the dimers leading to the destabilization observed.

C-terminus interaction with the C surface

The C surface is the oligomerization surface of the dimer, the building blocks of the protein. It is located at a right angle to the A surface. Mutations disrupting this interface lead to an abolishment of the enzyme activity (126). As described earlier, the oligomerization at the C surface is crucial for activity. The interactions at this interface are thought to help position one catalytic residues E136 in the active site (68). A disruption of these interactions means a disruption of the active site thus inactivity of the enzyme.

The domain GERDST was shown to be crucial for $CynD_{stut}$ activity (FIG.4.5). The $CynD_{stut\text{-}pum}$ hybrid was inactive due to the absence of this domain in $CynD_{pum}$ C-terminus (FIG.4.4). The GERDST domain partially restored activity to the $CynD_{stut\text{-}pum}$ hybrid, 30% that of wild-type $CynD_{stut}$. This partial activity might be caused by the instability of the mutant. The lack of activity in cell lysates can be due to unfolding or aggregation of the enzyme similar to the phenotype seen with the C-terminal deletions.

Thus, the GERDST domain might be interacting with the C surface and help reposition the catalytic residue E136 in the active site. Even though $CynD_{stut}$ Δ310 had most of its tail deleted, it was still 13% active compared to the wild-type. This partial activity might be due to the presence of part of GERDST domain, 306GERD309 residues. A larger deletion beyond this domain rendered the enzyme inactive ($CynD_{stut}$ Δ302).

CONCLUSION

In this study, I characterized the effect of the C-terminal deletions on the activity and stability of three nitrilases: $CynD_{pum}$, $CynD_{stut}$ and CHT_{crassa}. With increasing deletion size, the stability and the activity of the enzymes decreased. A domain in $CynD_{stut}$ was shown to be necessary for the activity of the enzyme explaining the inactivity of the $CynD_{stut\text{-}pum}$ hybrid. We speculate that this domain might be interacting with the C surface leading to the positioning of the catalytic residues in the active site.

CHAPTER V

CHARACTERIZATION OF A HIGHLY STABLE pH TOLERANT $CynD_{pum}$ MUTANT

OVERVIEW

The interest in biodetoxification of cyanide contaminated waste waters has increased due to the dangerous effects and high cost of chemical detoxification (93). The bioremediation of cyanide promises a safer and less expensive process since it replaces the use of expensive and harmful chemicals.

Several enzymes capable of degrading cyanide have been found in different bacteria, fungi and plants (71, 111). Despite having the same substrate, these enzymes differ in their reaction mechanism and reaction conditions such as the presence of cofactors and secondary substrates (29, 50). Cyanide dihydratase (CynD), a member of the nitrilase family hydrolyses cyanide into formate and ammonia (104). The reaction does not require any cofactors or additional substrates during the hydrolysis process. This enzyme has been purified from three disparate bacterial strains; *Alcaligenes xylosoxidans subsp. denitrificans* (60), *Pseudomonas stutzeri* AK61 (146) and *Bacillus pumilus* C1 (87).

Bacillus pumilus C1 was isolated from a cyanide wastewater dam in South Africa (86). The expression of the nitrilase gene was not regulated by the presence of cyanide in the medium. Instead, it was found to be regulated by the SpoOA regulator of the sporulation pathway and can be induced by addition of Mn^{2+} (87).

The activity of the enzyme is optimal between 37^{o}C and 42^{o}C and its maximal activity is in the range of pH 7-8 (63). However, at alkaline pH the enzyme has no activity. This is a major drawback for the industrial use of this enzyme since cyanide solutions are kept alkaline to avoid cyanide volatilization.

CynD$_{pum}$ has 330 amino acids and forms a 37 KDas subunit. At pH 7-8, its optimal pH, the subunits oligomerize and form an 18-subunit spiral. However, at pH 5.4 the enzyme subunits associate to form extended rods (62). A model for the enzyme has been proposed based on low resolution electro-microscopy and alignment of sequences of related crystallographically determined structures (62).The monomers are inactive but fold into αββα structure and dimerize to form αββα-αββα dimers which are the building blocks for the active oligomeric structure.

The CynD$_{pum}$ C-terminus is an extension not found in other members of the superfamily whose crystal structure was solved. The lack of information on this region made it difficult to localize the C-terminus in the model but some predictions on its localization and role have been proposed based on mutational studies of this region (126, 135). E327G, a mutation in the C-terminus, increased the thermostability of the enzyme (144) whereas, deletions of the C-terminal 28 amino acids did not affect the activity of CynD$_{pum}$ extensively; CynD$_{pum}$ Δ303 had 87% activity compared to the parent enzyme (Chapter IV, TABLE 4.6). However, the deletion destabilized the enzyme which lost 90% of its activity within 15 min incubation at 38^{o}C (Chapter IV FIG.4.2). These results show a role of the C-terminus on the protein stability suggesting its localization may be around interfaces important for the formation of the oligomeric structure of the enzyme.

A set of C-terminal swaps were created with other members of the superfamily, an arylacetonitrilase from *Pseudomonas fluorescens* EBC191 (69). This nitrilase catalyzes the conversion of different phenylacetonitriles to the corresponding carboxylic acids and shows some enantioselectivity. Its C-terminus was swapped with that of nitrilases from *Rhodococcus rhodochrous* or *Alcaligenes faecalis*. The hybrid enzymes were shown to be similar to the parent enzyme regarding activity and enantioselectivity.

When the C-terminus was swapped between two highly similar cyanide dihydratases from *Pseudomonas stutzeri* and *Bacillus pumilus*, the hybrid enzymes did not behave similarly. The hybrid CynD$_{pum\text{-}stut}$ had full activity relative to CynD$_{pum}$ unlike CynD$_{stut\text{-}pum}$ hybrid which was inactive (126). The high similarity between these two cyanide dihydratase is not conserved in the C-terminus. In fact, alignment of CynD$_{stut}$ and CynD$_{pum}$ C-termini show two regions formed of 6 to 9 amino acids each that differed in polarity or charge. CynD$_{stut}$ does not tolerate changes to its C-terminus; its activity and stability decreased when deletions were made in its C-terminus. These results show the robustness of CynD$_{pum}$ which activity was not altered regardless of deletion or substitution of its C-terminus.

The phenotype of the CynD$_{pum\text{-}stut}$ hybrid was not known other than it was active. Since CynD$_{pum}$ activity does not require a C-terminus, the hybrid CynD$_{pum\text{-}stut}$ could have a phenotype similar to CynD$_{pum}$ Δ303, meaning active but unstable. On the other hand, CynD$_{stut}$ C-terminus might have special properties since only it functions with the CynD$_{stut}$ enzyme. Investigating the phenotype of CynD$_{pum\text{-}stut}$ could be informative of the

role of the C-terminus and especially the interactions of residues in this region with the rest of the protein.

In this chapter, I chose to characterize $CynD_{pum\text{-}stut}$ and look at the effect of $CynD_{stut}$ C-terminus on the stability and activity of the hybrid. $CynD_{pum\text{-}stut}$ hybrid was found to be several-fold more stable than $CynD_{pum}$. This same hybrid exhibited 100% activity at pH 9, a pH where the parent enzyme is inactive, and retained 40% of its activity at pH 9.5 making it a true pH tolerant mutant.

MATERIALS AND METHODS

Culture media and reagents

All strains were grown in LB broth. Antibiotics were used at concentrations of 100 ug/ml of ampicillin, 25 ug/ml of kanamycin or 25 ug/ml of chloramphenicol.

Bacterial strains and plasmids

E.coli strain MB3436 [Δ*endA thiA hsdR17 supE44 lacI*^{q}*ZΔM15*] was used as the host strain for DNA manipulations. *E.coli* strain MB1837 [BL21 (DE3) pLysS] was used to express the proteins. The plasmids used are described in TABLE 5.1.

TABLE 5.1 List of plasmids used in this study.

Plasmid	Description	Reference
p5277	pEt28 carrying synthetic *P. stutzeri cynD*	This work
p2890	pEt26b carrying *B. pumilus* C1 *cynD*	Jandhyala *et al.* 2003
p4406	pEt28a carryimg *B. pumilus* C1 *cynD*	This work
p3411	pEt26b carrying $CynD_{pum\text{-}stut}$	Sewell *et al.* 2005
p5389	pEt28a carrying $CynD_{pum\text{-}stut}$	This work
p5383	5389 K93R	This work
p5467	pEt28b carrying $CynD_{pum}$ 306GERDST311	This work

Protein expression and purification

Genes were cloned into pEt28a creating expression constructs with an N-terminal his-tag and transformed into MB1837 (BL21 pLysS). Overnight cultures were diluted 1:100 in 50ml LB Kanamycin and grown to an OD600 of 0.3 at 37^{o}C. 1 mM IPTG was added and induction continued at 30^{o}C for 3-4 hours. Cells were then pelleted by centrifugation at 3750 rpm for 10 min and were washed two times with 0.1 M MOPS pH 7.7. The pellet was stored at -20^{o}C overnight. Cells were then thawed and lysed at room temperature with B-PER II Protein Extraction Reagent (Thermo Scientific). 2mL of B-PER II reagent per gram of cell pellet was used with 0.5 mg/ml lysozyme, 10ug/ml DNase and 1X EDTA-free protease inhibitors as recommended by the manufacturer. The cell lysate was centrifuged at 13,000 rpm for 15 min at 4^{o}C. Purification of hexahistidine-tagged proteins was performed at 4^{o}C using the HisPur Cobalt purification

kit (Thermo Scientific). Buffer exchange of the purified protein at 4^{o}C used Zeba Spin Desalting Columns (Thermo Scientific) and the protein was resuspended in 0.1 M MOPS pH 7.7. Protein concentration was determined using the NanoDrop ND-1000 at 280 nm with the predicted his-tagged protein extinction coefficient of 54770 cm^{-1} M^{-1} and molecular weight of 40,013 g/mol for both purified enzymes from p5383 and p5389 plasmids. SDS-PAGE confirmed the purity of the protein. Purified proteins were stored in aliquots at -80^{o}C.

Kinetic measurements

3.9 ug of enzyme was used for kinetics analysis in 1 ml total volume. A stock solution of 1 M of cyanide was prepared in a 1 M MOPS pH 7.7. Reactions were done at room temperature in 50 mM MOPS at pH 7.7 at different concentrations of cyanide. Kinetic measurements were also repeated using 50 mM Tris-HCl at pH 7.7 and pH 9. Each reaction was run for 5 min and time points were taken every 1 min. The reaction rates over the first 5 min were linear and $V_{initial}$ was calculated by monitoring ammonia produced in 100ul of reaction mixed with 100 ul of diluted Nessler reagent (1:3 in MQ H_2O) and using a 96-well plate reader (Bio-Rad) the absorbance was determined at 420 nm to determine the concentration of produced ammonia. Lineweaver Burk plots were used to calculated K_m and V_{max}. For each enzyme, the final K_m and V_{max} values are averages from 3 separate protein preps. V_{max} was used to calculate K_{cat}. All enzymes were considered as 18-subunits spirals with molecular weight of 713,772 g/mole.

pH activity measurements

5.5 ug of enzyme was used for pH activity analysis in 1ml total volume. Three 1M cyanide stock solutions were prepared: 1 M citric acid/Na_2HPO_4 at pH 5.5, 1 M MOPS pH 7.7 or 1 M CAPS at pH 9.5. Reactions were done at room temperature in a fume hood at a final concentration of cyanide of 4 mM. The activity of the purified enzyme was measured over the pH range 4-10. Buffers used are as follow; 50 mM citric acid/ Na_2HPO_4 (pH 4, 5 and 6), 50 mM MOPS (pH 7), 50 mM Tris HCl (pH 8) and 50 mM glycine/NaOH (pH 9 and 9.5). The activity was monitored for the first 5 min and time points were taken every min. Ammonia production was measured as described above. Final values are averages from 3 separate protein preps.

Enzyme stability

The thermostability of the enzyme was determined by incubating 80 ug of purified enzyme in a total volume of 8 ml of 50 mM MOPS pH 7.7 in a water bath at 42^{o}C. At different times, 0.5 ml aliquots were removed into a new 1.5 ml Eppendorf tube and left at room temperature for 3 min before adding cyanide in 1 M MOPS pH 7.7 to a final concentration of 4 mM. The reaction continued at room temperature and the activity was monitored for the first 5 min with time points taken every min to measure ammonia production as described above. The reaction rate was calculated using the zero time value considered as 100% activity rate and the relative activity of the enzyme at the different incubation times was then calculated. Final values are averages from 3 separate protein preps.

Gel filtration

Size-exclusion chromatography of the purified enzymes was done using Superdex 200 10/300 GL column and BioLogic DuoFlow chromatography system from Biorad equilibrated with 0.1 M MOPS pH 7.7. 200 ul of 2-3mg/ml purified enzyme resuspended in 0.1 M MOPS pH 7.7 were loaded on the column. 0.1 M MOPS pH 7.7 was used to as mobile phase to elute the protein and the elution was monitored by absorbance at 280 nm. The size standard kit used was Gel Filtration Markers Kit weights 29,000 – 700,000 Das from Sigma (Carbonic Anhydrase 29 KDa, Albumin 66 KDa, Alcohol dehydrogenase 150 KDa, β-Amylase 200 KDa, Apoferritin 443 KDa, Thyroglobulin 669 KDa, Blue dextran, 2,000 KDa).

RESULTS

Characterizing the stability of CynD$_{pum\text{-}stut}$ hybrid

Unlike the CynD$_{stut\text{-}pum}$ hybrid, CynD$_{pum\text{-}stut}$ hybrid was fully active *in vivo* with a reaction rate of 100% compared to CynD$_{pum}$ as shown in Chapter IV. On the other hand, CynD$_{pum}$ Δ303, lacking much of the C-terminus, had 87% of the activity of the parent enzyme but was highly unstable.

To analyze the stability of the CynD$_{pum\text{-}stut}$ hybrid, purified enzymes of CynD$_{pum}$, CynD$_{stut}$ and CynD$_{pum\text{-}stut}$ were incubated in a water bath at 42^{o}C for various times and the remaining activity of the enzyme was tested (FIG.5.1).

The CynD$_{pum\text{-}stut}$ hybrid had a much higher stability than either wild type CynD$_{pum}$ or CynD$_{stut}$ (FIG.5.1). CynD$_{pum}$ and CynD$_{stut}$ had a similar level of stability;

both enzymes retained 50 % of their activity after less than 1 h of incubation at 42^{o}C. The CynD$_{pum\text{-}stut}$ hybrid retained 50% of its activity after 17 h of incubation at 42^{o}C. Even after 48 h incubation, the hybrid had 13% of its activity remaining.

The results clearly affirm the importance of the C-terminus and its effect on stability, confirming previous results that deletions in the C-terminus disrupted the stability of the enzyme. These experiments also suggest that the C-terminus of CynD$_{pum}$ is not optimal for the stability of that protein.

In chapter III, I described other CynD$_{pum}$ mutants: E327K, D172N and K93R. All these mutations increased the stability of CynD$_{pum}$ with K93R having the largest effect. CynD$_{pum\text{-}stut}$ is much more stable that the single mutant K93R. I speculated that this mutation is involved in the A and D/E surfaces whereas the C-terminus is thought to interact with the A and C surface. For this reason, I hypothesized that K93R mutation might have a synergistic effect and therefore I created CynD$_{pum\text{-}stut}$ K93R mutant and the thermostability of the construct was tested (FIG.5.2).

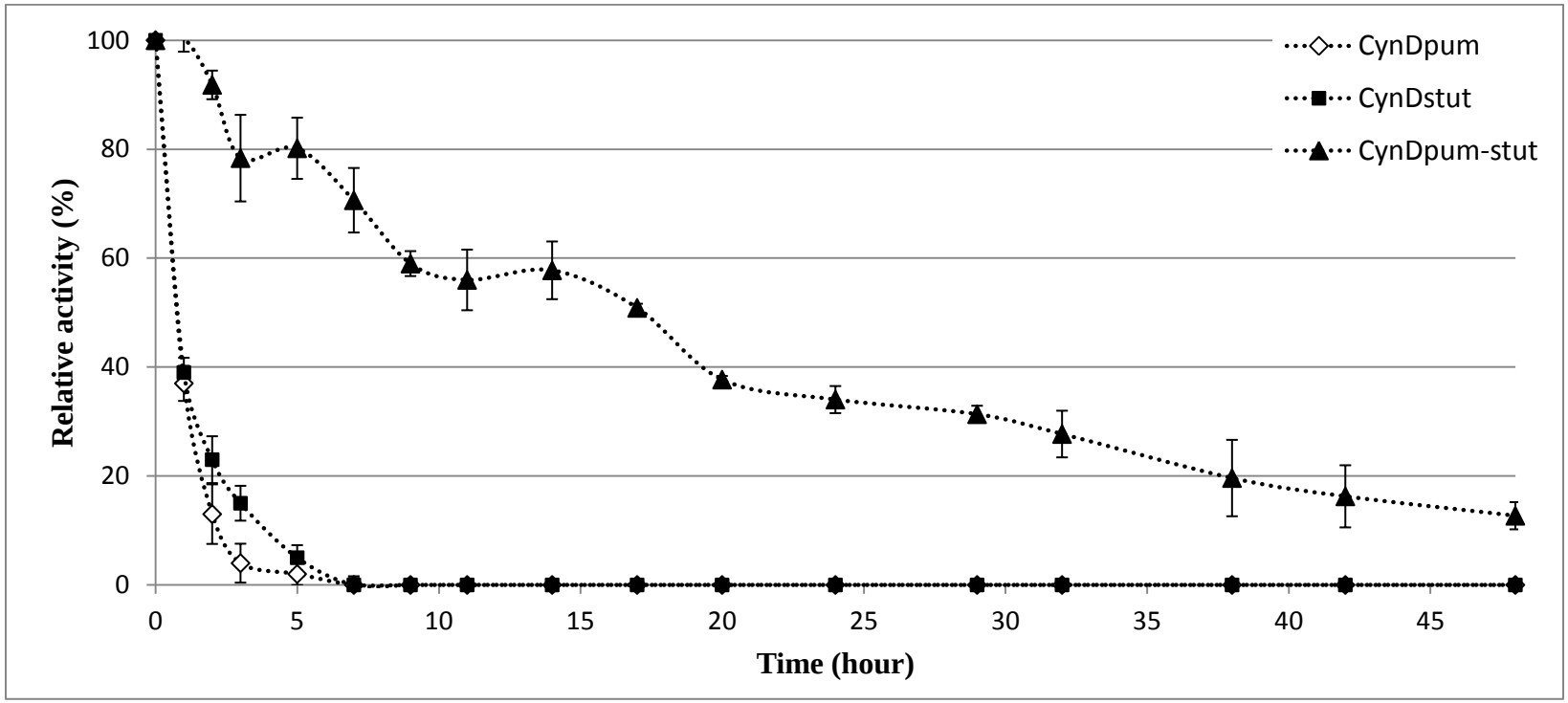

FIG.5.1. Comparison of $CynD_{pum\text{-}stut}$ hybrid and wild-type thermostability. Purified enzymes were incubated in a water bath at 42^{o}C for designated times and aliquots removed to assay. Residual activity was tested at room temperature. Error bars indicate the standard deviation of the average from experiments conducted with three separate protein preps.

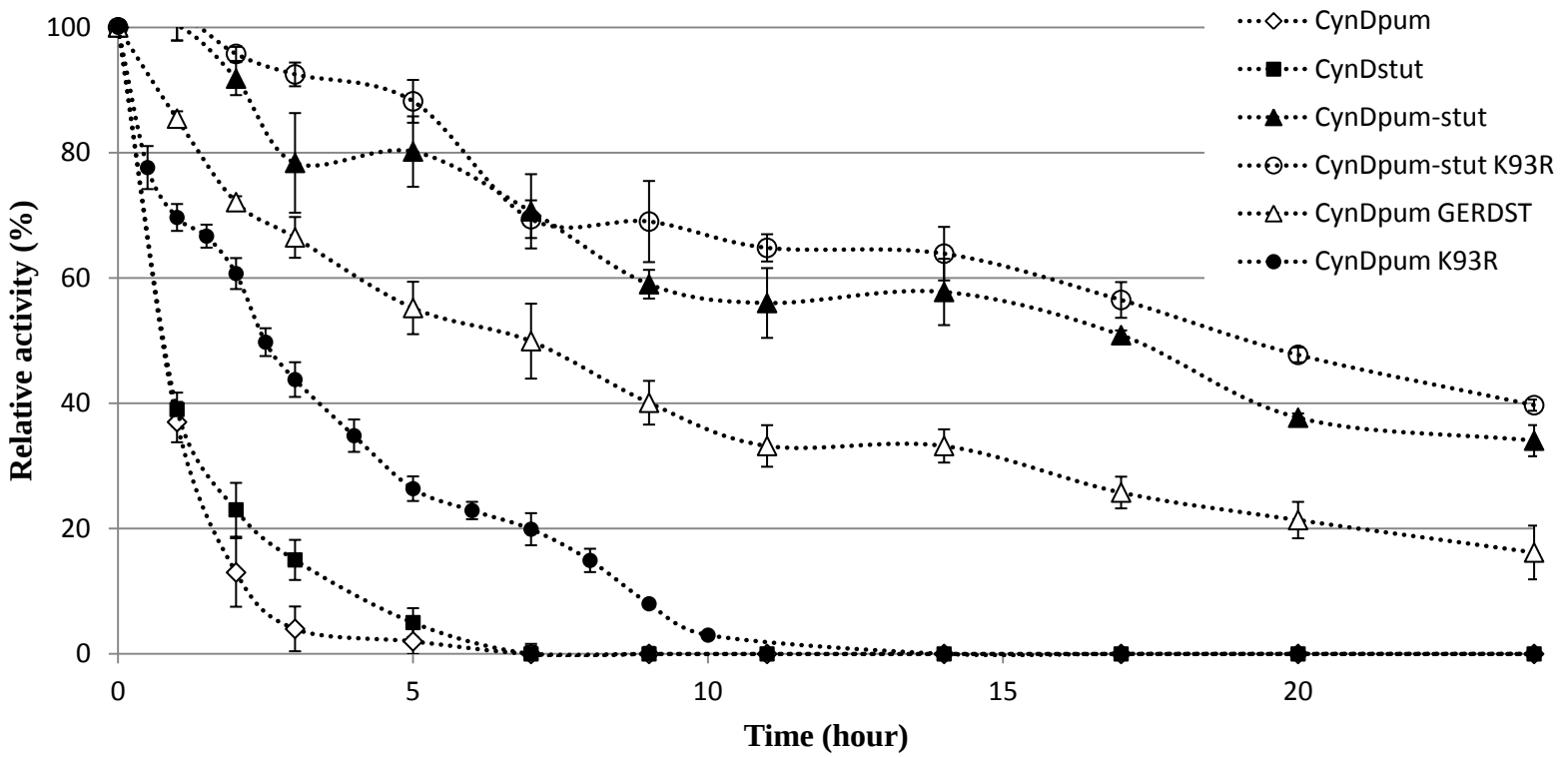

FIG.5.2. Thermostability of different $CynD_{pum}$ mutants. Purified enzymes were incubated in a water bath at 42^{o}C for the designated times. Residual activity was tested at room temperature. Error bars indicate the standard deviation of the average from experiments conducted with three separate protein preps.

CynD$_{pum\text{-}stut}$ K93R was in fact somewhat more stable than CynD$_{pum\text{-}stut}$ (FIG.5.2). K93R and the C-terminus may be stabilizing different aspects of the structure, the D/E surface and A/C surface respectively.

Another construct, CynD$_{pum}$ GERDST was also created based on the observations found in chapter IV. This GERDST domain is located in the C-terminus of CynD$_{stut}$ at position 306 to 311. In the previous study, this region was shown to be necessary for the activity and stability of the CynD$_{stut}$. The restoration of this domain in the inactive CynD$_{stut\text{-}pum}$ hybrid restores the activity to the enzyme. On the other hand, alanine substitution of the residues of this domain decreased the stability of CynD$_{stut}$.

However, this domain is not found in CynD$_{pum}$ C-terminus. Instead, the domain has a sequence of NHQKNE found at position 307 to 312. Due to the importance of this region on CynD$_{stut}$ and the high stability that CynD$_{stut}$ C-terminus has conferred to CynD$_{pum}$, it was then decided to build a CynD$_{pum}$ GERDST mutant by replacing CynD$_{pum}$ residues 307NHQKNE312 with CynD$_{stut}$ sequence 307GERDST.

The CynD$_{pum}$ GERDST showed an increased in the stability (FIG.5.2). This increase was larger than the one seen in the single mutant K93R but not as high as the CynD$_{pum\text{-}stut}$ hybrid. CynD$_{pum}$ GERDST kept 50% of its activity after 7 h incubation at 42^{o}C. However, K93R mutant lost 50% of activity within 2.5 h of incubation at 42^{o}C.

The CynD$_{pum\text{-}stut}$ hybrid was still more stable than CynD$_{pum}$ GERDST indicating that 307GERDST312 is not the only region involved in this stability increase and other residues are important as well.

pH activity profile

A link between stability and pH activity has been described for $CynD_{pum}$. Previously identified mutants showed an increase in cyanide degrading activity at pH 9 *in vivo*. These point mutations, E327K and E327G increased the stability of $CynD_{pum}$ and were able to degrade cyanide at pH 9, a pH where the wild-type is inactive. Since several mutants described here have shown an increase in stability, their pH activity profile was tested and compared to $CynD_{pum}$ (FIG.5.3).

At different pHs, the purified enzyme was assayed with 4 mM cyanide at room temperature. Ammonia production was measured using Nessler's reagent and the absorbance at 420 nm was used to determine the concentration of ammonia generated and the reaction rate was then calculated.

Wild-type $CynD_{pum}$ and $CynD_{pum}$ GERDST had a similar pH activity profile. Their maximal activity was at pH 8. However, at pH 9, $CynD_{pum}$ was inactive and $CynD_{pum}$ GERDST had only 5% activity at pH 9 (FIG.5.3).

The $CynD_{pum\text{-}stut}$ hybrid had a very different pH activity profile. Its reaction rate in acidic solutions showed a dramatic increase compared to wild- type; 60% increase at pH 4, 50% increase at pH 5 and 40% increase at pH 6. At alkaline pH, the effect was even more dramatic. The hybrid $CynD_{pum\text{-}stut}$ had its maximal activity at pH 9 unlike wild type $CynD_{pum}$ which was essentially inactive at that pH. Even at pH 9.5, the hybrid $CynD_{pum\text{-}stut}$ was still active, retaining 40% to 50% of its maximal activity but the wild-type $CynD_{pum}$ was completely inactive. However, at pH 10, only about 5% of the activity was detected.

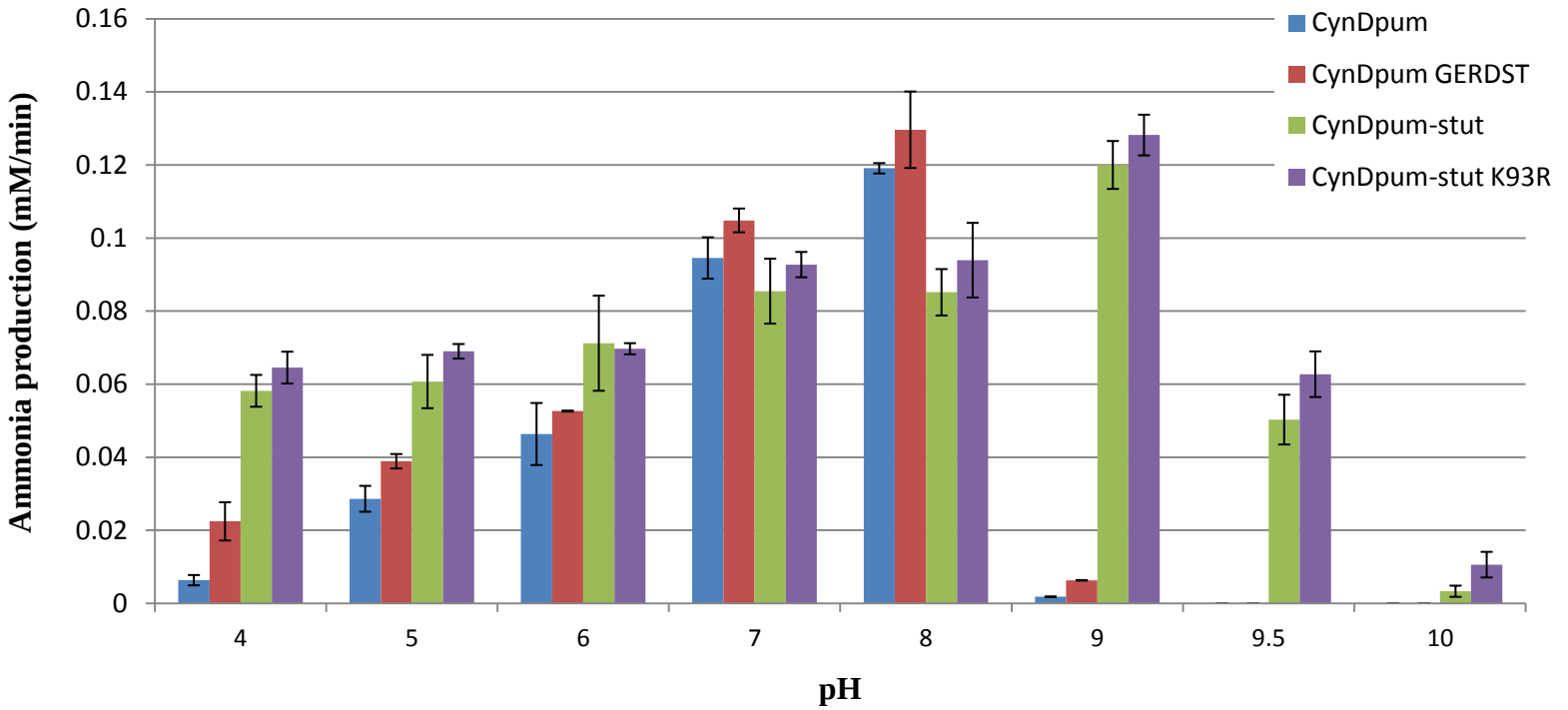

FIG.5.3. pH activity profile of $CynD_{pum}$ mutants. Purified enzyme was tested with 4 mM cyanide and the ammonia production was measured at different pHs. Error bars indicate the standard deviation of the average from experiments conducted with three separate protein preps.

The K93R mutation had a slight but not a significant effect on the CynD$_{pum\text{-}stut}$ hybrid at the different pHs.

Even though CynD$_{pum}$ GERDST had a large increase in its stability, this mutant was still essentially inactive at pH 9 just like the parent enzyme. This phenotype is similar to that seen with the K93R single mutant described in chapter III. K93R mutant had a higher stability than wild-type but had no activity at pH 9. Hence the activity at pH 9 of the CynD$_{pum\text{-}stut}$ hybrid might not be only the consequence of an increase in stability but the result of a specific interaction taking place at the active site or in the vicinity of it leading to changes in the chemical reaction of the enzyme at this alkaline pH. Nevertheless, the increase in reaction rate in acidic solution might be the result of the protein stability.

Kinetic measurement

The increase in reaction rate seen in the previous experiment at pH 9 (FIG.5.3) shows that the CynD$_{pum\text{-}stut}$ hybrid optimal pH shifted from pH 8 to pH 9. To test if this pH shift had an effect on catalysis, kinetics parameters of CynD$_{pum\text{-}stut}$ hybrid were measured at pH 7.7 and pH 9 and compared to that of wild-type CynD$_{pum}$ (TABLE 5. 2).

At pH 7.7, CynD$_{pum}$ and CynD$_{pum\text{-}stut}$ exhibited comparable kinetic properties. Both enzymes had similar K_m and V_{max} values (TABLE 5.2). When tested at pH 9, CynD$_{pum\text{-}stut}$ hybrid displayed a 2-fold increase in affinity for the substrate but a slight decrease in V_{max}. The wild-type enzyme was inactive at pH 9 and therefore could not be measured.

TABLE 5.2 Kinetic measurement of CynD$_{pum\text{-}stut}$ at pH 7.7 and pH 9.

		CynD$_{pum}$	CynD$_{pum\text{-}stut}$
pH 7.7	K_m (mM)	2.9 ± 0.5	2.4 ± 0.8
	V_{max} (mmole/min.mg)	0.038 ± 0.004	0.03 ± 0.003
	K_{cat} (min^{-1})	2.63 x10^4	2.15 x10^4
pH 9	K_m (mM)	N/A	1.3 ± 0.3
	V_{max} (mmole/min.mg)	N/A	0.025 ± 0.002
	K_{cat} (min^{-1})	N/A	1.8 x10^4

Size exclusion chromatography

The role of the C-terminus in the oligomerization of the nitrilase has been seen in several members of the superfamily. CynD$_{pum}$ C1 changes its structure from an 18-subunit spiral at pH 8 to long helix at pH 5 (62). This effect is thought to implicate the involvement of three histidines found in the C-terminus which become protonated at this pH. Thus, the C-termini from the different subunits located in the central of the spiral repulse leading to an expansion of the spiral radius and elongation of the helix (135). This change was accompanied with a slight increase in activity (63). However a highly similar nitrilase, CynD$_{pum}$ 8A3 does not show a structural change at pH 5 nor does it have any histidines in its C-terminus (123).

Another example comes from the nitrilase of *Rhodococcus rhodochrous* J1. Following the autocleavage of 39 C-terminal residues, the enzyme structure changed from inactive 80 KDa dimers to active 410 KDa helical oligomers (96, 136).

Wang *et al.* (144) described $CynD_{pum}$ mutants that showed increased stability. Two of these mutations were located in the C-terminus. Using negative stain electron microscopy, the quaternary structure of these mutants was compared to wild-type at pH 8. The C-terminal mutant E327G formed a spiral similar in length to wild-type whereas the mutations affecting other interfaces in the protein displayed helices with an average of 2.5 times the length of wild-type.

With these observations in mind, it was interesting to see if $CynD_{pum}$ Δ303 and $CynD_{pum\text{-}stut}$ had any effect on the quaternary structure of the enzyme. A comparison of the oligomer size between $CynD_{pum}$ Δ303, $CynD_{pum\text{-}stut}$ and wild-type $CynD_{pum}$ was done using the size exclusion chromatography to detect structural changes.

The $CynD_{pum}$ monomer has a size of 37 KDa and assembles into an 18-subunit spiral. Thus, the elution peak of $CynD_{pum}$ aligned with that of the protein standard of 669 KDa as expected (FIG.5.4).

However, $CynD_{pum}$ Δ303 showed a smaller structure. A small peak eluted at 669 KDa suggesting some 18-subunit spiral structure existed but the majority of the purified protein eluted as protein of 150- 180 KDa (FIG.5.4), suggesting a tetramer.

On the other hand, $CynD_{pum\text{-}stut}$ eluted at the same time as $CynD_{pum}$ suggesting its structure is similar to the parent enzyme (FIG.5.5).

DISCUSSION

The C-termini of nitrilases have highly variable length and sequences. Changes and deletions to this region had different effects on the enzyme parameters (69, 126) . In this study, I showed that the C-terminus of $CynD_{stut}$ was more favorable to $CynD_{pum}$ than its own natural C-terminus. The hybrid $CynD_{pum\text{-}stut}$ was highly stable and was fully active at pH 9.

The use of enzymes in the bioremediation of cyanide has been long discussed in literature. Several enzymes can degrade cyanide into less toxic products as described in the first chapter. The cyanide dihydratase enzymes are thought to be prominent candidates for this biocatalysis since they hydrolyze cyanide into two simple products and do not require any cofactors.

However, two major parameters are required before these enzymes can be successfully used in industry; increased stability and activity in alkaline pH. Enzymes with higher stability are important for high temperature procedures and they reduce the process cost due to their longer lifetime. Activity of these enzymes at alkaline pH is crucial for cyanide degradation. Cyanide contaminated wastewaters are kept at pH 9 or higher to prevent the production of poisonous hydrocyanic acid.

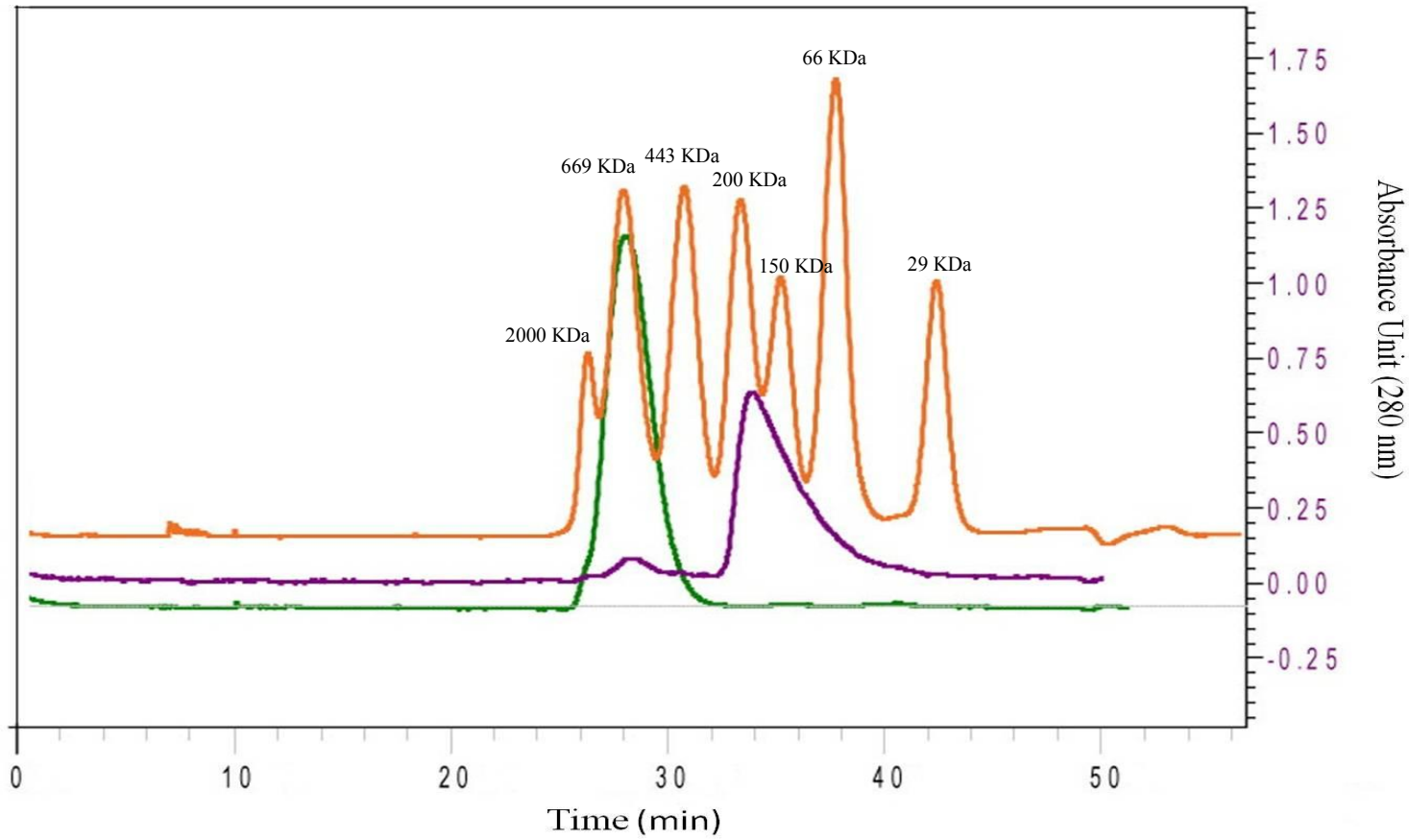

FIG.5.4. Gel filtration chromatography of $CynD_{pum}$ and $CynD_{pum}$ Δ303. $CynD_{pum}$ is in green and $CynD_{pum}$ Δ303 in purple and standards in orange. 2 to 3 mg/ml of purified enzymes were loaded on Superdex 200 10/300 GL column and 0.1 M MOPS was used as mobile phase Elution was monitored by absorbance at 280 nm.

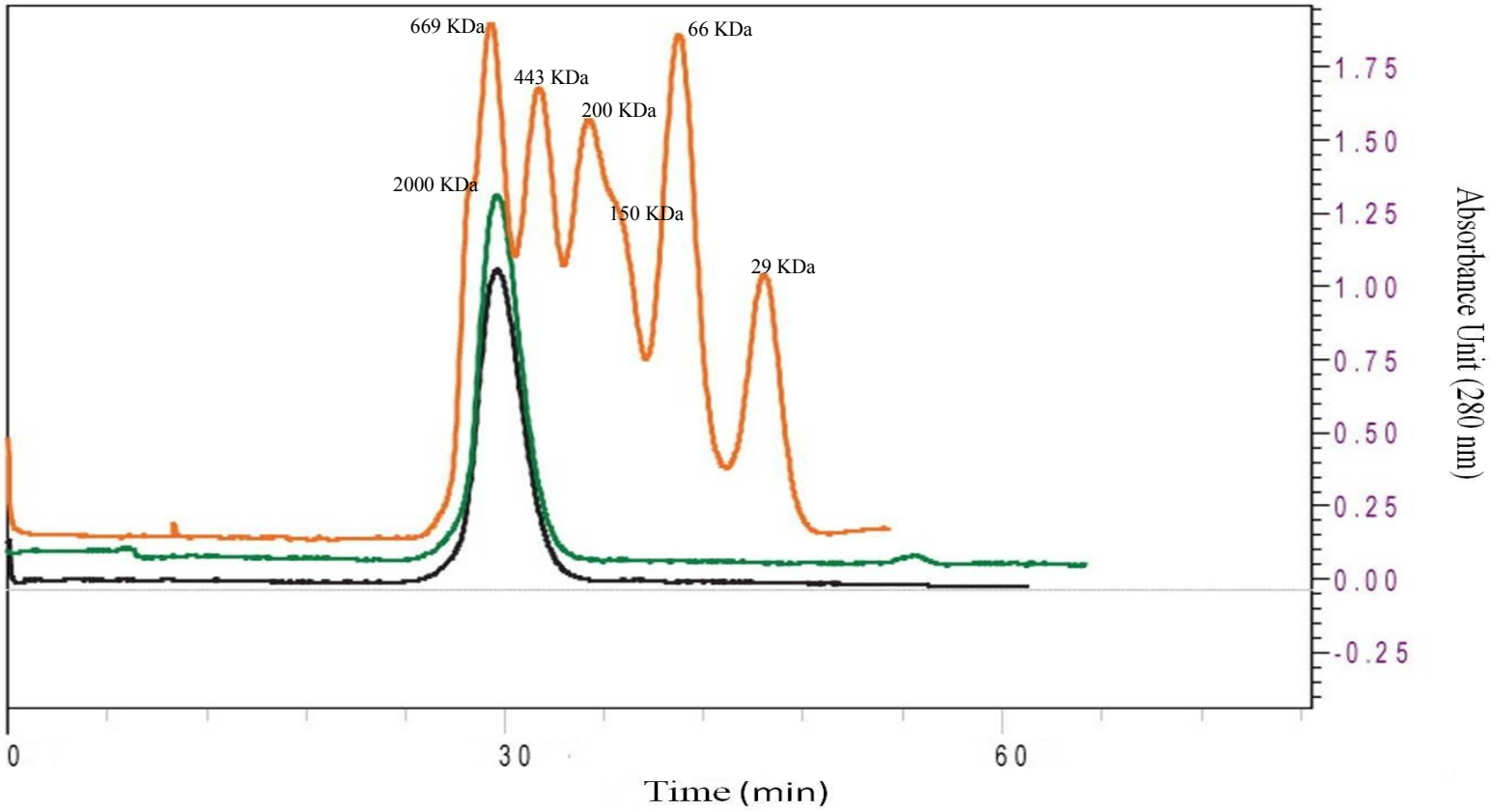

FIG.5.5. Gel filtration chromatography of $CynD_{pum}$ and $CynD_{pum\text{-}stut}$. $CynD_{pum}$ is in green and $CynD_{pum\text{-}stut}$ in black and standards in orange. 2 to 3 mg/ml of purified enzymes were loaded on Superdex 200 10/300 GL column and 0.1 M MOPS was used as mobile phase. Elution was monitored by absorbance at 280 nm.

The hybrid CynD$_{pum\text{-}stut}$ demonstrated remarkable stability compared to wild-type (FIG.5.1). It only lost 50% of its activity after 17 h incubation at 42^{o}C whereas the wild-type lost 50% of its activity in less than 1 h of incubation.

In addition, the CynD$_{pum\text{-}stut}$ hybrid showed a shift in its optimal pH from pH 8 to pH 9 (FIG.5.3). CynD$_{pum}$ rapidly lost its activity when the pH increased above pH 8. The hybrid had 100% activity at pH 9 and kept 45% of its activity at pH 9.5.

No other previously described CynD$_{pum}$ mutants have shown such an improvement in stability or catalysis at alkaline pH. The CynD$_{pum\text{-}stut}$ hybrid shows great potential to be used in bioremediation of cyanide.

The current model suggests that the C-terminus is involved at the A surface, the dimerization surface and C surface, the oligomerization surface. Both these surfaces were shown to be important for stability and activity of the enzyme (126). Mutations at the A surface abolished the activity of the enzyme such as A202T mutant described in chapter III. However, another A surface mutant, D172N also described in chapter III increased the stability of CynD$_{pum}$ and the affinity to the substrate at pH 7.7.

The C surface is important for oligomerization. Interactions at this interface help position a catalytic residue, E141 in the active site (58). Deletion of residues in this region destroyed the activity (126).

Residues found in CynD$_{stut}$ seem to be more favorable for CynD$_{pum}$. The different charges or polarity of the side chains might be forming better interactions with the C surface and A surface thus increasing stability of the enzyme.

In the previous chapter, CynD$_{pum}$ Δ303 was demonstrated to be highly unstable losing all of its activity within 30 minutes of incubation at 38^{o}C. However, its activity *in vivo* was 86% compared to wild-type CynD$_{pum}$. Gel filtration showed a destabilization of the 18-subunits oligomeric structure leading to pentamers or tetramers. The high instability and reduced activity *in vitro* might be the result of this spiral disruption and the small residual activity detected might be due to the small population of 18-subunit oligomers. However, *in vivo* chaperones might be helping stabilizing the structure and rescuing the activity of the mutant.

CynD$_{stut}$ C-terminus did not affect the structure of the hybrid despite the tremendous improvement on stability and pH activity. The gel filtration does not show long helices and suggests that the hybrid has a similar length as the wild-type.

CONCLUSION

Despite its high variability among the members of the nitrilase superfamily, the C-terminus seems to have a major role on CynD activity and stability. Unfortunately, no structural data of this domain are yet available due to this variability. The importance of the tail comes from its interactions with two major interfaces, surface A and C. These surfaces are crucial for the activity and stability of CynD. Thus, it is not too surprising that this domain would have major effects on the enzyme parameters. High resolution crystal structure of the protein would be helpful to understand the specific interactions taking place between this domain and the rest of protein. Taking advantage of our

studies on the C-terminus has enabled me to construct a novel protein with remarkable stability and tolerance to alkaline conditions, features essential for industrial application.

CHAPTER VI

CONCLUSION AND FUTURE WORK

Cyanide is a simple nitrile found naturally in some foods such as cassava roots, apple seeds and bitter almonds. It is produced by some microorganisms and plants and thought to be a defense mechanism against predators (24, 71). Cyanide is also used in several industries, mainly mining, electroplating, plastics, pesticides and adhesives. These applications result in waste waters contaminated with cyanide which have to be discharged properly due to the high toxicity of cyanide.

A simple, safe and cost efficient method for detoxification of these waters can be developed with the use of enzymes that convert cyanide into non-toxic products. One major group of enzymes considered for this bioremediation process is the nitrilase enzymes specifically the cyanide dihydratase enzyme from *Bacillus pumilus* (87) and *Pseudomonas stutzeri* (146). These enzymes hydrolyze cyanide into formate and ammonia without the use of cofactors, external energy or additional substrates.

The selection of enzymes for industrial use is based on the criteria relevant to the application, in this case that would be specificity, reaction rate, stability, optimal pH and temperature. The goal of this study is to improve $CynD_{pum}$ and $CynD_{stut}$ especially with regards to stability and activity at alkaline pH.

Directed evolution was used to improve the properties of $CynD_{pum}$ and error-prone PCR was used to mutagenize the gene. The advantage of this method is that the structure of the enzyme does not have to be known. However, its success depends on the

screening a large pool of randomly mutagenized clones. For this purpose, I optimized various parameters of an *in vivo* cloning method which was successful in generating a library with more than 10^4 clones from as little as 1 pmole of PCR fragment and 0.25 pmole of linearized plasmid (2). The method relies on *in vivo* recombination of the PCR fragments with a linearized vector using the lambda phage Red recombinase enzymes. Using a positive selection vector the recombination rate was increased from around 60% to 99 % by eliminating both religated and unlinearized vectors. This method shows great promise for the creation of random mutational libraries generated from error-prone PCR and used in directed evolution and protein engineering applications.

CynD$_{pum}$ STABILITY MUTANTS

Using the *in vivo* cloning technique combined with error-prone PCR, 3 CynD$_{pum}$ mutants with higher catalysis activity at pH 7.7 were found, mutants CD12 and DD3 with one amino acid change each, E327K and K93R respectively and 7G8 with two mutations D172N and A202T. The point mutations from these mutants were characterized individually and their effect on kinetics, stability and pH activity were studied in combination with structural modeling of their location in the protein structure.

The A202 residue is highly conserved in many members of the superfamily and it is located at the A surface. This surface is the dimerization surface and is formed of 2 α helices, α5 and α6. The A202T mutation, located on the α6, abolished the activity of the enzyme similarly to other α6 A surface mutations and deletions (126). The protein was found aggregated in the pellet suggesting the mutant is not assembled normally. Due to

the importance of the α6 A surface on the dimerization of the protein, A202T may disrupt critical interactions between the two dimers and thus destabilize the protein.

On the other hand, residue D172 is located at the α5 A surface and the mutant D172N retained full activity while showing an increase in thermostability as well as a 2-fold increase in affinity for the substrate at pH 7.7. These results emphasize the role of the A surface on the stability of the enzyme by disrupting (A202T) or strengthening (D172N) the interactions taken place at the interface between the monomers. Additionally, previously published results showed a role of the A surface, especially the α5 helix on the positioning of the catalytic residues in the active site (74).

Another mutant, K93R was also characterized. This residue is located on the α3 helix and is proposed to be involved in the interactions at the D/E surface. The E surface is thought to terminate the helix by tilting the last dimer, reducing the diameter of the spiral and thus preventing additional dimers from adding. It is formed of highly conserved negative charged residues 267EID269 at the end of strand β14 and the positive charged residues 93KR94 on the carboxy-terminal end of α3. On the other hand, the D surface is formed by α1 and α3 helices where interactions occur as the spiral completes one turn. Based on the location of the mutation, K93R might be stabilizing the interactions at either the D surface or the E surface. Previously isolated D surface mutants showed an elongation of the spiral, hence it would be interesting in future work to look at the length of K93R mutant and check for a similar structural change.

A final mutation E327K was located in the C-terminal region of $CynD_{pum}$. Structural modelling of this region is not available due to lack of sequence identity with

related crystallographically determined structure. However, it is speculated that this domain interacts with the A surface and the C surface, the oligomerization surface. The C surface interactions are crucial for the activity. It is thought that one of the catalytic residues is positioned in the active site following the oligomerization at the C surface (68).

Even though the screen was aimed at finding mutants with higher catalysis activity at pH 7.7, no mutants were found in the active site or the C surface. Some of the mutants did show an increase in affinity or maximal reaction rate but their effect on the stability of the enzyme was more prominent. The location of the mutations at the A, D/E surfaces as well as the C-terminus shows the importance of these domains on the stability of the enzyme. The mechanism of this phenotype as well as the interactions at these interfaces would be better understood once a high resolution crystal structure of $CynD_{pum}$ is obtained.

INTERACTION OF THE C-TERMINUS WITH THE A AND C SURFACES

The C-terminus is thought to interact with the C surface and then reach across to the A surface (31). Due to the importance of these surfaces on the activity of the nitrilase, the C-terminus seems to play an essential role at these interfaces. Because the C-terminus sequence diverges among all the members of the superfamily, its interactions with the other surfaces of the protein are hard to predict.

Deletion of the C-terminus in $CynD_{pum}$ led to a decrease in stability even though the cyanide degradation activity did not change when tested in whole cells. However,

purified mutant protein lost activity rapidly and showed a dissociation of the spiral structure as seen by gel filtration. A small peak eluted as an 18-mer similar to wild-type but the majority of the enzyme eluted as tetramers. These results suggest that the stable oligomerization of the dimers is altered, indicating a role of the C-terminus on the C surface interactions.

Even though the sequence of the C-terminus differs between the members of the nitrilase family, exchanging C-terminal regions had different effect on the enzyme. CHT_{crassa} and $CynD_{stut}$ lost all activity when their C-terminus was swapped with that of each other or $CynD_{pum}$. This was not the case with $CynD_{pum}$ which kept 50% of its activity when its C-terminus was swapped with that from CHT_{crassa} and had full activity with $CynD_{stut}$ C-terminus. These results indicate the presence of C-terminal domains required for the activity of some nitrilases but are missing in the other members. Such a domain was identified as $CynD_{stut}$ 306GERDST311. The $CynD_{stut\text{-}pum}$ hybrid was inactive due to the absence of this domain in $CynD_{pum}$ C-terminus. Introducing the GERDST domain in $CynD_{stut\text{-}pum}$ hybrid partially restored activity to the $CynD_{stut\text{-}pum}$ hybrid, however the mutant remained unstable. Thus, the GERDST domain might be interacting with the C surface and help reposition the catalytic residue E136 of $CynD_{stut}$ in the active site. Other $CynD_{stut}$ C-terminal residues seem to be required to ensure the stability of the enzyme.

On the other hand, $CynD_{pum\text{-}stut}$ showed a remarkable increase in stability compared to wild-type $CynD_{pum}$ and $CynD_{stut}$. The hybrid had 100% activity at pH 9 and kept 45% of its activity at pH 9.5, conditions where the parent enzymes are completely

inactive. The GERDST domain increased the stability of CynD$_{pum}$ but did not affect the activity of the enzyme at pH 9. This indicates that other residues in the C-terminus are responsible for this phenotype.

Since the C-terminus is speculated to interact with the A surface, it would be very interesting to test the stability and activity of the enzyme when D172N and/or A202T are introduced in the hybrid.

The CynD$_{pum\text{-}stut}$ hybrid shows great potential to be used in bioremediation of cyanide. Thus, its cyanide degrading activity should be tested with samples from industrial cyanide wastewaters contaminated with different metals. The metals might inhibit the activity of the enzyme as seen previously in the wild-type CynD$_{pum}$ (63) or the hybrid might show a higher tolerance to metals than that of the parent enzyme.

REFERENCES

1. **Abdallah I, Fischer AJ, Elmore CL, Saltveit ME, Zaki M.** 2006. Mechanism of resistance to quinclorac in smooth crabgrass (*Digitaria ischaemum*). Pestic. Biochem. Physiol. **84:**38-48.

2. **Abou-Nader M, and Benedik MJ.** 2010. Rapid generation of random mutant libraries. Bioeng. Bugs. **1:**337-340.

3. **Agarkar VB, Kimani SW, Cowan DA, Sayed MF, Sewell BT.** 2006. The quaternary structure of the amidase from *Geobacillus pallidus* RAPc8 is revealed by its crystal packing. Acta Crystallogr. Sect. F. Struct. Biol. Cryst. Commun. **62:**1174-1178.

4. **Akopyan TN, Braunstein AE, Goryachenkova EV.** 1975. Beta-cyanoalanine synthase: purification and characterization. Proc. Natl. Acad. Sci. U. S. A. **72:**1617-1621.

5. **Anderson PM, and Little RM.** 1986. Kinetic properties of cyanase. Biochem. **25:**1621-1626.

6. **Andrade J, Karmali A, Carrondo MA, Frazao C.** 2007. Structure of amidase from *Pseudomonas aeruginosa* showing a trapped acyl transfer reaction intermediate state. J. Biol. Chem. **282:**19598-19605.

7. **Baker RT, and Varshavsky A.** 1995. Yeast N-terminal amidase. A new enzyme and component of the N-end rule pathway. J. Biol. Chem. **270:**12065-12074.

8. **Barber CV, and Pratt VR.** 1998. Poison and profits: cyanide fishing in the Indo-Pacific. Environment. **40:**4-9.

9. **Barclay M, Tett VA, Knowles CJ.** 1998. Metabolism and enzymology of cyanide/metallocyanide biodegradation by *Fusarium solani* under neutral and acidic conditions. Enzyme Microb. Technol. **23:**321-330.

10. **Basile LJ, Willson RC, Sewell BT, Benedik MJ.** 2008. Genome mining of cyanide-degrading nitrilases from filamentous fungi. Appl. Microbiol. Biotechnol. **80:**427-435.

11. **Baxter J, and Cummings SP.** 2006. The current and future applications of microorganism in the bioremediation of cyanide contamination. Antonie Van Leeuwenhoek. **90:**1-17.

12. **Beamer WC, Shealy RM, Prough DS.** 1983. Acute cyanide poisoning from laetrile ingestion. Ann. Emerg. Med. **12:**449-451.

13. **Beckman RA, Mildvan AS, Loeb LA.** 1985. On the fidelity of DNA replication: manganese mutagenesis in vitro. Biochemistry. **24:**5810-5817.

14. **Belani KG, Singh H, Beebe DS, George P, Patterson SE, Nagasawa HT, Vince R.** 2012. Cyanide toxicity in juvenile pigs and its reversal by a new prodrug, sulfanegen sodium. Anesth. Analg. **114:**956-961.

15. **Blenis PV, Chow PS, Duncan I, Knowles NR.** 2004. Cyanide levels near fairy rings affect the growth of grasses and fungi. Can. J. Bot. **82:**1324-1329.

16. **Blumenthal-Goldschmidt S, Butler GW, Conn EE.** 1963. Incorporation of hydrocyanic acid labelled with carbon-14 into asparagine in seedlings. Nature. **197:**718-719.

17. **Borron SW, Baud FJ, Mégarbane B, Bismuth C.** 2007. Hydroxocobalamin for severe acute cyanide poisoning by ingestion or inhalation. Am. J. Emerg. Med. **25:**551-558.

18. **Botz MM.** 2000. Modeling of natural cyanide attenuation in tailings impoundments. Miner. Mettal. Proc. **17:**228-233.

19. **Brenner M, Kim JG, Lee J, Mahon SB, Lemor D, Ahdout R, Boss GR, Blackledge W, Jann L, Nagasawa HT, Patterson SE.** 2010. Sulfanegen sodium treatment in a rabbit model of sub-lethal cyanide toxicity. Toxicol. Appl. Pharmacol. **248:**269-276.

20. **Broderius SJ.** 1981. Determination of hydrocyanic acid and free cyanide in aqueous solution. Anal. Chem. **53:**1472-1477.

21. **Brysk MM, Corpe WA, Hankes LV.** 1969. Beta-cyanoalanine formation by *Chromobacterium violaceum*. J. Bacteriol. **97:**322-327.

22. **Brysk MM, and Ressler C.** 1970. γ-Cyano-α-l-aminobutyric acid. J. Biol. Chem. **245:**1156-1160.

23. **Cadwell RC, and Joyce GF.** 1992. Randomization of genes by PCR mutagenesis. PCR Methods Appl. **2:**28-33.

24. **Castric PA, Farnden KJF, Conn EE.** 1972. Cyanide metabolism in higher plants: V. The formation of asparagine from β-cyanoalanine. Arch. Biochem. Biophys. **152:**62-69.

25. **Clark JM.** 1988. Novel non-templated nucleotide addition reactions catalyzed by procaryotic and eucaryotic DNA polymerases. Nucleic Acids Res. **16:**9677-9686.

26. **Clennell JE.** 1910. The cyanide handbook. New York [etc.] McGraw-Hill Book Company, New York.

27. **Cooper AJ, Haber MT, Meister A.** 1982. On the chemistry and biochemistry of 3-mercaptopyruvic acid, the alpha-keto acid analog of cysteine. J. Biol. Chem. **257:**816-826.

28. **Dao-Thi MH, Van Melderen L, De Genst E, Afif H, Buts L, Wyns L, Loris R.** 2005. Molecular basis of gyrase poisoning by the addiction toxin CcdB. J. Mol. Biol. **348:**1091-1102.

29. **Dash RR, Gaur A, Balomajumder C.** 2009. Cyanide in industrial wastewaters and its removal: A review on biotreatment. J. Hazard. Mater. **163:**1-11.

30. **Datsenko KA, and Wanner BL.** 2000. One-step inactivation of chromosomal genes in *Escherichia coli* K-12 using PCR products. Proc. Natl. Acad. Sci. U. S. A. **97:**6640-6645.

31. **Dent KC, Weber BW, Benedik MJ, Sewell BT.** 2009. The cyanide hydratase from *Neurospora crassa* forms a helix which has a dimeric repeat. Appl. Microbiol. Biotechnol. **82:**271-278.

32. **DeSantis G, Wong K, Farwell B, Chatman K, Zhu Z, Tomlinson G, Huang H, Tan X, Bibbs L, Chen P, Kretz K, Burk MJ.** 2003. Creation of a productive, highly enantioselective nitrilase through gene site saturation mutagenesis (GSSM). J. Am. Chem. Soc. **125:**11476-11477.

33. **Devuyst EA.** 1989. A cyanide removal process using sulfur dioxide and air. JOM. **41:**43-45.

34. **Dixon R, and Kahn D.** 2004. Genetic regulation of biological nitrogen fixation. Nat. Rev. Microbiol. **2:**621-631.

35. **Dorr PK, and Knowles CJ.** 1989. Cyanide oxygenase and cyanase activities of *Pseudomonas fluorescens* NCIMB 11764. FEMS Microbiol. Lett. **60:**289-294.

36. **Dumestre A, Chone T, Portal J, Gerard M, Berthelin J.** 1997. Cyanide degradation under alkaline conditions by a strain of *Fusarium solani* isolated from contaminated soils. Appl. Environ. Microbiol. **63:**2729-2734.

37. **Dunnill PM, and Fowden L.** 1965. Enzymatic formation of beta-cyanoalanine from cyanide by *Escherichia coli* extracts. Nature. **208:**1206-1207.

38. **Eckert KA, and Kunkel TA.** 1990. High fidelity DNA synthesis by the Thermus aquaticus DNA polymerase. Nucleic Acids Res. **18:**3739-3744.

39. **El-Deiry WS, Downey KM, So AG.** 1984. Molecular mechanisms of manganese mutagenesis. Proc. Natl. Acad. Sci. U. S. A. **81:**7378-7382.

40. **Enright AJ, and Ouzounis CA.** 2001. Functional associations of proteins in entire genomes by means of exhaustive detection of gene fusions. Genome Biol. **2:**R34.1-R34.7.

41. **Fernandez RF, Dolghih E, Kunz DA.** 2004. Enzymatic assimilation of cyanide via pterin-dependent oxygenolytic cleavage to ammonia and formate in *Pseudomonas fluorescens* NCIMB 11764. Appl. Environ. Microbiol. **70:**121-128.

42. **Fernandez RF, and Kunz DA.** 2005. Bacterial cyanide oxygenase is a suite of enzymes catalyzing the scavenging and adventitious utilization of cyanide as a nitrogenous growth substrate. J. Bacteriol. **187:**6396-6402.

43. **Fisher FB.** 1952. Colorimetric determination of cyanide in stack gas and waste water. Anal. Chem. **24:**1440.

44. **Gallagher LA, and Manoil C.** 2001. *Pseudomonas aeruginosa* PAO1 kills*Caenorhabditis elegans* by cyanide poisoning. J. Bacteriol. **183:**6207-6214.

45. **Gantzer CJ.** 1990. Biological degradation of cyanide by nitrogen-fixing cyanobacteria. U.S. Environmental Protection Agency, Risk Reduction Engineering Laboratory, Cincinnati, OH.

46. **Getzoff ED, Cabelli DE, Fisher CL, Parge HE, Viezzoli MS, Banci L, Hallewell RA.** 1992. Faster superoxide dismutase mutants designed by enhancing electrostatic guidance. Nature. **358:**347-351.

47. **Gracia R, and Shepherd G.** 2004. Cyanide poisoning and its treatment. Pharmacotherapy. **24:**1358-1365.

48. **Greener A, Callahan M, Jerpseth B.** 1997. An efficient random mutagenesis technique using an *E. coli* mutator strain. Mol. Biotechnol. **7:**189-195.

49. **Grossmann K.** 2010. Auxin herbicides: current status of mechanism and mode of action. Pest. Manag. Sci. **66:**113-120.

50. **Gupta N, Balomajumder C, Agarwal VK.** 2010. Enzymatic mechanism and biochemistry for cyanide degradation: a review. J. Hazard. Mater. **176:**1-13.

51. **Gupta SD, and Wu HC.** 1991. Identification and subcellular localization of apolipoprotein N-acyltransferase in *Escherichia coli*. FEMS Microbiol. Lett. **78:**37.

52. **Hardy RW, and Knight E,Jr.** 1967. ATP-dependent reduction of azide and HCN by N2-fixing enzymes of Azotobacter vinelandii and Clostridium pasteurianum. Biochim. Biophys. Acta. **139:**69-90.

53. **Harris RE, and Knowles CJ.** 1983. The conversion of cyanide to ammonia by extracts of a strain of *Pseudomonas fluorescens* that utilizes cyanide as a source of nitrogen for growth. FEMS Microbiol. Lett. **20:**337-341.

54. **Harris R, and Knowles CJ.** 1983. Isolation and growth of a *Pseudomonas* species that utilizes cyanide as a source of nitrogen. J. Gen Microbiol. **129:**1005-1011.

55. **Hartley JL, Temple GF, Brasch MA.** 2000. DNA cloning using in vitro site-specific recombination. Genome Res. **10:**1788-1795.

56. **Hatzfeld Y, Maruyama A, Schmidt A, Noji M, Ishizawa K, Saito K.** 2000. β-cyanoalanine synthase is a mitochondrial cysteine synthase-like protein in spinach and *Arabidopsis*. Plant Physiol. **123:**1163-1172.

57. **Hughes J, Decarvalho JPC, Hughes MA.** 1994. Purification, characterization, and cloning of α-hydroxynitrile lyase from cassava (*Manihot esculenta Crantz*). Arch. Biochem. Biophys. **311:**496-502.

58. **Hung CL, Liu JH, Chiu WC, Huang SW, Hwang JK, Wang WC.** 2007. Crystal structure of Helicobacter pylori formamidase AmiF reveals a cysteine-glutamate-lysine catalytic triad. J. Biol. Chem. **282:**12220-12229.

59. **Hymes J.** 1996. Biotinidase and its roles in biotin metabolism. Clin. Chim. Acta. **255:**1-11.

60. **Ingvorsen K, Højer-Pedersen B, Godtfredsen SE.** 1991. Novel cyanide-hydrolyzing enzyme from *Alcaligenes xylosoxidans subsp. denitrificans*. Appl. Environ. Microbiol. **57:**1783-1789.

61. **Jaeger KE, and Eggert T.** 2004. Enantioselective biocatalysis optimized by directed evolution. Curr. Opin. Biotechnol. **15:**305-313.

62. **Jandhyala D, Berman M, Meyers PR, Sewell BT, Willson RC, Benedik MJ.** 2003. CynD, the cyanide dihydratase from *Bacillus pumilus*: gene cloning and structural studies. Appl. Environ. Microbiol. **69:**4794-4805.

63. **Jandhyala DM, Willson RC, Sewell BT, Benedik MJ.** 2005. Comparison of cyanide-degrading nitrilases. Appl. Microbiol. Biotechnol. **68:**327-335.

64. **Jones RJ, and Steven AL.** 1997. Effects of cyanide on corals in relation to cyanide fishing on reefs. Mar. Freshwater Res. **48:**517-522.

65. **Kao CM, Liu JK, Lou HR, Lin CS, Chen SC.** 2003. Biotransformation of cyanide to methane and ammonia by *Klebsiella oxytoca*. Chemosphere. **50:**1055-1061.

66. **Kelly M, and Clarke PH.** 1962. An inducible amidase produced by a strain of *Pseudomonas aeruginosa*. Journal of General Microbiology. **27:**305-316.

67. **Keusgen M, Kloock JP, Knobbe D-, Jünger M, Krest I, Goldbach M, Klein W, Schöning MJ.** 2004. Direct determination of cyanides by potentiometric biosensors. Sensor. Actuat. B-Chem. **103:**380-385.

68. **Kimani S, Agarkar V, Cowan D, Sayed MF-, Sewell BT.** 2007. Structure of an aliphatic amidase from *Geobacillus pallidus* RAPc8. Acta Crystallogr. D. **63:**1048-1058.

69. **Kiziak C, Klein J, Stolz A.** 2007. Influence of different carboxy-terminal mutations on the substrate-, reaction- and enantiospecificity of the arylacetonitrilase from *Pseudomonas fluorescens* EBC191. Protein Eng. Des. Sel. **20:**385-396.

70. **Knorre H, and Griffiths A.** 1984. Cyanide detoxification with hydrogen peroxide using the Degussa process. Conference on Cyanide and the Environment, Tucson Arizona.

71. **Knowles CJ.** 1976. Microorganisms and cyanide. Bacteriol. Rev. **40:**652-680.

72. **Kovac C.** 2000. Cyanide spill threatens health in Hungary. Brit. Med. J. **320:**536.

73. **Kuhn DD, and Young TC.** 2005. Photolytic degradation of hexacyanoferrate (II) in aqueous media: the determination of the degradation kinetics. Chemosphere. **60:**1222-1230.

74. **Kumaran D, Eswaramoorthy S, Gerchman SE, Kycia H, Studier FW, Swaminathan S.** 2003. Crystal structure of a putative CN hydrolase from yeast. Proteins. **52:**283-291.

75. **Kunz DA, Fernandez RF, Parab P.** 2001. Evidence that bacterial cyanide oxygenase is a pterin-dependent hydroxylase. Biochem. Biophys. Res. Commun. **287:**514-518.

76. **Kunz DA, and Nagappan O.** 1989. Cyanase-mediated utilization of cyanate in *Pseudomonas fluorescens* NCIB 11764. Appl. Environ. Microbiol. **55:**256-258.

77. **La Brooy SR.** 1994. Review of gold extraction from ores. Minerals Eng. **7:**1213-1241.

78. **Lauinger C, and Ressler C.** 1970. β-Cyanoalanine as a substrate for asparaginase stoichiometry, kinetics, and inhibition. Biochim. Biophys. Acta. **198:**316-323.

79. **Li J, Burgess BK, Corbin JL.** 1982. Nitrogenase reactivity: cyanide as substrate and inhibitor. Biochemistry. **21:**4393-4402.

80. **Li MZ, and Elledge SJ.** 2005. MAGIC, an in vivo genetic method for the rapid construction of recombinant DNA molecules. Nat. Genet. **37:**311-319. doi: 10.1038/ng1505.

81. **Liang W.** 2003. Drought stress increases both cyanogenesis and β-cyanoalanine synthase activity in tobacco. Plant Sci. **165:**1109-1115.

82. **Macadam AM, and Knowles CJ.** 1984. Purification and properties of β-cyano-l-alanine synthase from the cyanide-producing bacterium, *Chromobacterium violaceum*. Biochim. Biophys. Acta. **786:**123-132.

83. **Marcotte EM, Pellegrini M, Ng HL, Rice DW, Yeates TO, Eisenberg D.** 1999. Detecting protein function and protein-protein interactions from genome sequences. Science. **285:**751-753.

84. **Marsden JO.** 2006. Overview of gold processing techniques around the world. Miner. Metall. Proc. **23:**121-125.

85. **Materassi R, Balloni W, Florenzano G.** 1977. Cyanide reduction by nitrogenase in intact cells of *Rhodopseudomonas gelatinose* Molisch. Zentralbl. Bakteriol. Parasitenkd. Infektionskr. Hyg. **132:**413-417.

86. **Meyers PR, Gokool P, Rawlings DE, Woods DR.** 1991. An efficient cyanide-degrading Bacillus pumilus strain. J. Gen. Microbiol. **137:**1397-1400.

87. **Meyers PR, Rawlings DE, Woods DR, Lindsey GG.** 1993. Isolation and characterization of a cyanide dihydratase from *Bacillus pumilus C1*. J. Bacteriol. **175:**6105-6112.

88. **Michaels R, and Corpe WA.** 1965. Cyanide formation by *Chromobacterium violaceum*. J. Bacteriol. **89:**106-112.

89. **Miller JD, Parga JR, Wan RY.** 1988. zinc-dust cementation of silver from alkaline cyanide solution - analysis of Merrill Crowe plant data. Miner. Metall. Proc. **5:**170-176.

90. **Miller JM, and Conn EE.** 1980. Metabolism of hydrogen cyanide by higher plants. Plant Physiol. **65:**1199-1202.

91. **Mkpong O, Yan H, Chism G, Sayre R.** 1990. Purification, characterization, and localization of linamarase in cassava. Plant Physiol. **93:**176-181.

92. **Moertel CG, Fleming TR, Rubin J, Kvols LK, Sarna G, Koch R, Currie VE, Young CW, Jones SE, Davignon JP.** 1982. A clinical trial of amygdalin (Laetrile) in the treatment of human cancer. N. Engl. J. Med. **306:**201-206.

93. **Mosher JB, and Figueroa L.** 1996. Biological oxidation of cyanide: A viable treatment option for the minerals processing industry? Minerals Eng. **9:**573-581.

94. **Mundy BP, Liu FH, Strobel GA.** 1973. Alpha-aminobutyronitrile as an intermediate in cyanide fixation by *Rhizoctonia solani*. Can. J. Biochem. **51:**1440-1442.

95. **Murphy KC.** 1998. Use of bacteriophage lambda recombination functions to promote gene replacement in *Escherichia coli*. J. Bacteriol. **180:**2063-2071.

96. **Nagasawa T, Wieser M, Nakamura T, Iwahara H, Yoshida T, Gekko K.** 2000. Nitrilase of *Rhodococcus rhodochrous* J1. Conversion into the active form by subunit association. Eur. J. Biochem. **267:**138-144.

97. **Nakada Y, Jiang Y, Nishijyo T, Itoh Y, Lu CD.** 2001. Molecular characterization and regulation of the aguBA operon, responsible for agmatine utilization in *Pseudomonas aeruginosa* PAO1. J. Bacteriol. **183:**6517-6524.

98. **Nakai T, Hasegawa T, Yamashita E, Yamamoto M, Kumasaka T, Ueki T, Nanba H, Ikenaka Y, Takahashi S, Sato M, Tsukihara T.** 2000. Crystal structure of N-carbamyl-D-amino acid amidohydrolase with a novel catalytic framework common to amidohydrolases. Structure. **8:**729-737.

99. **Negrón-mendoza A, Draganić ZD, Navarro-gonzález R, Draganić IG.** 1983. Aldehydes, ketones, and carboxylic acids formed radiolytically in aqueous solutions of cyanides and simple nitriles. Radiat. Res. **95:**248.

100. **Nichols M, and Willits C.** 1934. Reactions of Nessler's solution. J. Am. Chem. Soc. **56:**769-774.

101. **Ogunlabi OO, and Agboola FK.** 2007. A soluble β-cyanoalanine synthase from the gut of the variegated grasshopper *Zonocerus variegatus* (L.). Insect Biochem. Mol. Biol. **37:**72-79.

102. **Ogura T, and Hiraga S.** 1983. Mini-F plasmid genes that couple host cell division to plasmid proliferation. Proc. Natl. Acad. Sci. U. S. A. **80:**4784-4788.

103. **Oliner JD, Kinzler KW, Vogelstein B.** 1993. *In vivo* cloning of PCR products in *E.coli*. Nucleic Acids Research. **21:**5192-5197.

104. **Pace HC.** 2001. The nitrilase superfamily: classification, structure and function. Genome. Biol. **2:**1-9.

105. **Pace HC, Hodawadekar SC, Draganescu A, Huang J, Bieganowski P, Pekarsky Y, Croce CM, Brenner C.** 2000. Crystal structure of the worm NitFhit Rosetta Stone protein reveals a Nit tetramer binding two Fhit dimers. Current Biology. **10:**907-917.

106. **Padmaja G, and Balagopal C.** 1985. Cyanide degradation by *Rhizopus oryzae*. Can. J. Microbiol. **31:**663-669.

107. **Peiser GD, Wang T, Hoffman NE, Yang S, Liu H, Walsh CT.** 1984. Formation of cyanide from carbon 1 of 1-aminocyclopropane-1-carboxylic acid during its conversion to ethylene. Proc. Natl. Acad. Sci. **81:**3059-3063.

108. **Pekarsky Y, Campiglio M, Siprashvili Z, Druck T, Sedkov Y, Tillib S, Draganescu A, Wermuth P, Rothman JH, Huebner K, Buchberg AM, Mazo A, Brenner C, Croce CM.** 1998. Nitrilase and Fhit homologs are encoded as fusion proteins in *Drosophila melanogaster* and *Caenorhabditis elegans*. Proc. Natl. Acad. Sci. **95:**8744-8749.

109. **Poole CJ, and Kind PR.** 1986. Deficiency of thiosulphate sulphurtransferase (rhodanese) in Leber's hereditary optic neuropathy. Br. Med. J. (Clin. Res. Ed). **292:**1229-1230.

110. **Porter N, and Knowles CJ.** 1979. Cyanide-resistant growth in *Citrobacter freundii* and other *Enterobacteriaceae*. FEMS Microbiol. Lett. **5:**323-326.

111. **Poulton JE.** 1990. Cyanogenesis in plants. Plant Physiol. **94:**401-405.

112. **Prasad MS.** 1991. Modern trends in gold processing--overview. Minerals Eng. **4:**1257-1277.

113. **Qian D, Jiang L, Lu L, Wei C, Li Y.** 2011. Biochemical and structural properties of cyanases from *Arabidopsis thaliana* and *Oryza sativa*. PLoS One. **6:**e18300.

114. **Ressler C, Abe O, Kondo Y, Cottrell B, Abe K.** 1973. Purification and characterization from *Chromobacterium violaceum* of an enzyme catalyzing the synthesis of gamma-cyano-alpha-aminobutyric acid and thiocyanate. Biochem. **12:**5369-5377.

115. **Rico M, Benito G, Salgueiro AR, Díez-Herrero A, Pereira HG.** 2008. Reported tailings dam failures: A review of the European incidents in the worldwide context. J. Hazard. Mater. **152:**846-852.

116. **Ritcey GM.** 2005. Tailings management in gold plants. Hydrometallurgy. **78:**3-20.

117. **Robey H.** 2004. Thermal hydrolysis of cyanide. Pollut. Eng. **36:**22-26.

118. **Rodgers PB, and Knowles CJ.** 1978. Cyanide production and degradation during growth of *Chromobacterium violaceum*. J. Gen. Microbiol. **108:**261-267.

119. **Romero PA, and Arnold FH.** 2009. Exploring protein fitness landscapes by directed evolution. Nat. Rev. Mol. Cell Biol. **10:**866-876.

120. **Rudrappa T.** 2008. Cyanogenic pseudomonads influence multitrophic interactions in the rhizosphere. PloS One. **3:**e2073.

121. **Russell CB, Thaler DS, Dahlquist FW.** 1989. Chromosomal transformation of *Escherichia coli recD* strains with linearized plasmids. J. Bacteriol. **171:**2609-2613.

122. **Scharf SJ, Horn GT, Erlich HA.** 1986. Direct cloning and sequence analysis of enzymatically amplified genomic sequences. Science. **233:**1076-1078.

123. **Scheffer MP.** 2006. Helical structures of the cyanide degrading enzymes from *Gloeocercospora sorghi* and *Bacillus pumilus* providing insights into nitrilase quaternary interactions. Master's thesis. University of Cape Town, South Africa.

124. **Schoemaker HE, Mink D, Wubbolts MG.** 2003. Dispelling the myths--biocatalysis in industrial synthesis. Science. **299:**1694-1697.

125. **Sewell BT, Berman MN, Meyers PR, Jandhyala D, Benedik MJ.** 2003. The cyanide degrading nitrilase from *Pseudomonas stutzeri* AK61 is a two-fold symmetric, 14-subunit spiral. Structure. **11:**1413-1422.

126. **Sewell BT, Thuku RN, Zhang X, Benedik MJ.** 2005. Oligomeric structure of nitrilases: effect of mutating interfacial residues on activity. Ann. N. Y. Acad. Sci. **1056:**153-159.

127. **Shragg T, Albertson T, Fisher C.** 1982. Cyanide poisoning after bitter almond ingestion. West. J. Med. **136:**65-69.

128. **Singer B, and Kusmierek JT.** 1982. Chemical mutagenesis. Annu. Rev. Biochem. **51:**655-691.

129. **Singh R, Sharma R, Tewari N, Geetanjali, Rawat DS.** 2006. Nitrilase and its application as a "Green" catalyst. Chem. Biodiv. **3:**1279-1287.

130. **Skandalis A, Encell LP, Loeb LA.** 1997. Creating novel enzymes by applied molecular evolution. Chem. Biol. **4:**889-898.

131. **Smith GR.** 1987. Mechanism and control of homologous recombination in *Escherichia coli*. Annu. Rev. Genet. **21:**179-201.

132. **Stuehr J, Yeager E, Sachs T, Hovorka F.** 1963. Ultrasonic investigation of the rate of hydrolysis of potassium cyanide. J. Chem. Phys. **38:**587-593.

133. **Sugino A, Higgins NP, Cozzarelli NR.** 1980. DNA gyrase subunit stoichiometry and the covalent attachment of subunit A to DNA during DNA cleavage. Nucleic Acids Res. **8:**3865-3874.

134. **Thimann KV, and Mahadevan S.** 1964. Nitrilase. I. occurrence, preparation, and general properties of the enzyme. Arch. Biochem. Biophys. **105:**133-141.

135. **Thuku RN, Brady D, Benedik MJ, Sewell BT.** 2009. Microbial nitrilases: versatile, spiral forming, industrial enzymes. J. Appl. Microbiol. **106:**703-727.

136. **Thuku RN, Weber BW, Varsani A, Sewell BT.** 2007. Post-translational cleavage of recombinantly expressed nitrilase from *Rhodococcus rhodochrous* J1 yields a stable, active helical form. FEBS J. **274:**2099-2108.

137. **Tindall KR, and Kunkel TA.** 1988. Fidelity of DNA synthesis by the *Thermus aquaticus* DNA polymerase. Biochem. **27:**6008-6013.

138. **Unger RC, and Clark AJ.** 1972. Interaction of the recombination pathways of bacteriophage lambda and its host *Escherichia coli* K12: effects on exonuclease V activity. J. Mol. Biol. **70:**539-548.

139. **United States Environmental Protection Agency Office of Solid Waste Special,Waste Branch.** 1994. Treatment of cyanide heap leaches and tailings : technical report. http://www.epa.gov/osw/nonhaz/industrial/special/mining/techdocs/cyanide.pdf.

140. **USEPA.** 1985. Drinking water criteria document for cyanide. Environ. Protection Agency U. S. Environment Criteria and Assessment Office, Cincinnati, EPA/600/X-84-192-1.

141. **Van Melderen L.** 2002. Molecular interactions of the CcdB poison with its bacterial target, the DNA gyrase. Int. J. Med. Microbiol. **291:**537-544.

142. **Van Melderen L, Bernard P, Couturier M.** 1994. Lon-dependent proteolysis of CcdA is the key control for activation of CcdB in plasmid-free segregant bacteria. Mol. Microbiol. **11:**1151-1157.

143. **Wang C, Kunz DA, Venables BJ.** 1996. Incorporation of molecular oxygen and water during enzymatic oxidation of cyanide by *Pseudomonas fluorescens* NCIMB 11764. Appl. Environ. Microbiol. **62:**2195-2197.

144. **Wang L, Watermeyer JM, Mulelu AE, Sewell BT, Benedik MJ.** 2012. Engineering pH-tolerant mutants of a cyanide dihydratase. Appl. Microbiol. Biotechnol. **94:**131-140.

145. **Wang P, Matthews DE, VanEtten HD.** 1992. Purification and characterization of cyanide hydratase from the phytopathogenic fungus *Gloeocercospora sorghi*. Arch. Biochem. Biophys. **298:**569-575.

146. **Watanabe A, Yano K, Ikebukuro K, Karube I.** 1998. Cyanide hydrolysis in a cyanide-degrading bacterium, *Pseudomonas stutzeri* AK61, by cyanidase. Microbiol. **144:**1677-1682.

147. **Watanabe A, Yano K, Ikebukuro K, Karube I.** 1998. Investigation of the potential active site of a cyanide dihydratase using site-directed mutagenesis. Biochim. Biophys. Acta. **1382:**1-4.

148. **Way JL, Leung P, Cannon E, Morgan R, Tamulinas C, Leong-Way J, Baxter L, Nagi A, Chui C.** 1988. The mechanism of cyanide intoxication and its antagonism. Ciba found. Symp. **140:**232-243.

149. **White J, Jones D, Huang D, Gauthier J.** 1988. Conversion of cyanide to formate and ammonia by a pseudomonad obtained from industrial wasterwater. J. Ind. Microbiol. Biotechnol. **3:**263-272.

150. **Winans SC, Elledge SJ, Krueger JH, Walker GC.** 1985. Site-directed insertion and deletion mutagenesis with cloned fragments in *Escherichia coli*. J. Bacteriol. **161:**1219-1221.

151. **World Health Organization.** 2004. Hydrogen cyanide and cyanides: human health aspects.Concise international chemical assessment document 61. World Health Organization, Geneva, Switzerland.

152. **Wu S, Fogiel AJ, Petrillo KL, Hann EC, Mersinger LJ, DiCosimo R, O'Keefe DP, Ben-Bassat A, Payne MS.** 2007. Protein engineering of *Acidovorax facilis* 72W nitrilase for bioprocess development. Biotechnol. Bioeng. **97:**689-693.

153. **Yamamoto K, Oishi K, Fujimatsu I, Komatsu K.** 1991. Production of R-(-)-mandelic acid from mandelonitrile by *Alcaligenes faecalis* ATCC 8750. Appl. Environ. Microbiol. **57:**3028-3032.

154. **Yip WK, and Yang SF.** 1988. Cyanide metabolism in relation to ethylene production in plant tissues. Plant Physiol. **88:**473-476.

155. **Zalkin H.** 1985. NAD synthetase. Methods Enzymol. **113:**297-302.

156. **Zheng YG, Chen J, Liu ZQ, Wu MH, Xing LY, Shen YC.** 2008. Isolation, identification and characterization of *Bacillus subtilis* ZJB-063, a versatile nitrile-converting bacterium. Appl. Microbiol. Biotechnol. **77:**985-993.